A Trajectory-Based Approach to Modeling Nonlinear Infrared Spectra: Interrogating Strong Hydrogen Bonds and Proton Transfer

by

Andrew D. Horning

B.S. Chemistry
University of Southern California, 2008

SUBMITTED TO THE DEPARTMENT OF CHEMISTRY IN PARTIAL FULMILLMENT OF THE REQUIREMENTS FOR THE DEGREE OF

MASTER OF SCIENCE IN CHEMISTRY
AT THE
MASSACHUSETTS INSTITUTE OF TECHNOLOGY

JUNE 2012

Signature of Author: _____
Department of Chemistry
May 7, 2012

Certified by: _____
Andrei Tokmakoff
Professor of Chemistry
Thesis Supervisor

Accepted by: _____
Robert W. Field
Robert T. Haslam and Bradley Dewey Professor of Chemistry
Chairman, Departmental Committee on Graduate Students

A Trajectory-Based Approach to Modeling
Nonlinear Infrared Spectra: Interrogating Strong
Hydrogen Bonds and Proton Transfer

by

Andrew D. Horning

Submitted to the Department of Chemistry
on May 7, 2012 in Partial Fulfillment of the
Requirements for the Degree of Master of Science in
Chemistry

ABSTRACT

This work describes a phenomenological approach for modeling linear and nonlinear infrared spectroscopy of condensed phase chemical systems, focusing on applications to strongly hydrogen bonded complexes. To overcome the limitations inherent in common analytical models, I construct full time trajectories for spectroscopic variables, here the vibrational frequencies and transition dipole moments, and use these as inputs to calculate the system response to an applied electric field. This method identifies key dynamical variables, treats these stochastically, and then constructs trajectories of spectroscopic variables from these stochastic quantities through mappings. The correspondence of such fluctuating coordinates and spectroscopic observables is demonstrated for a number of simple cases not adequately addressed using current approximations, including liquid water, strong hydrogen bonds, and proton transfer reactions using *ab initio* calculations, model potentials, and molecular dynamics. Dynamical information is bestowed upon these trajectories through either a Langevin-like Brownian oscillator model for the bath, full molecular dynamics calculations, or experimentally motivated empirical formulae. Utilizing the semiclassical approximation for the linear and nonlinear response functions, these constructed trajectories give us the ability to numerically calculate nonlinear spectroscopy to examine phenomena previously difficult with other methods, including non-Gaussian dynamics, correlated occurrences, highly anharmonic potentials, and complex system-bath relationships.

Thesis Supervisor: Andrei Tokmakoff
Title: Professor of Chemistry

TABLE OF CONTENTS

ACKNOWLEDGEMENTS

This research was supported in part by an award from the Department of Energy (DOE) Office of Science Graduate Fellowship Program (DOE SCGF). The DOE SCGF Program was made possible in part by the American Recovery and Reinvestment Act of 2009. The DOE SCGF program is administered by the Oak Ridge Institute for Science and Education for the DOE. ORISE is managed by Oak Ridge Associated Universities (ORAU) under DOE contract number DE-AC05-06OR23100. All opinions expressed in this paper are the author's and do not necessarily reflect the policies and views of DOE, ORAU, or ORISE.

This research was also supported in part by a BP MIT Energy Initiative (MITEI) Fellowship. I would like to thank both fellowship programs not only for financial support, but for exceptionally worthwhile academic, networking, and social opportunities which have proven tremendously intellectually stimulating and meaningful in my growth as a scientist and as a person.

Chapter 1 : THE HYDROGEN BOND AND PROTON TRANSFER

Atoms and molecules tend to stick together. The forces that cause this, however, are rather subtle and of many different forms, and many commonplace and seemingly simple intermolecular interactions are still not entirely understood. Attractive and repulsive forces between molecules were first postulated to account for observations of nonideality in gasses and liquids in the late 1800s [1]. Since this first introduction of bonds and molecular interactions, one peculiar rather weak attractive force - the hydrogen bond - has become perhaps the most important and useful chemical structural concepts in all of chemistry. A huge variety of chemical and biological phenomena can be traced back to hydrogen bonding, but despite its ubiquity, we still lack a coherent predictive theoretical understanding which captures the many varying properties of these intermediate strength chemical interactions. In part this is due to the difficulty in even defining what makes a hydrogen bond. It is an interaction which lies between the weak omnidirectional nonbonded dispersion forces and the strong full chemical bond, spanning a large range of possible energies and geometries.

Alfred Werner was among the first to investigate the unusual properties of the hydrogen bond when he proposed that ammonium salts contain a shared proton between the ammonia molecule and an anion in 1902, a full eleven years before Niels Bohr proposed his quantized model of the hydrogen atom [2]. Investigations of the hydrogen bond began in earnest as early as 1920 when the term first introduced by Latimer and Rodebush, and the consequences of this interaction on the absorption of infrared radiation was realized soon thereafter. Despite some sporadic early work, it is really Linus Pauling who cemented the idea firmly in the minds of chemists and first popularized the term, writing "...under certain conditions an atom of hydrogen is attracted by rather strong forces to two atoms, instead of only one, so that it may be considered to be acting as a bond between them. This is the hydrogen bond" [2-6].

HYDROGEN BONDS

At its core, the hydrogen bond is an attractive interaction between a proton donor D-H (X-H) and an acceptor moiety A (Y) [2, 6-8]:

$$\text{D-H} \cdots \text{A} \qquad \text{or} \qquad \text{X-H} \cdots \text{Y}$$

The recent IUPAC definition of this phenomenon emphasizes that "it is best considered as an electrostatic interaction, heightened by the small size of hydrogen, which permits proximity of the interacting dipoles or charges" [9]. That being said, this bond, depending on the strength, can have significant covalent and

dispersion character in addition to electrostatic, and many different pictures have been utilized to describe this interaction, including various orbital methods and valence bond frameworks [10, 11]. Much work has even found it fruitful to describe the character as part covalent bond and part charge transfer [12-15]. Hydrogen bonds are also unique because only the hydrogen atom lacks inner shell electrons, thus the bond itself is quite polarizable as the entire electron density around the hydrogen is directly influenced by the surrounding electrostatic environment [16]. As a result of this polarizability, the relative directionality of the donor-acceptor interaction is exceptionally important, as the dipoles involved are clearly oriented.

Despite its ubiquity, the hydrogen bond can be rather difficult to empirically define. Gilli and Gilli write that "the unique feature of the H-bond is that bonds made by the same donor-acceptor pair may display an extremely wide range of energies and geometries" [1]. There are a few general trends, however. A key feature of this interaction is the short X-Y internuclear distance upon bond formation, oftentimes shorter than the sum of the two van der Waals radii. In general, the stronger this attractive force, the more linear the X-H···Y angle, generally remaining above 110°. Linearity should be considered one of the main signatures of a hydrogen bond, as it is this directional anisotropy which structurally distinguishes it from isotropic van der Waals-like forces [17].

IMPORTANCE & INTEREST

Although weak compared to most chemical forces (spanning a rather wide energetic range, with a binding energy ΔE often between 1-20 kcal/mol), the hydrogen bond is responsible for a huge variety of macroscopic chemical phenomena, including the unique properties of water and ice, aqueous charge transport, protein folding and macromolecule stabilization, corrosion, and a variety of other phenomenon ranging from the interactions in the famous Watson–Crick base pairs of DNA to small molecule binding in enzymes [1, 18, 19]. The hydrogen bond is an especially important interaction in biological systems, where aqueous environments are common, proton motion is an important component of energy storage, and noncovalent interactions often work cooperatively to construct large polymers and molecular aggregates with well defined geometries.

Water is particularly significant with regards to hydrogen bonding and proton transfer, as each water molecule is capable of simultaneously donating and accepting multiple hydrogen bonds, and these interactions dominate the dynamics and structure of the condensed phases. The water dimer hydrogen bond, of energy approximately 5.5 kcal/mol, is of particular interest in biological systems as it is only one order of magnitude above k_BT at room temperature [20]. The relatively small energy of the hydrogen bond puts it in the "goldilocks zone" of chemical interactions for earth temperatures – not too strong, not to weak, but just right. kT at room temperature (298K) is 0.593 kcal/mol (256meV , 207cm^{-1}), which

means the energy of each interaction is just strong enough that the bonds are stable but weak enough that relatively small thermal fluctuations can lead to appreciable bond breaking or forming. This is in sharp contrast to the typical covalent bond, which is typically $O(100k_BT)$ at room temperature and requires significant effort to break.

THE GEOMETRY OF HYDROGEN BONDS

We can define a coordinate system for the prototypical hydrogen bond to describe the relative arrangement of each nucleus [2, 21]:

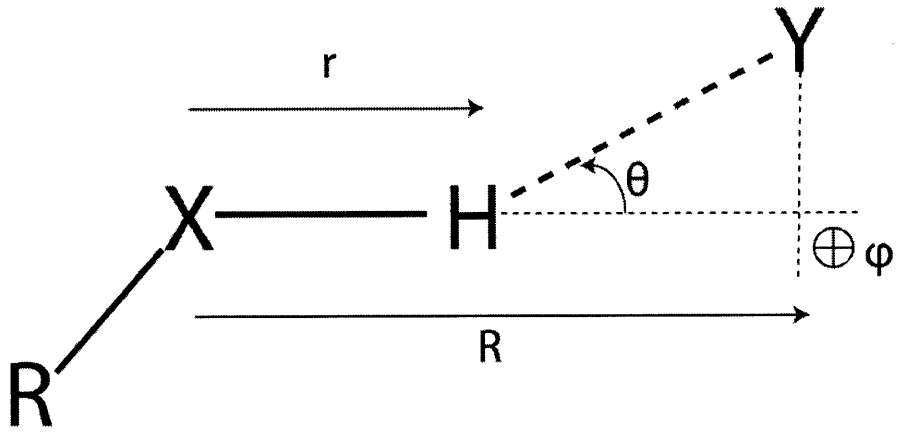

Figure 1: Hydrogen bonding coordinate system

This set of coordinates as defined specify the bond vector for the X-H bond r as well as the intermolecular coordinates R, θ, and φ describing the location and orientation of the acceptor. Motion along R serves to modulate the hydrogen bond distance, and motions along θ and φ (in water for instance these coordinates are connected to what are known as librational modes) allow the bond to deviate from linearity. In addition to this geometry, sometimes a proton transfer coordinate is defined as $\delta = r_{XH} - r_{YH}$, with donor acceptor distance R.

Common hydrogen bonding definitions are based upon instantaneous geometric criteria, examining these coordinates at any given moment in time and thus excluding any dynamics or large scale network properties [22, 23]. Typical hydrogen bond cutoff criteria are set somewhere near 3.5Å for the internuclear donor-acceptor R (coming from the first observed minimum in water's radial distribution function) and 30° deviation from linearity in θ and φ (a number chosen largely based upon the angular amplitude of librational motions in water). This picture ignores any motions or distortions, and simply focuses on the instantaneous geometric arrangement of the donor and acceptor. For example, a molecule undergoing a rapid rotation may pass these criteria fleetingly but continue rotating past the linear

arrangement, only qualifying as "hydrogen bonded" for a few femtoseconds. In their book "The Structure and Properties of Water," Eisenberg and Kauzmann attempt to incorporate timescale explicitly in defining the "structure" of water, with different aspects of the structure accessible at different time scales of measurement, but this is still a rather atypical definition [24].

With this geometric coordinate system defined, we can add in the electronic coordinates r_e for each electron e with mass m_e and momentum p_e which allows us to write the full system Hamiltonian for all nuclei and electrons:

$$H(r_e, r, R) = \sum_e \frac{p_e^2}{2m_e} + \frac{p^2}{2m} + \frac{P^2}{2M} + U(r_e, r, R) \tag{1.1}$$

where for a quantum mechanical system we use the momentum operators $p = -i\hbar\frac{\partial}{\partial r}$ and $P = -i\hbar\frac{\partial}{\partial R}$.

Applying the Born-Oppenheimer approximation to separate the fast electronic motions from the nuclear coordinates we can solve just the electronic portion of the wavefunction to obtain

$$H_{el}(r_e, r, R)\phi_{el}(r_e, r, R) = V(r, R)\phi_{el}(r_e, r, R) \tag{1.2}$$

Expanding this potential $V(r, R)$ about the minimum $V(r_0, R_0)$ as a power series we can write [21]:

$$V(r, R) = V(r_0, R_0) + \frac{1}{2}m\omega^2(R)(r - r_0)^2 + \frac{1}{2}M\Omega^2(R - R_0)^2 \tag{1.3}$$

Here we are expressing the anharmonic coupling between intermolecular position and X-H bond stretching as a frequency dependence in the intermolecular stretch, ω. This frequency dependence can be expanded in powers of R about minimum R_0:

$$\omega(R) = \omega(R_0) + (R - R_0)\frac{d\omega}{dR} + \frac{(R - R_0)^2}{2}\frac{\partial^2\omega}{\partial R^2} + \ldots \tag{1.4}$$

Assuming the electronic energy is minimized for a linear bond orientation ($\theta = 0, \phi = 0$) we can also include the bend or out of plane motion in this expansion:

$$\omega(R) = \omega(R_0) + (R - R_0)\frac{d\omega}{dR} + \frac{\theta^2}{2}\frac{\partial^2\omega}{\partial\theta^2} + \frac{\phi^2}{2}\frac{\partial^2\omega}{\partial\phi^2} + \frac{(R - R_0)^2}{2}\frac{\partial^2\omega}{\partial R^2} + \ldots \tag{1.5}$$

The overall observed linear IR spectrum then can contains absorptions at the transitions between these energies, $\hbar\omega$, and we should expect an anharmonic band with the potential for local minima and maxima in the spectrum. We can see here that bending intermonomer modes can shift the center of the vibrations and alter the overall shape. The electronic structure of the bond and thus the stretch are extremely sensitive to the nuclear position, especially that of the hydrogen atom itself, so this should come as no real surprise.

PROTON TRANSFER

Perhaps one of the greatest successes of modern theoretical mechanistic chemistry has been the development of both theoretical descriptions and experimental techniques with which to study electron transfer in condensed phases [25-30]. Ultrafast visible spectroscopy combined with synthetic ingenuity has allowed for the verification and investigation of various regimes of predicted behavior for this fundamental charge separation process, and the past 50 years has provided a wealth of understanding and insight regarding the transfer and translocation of electrons. Like electron transfer, proton transfer generally begins with neutral reactants and results in separated, stabilized charged product states. For a general donor-acceptor pair, we can compare the reactants and products of this acid-base reaction:

$$D + A \rightarrow D^+ + A^-$$

$$DH + A \rightarrow D^- + AH^+$$

Proton transfer, however, is only sometimes adequately described with the Marcus description, and difficulty in predicting the dynamics certainly is not due to relative importance or scarcity - the entire complex biological machinery of photosynthesis exists to ultimately create a proton gradient, and this occurs predictably many thousands of times per second in each cell. The most obvious reason for the continuing uncertainty is that unlike electron transfer, proton transfer involves the actual breaking and formation of a chemical bond with all the associated complex electronic consequences. With this comes the challenge of the proper picture for the transfer: one can consider it similar to the Marcus picture of solvent reorganization and a tunneling event, or as a more classical motion of the proton crossing over a barrier – both views are valid depending upon the reaction barrier height, shape, well depth, and corresponding proton wavefunction [21, 31-33].

Perhaps even less understood, local hydrogen bonding involving the proton of interest can greatly accelerate the transfer, serving to facilitate proton motion from donor to acceptor and define a reaction pathway. The structural rigidity provided by the hydrogen bond can also serve to pre-arrange the proton donor and acceptor in a favorable geometry - one can think of the proton transfer process as nothing more

than a large amplitude vibrational stretch in this prearranged donor-acceptor complex, and hydrogen bonds may be considered the semi-stable partially activated precursors to proton transfer reactions [7]. In fact, proton transfer in the absence of a guiding hydrogen bonds has only recently been observed in any system [34].

In densely hydrogen bonded compounds, it is known that proton diffusion is enhanced significantly. The "Grotthuss mechanism" describes the anomalously fast diffusion of protons in water as a topological defect propagation via structural diffusion – not unlike a string of marbles being pushed through a garden hose, with a concerned shift of protons along pre-arranged hydrogen bonding pathways [35-37]. This was proposed schematically by Theodor Christian Johann Dietrich von Grotthuß, who said that positive charges resulting from electrolysis could be transported in water through "structural diffusion," hopping from one molecule to another as seen from his original figure:

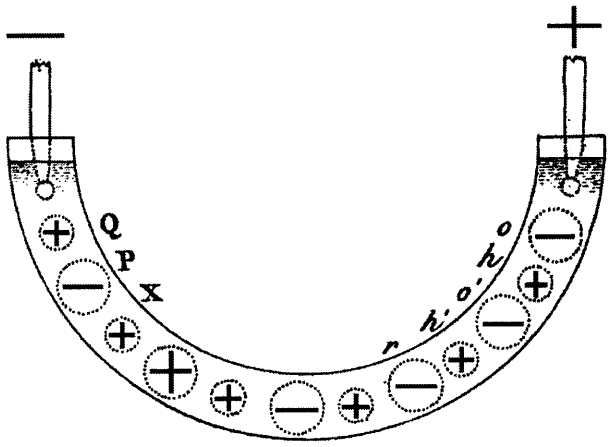

Figure 2: The original Grotthuss illustration of the propagation of charge (+) through a pre-arranged linear chain of chaged moieites [36]

Upon discovery of the proton (credited to Rutherford over 110 years after Grotthuss's publication!), this was proposed to be the mechanism of charge transport in water as well – that is, proton diffusion taking place via a series of bond breaking and formation events involving hydrogen bonded O-H···O bonds, resulting in net long-distance charge translocation without the long distance movement of any individual proton [38-41]. Hydrogen-bonded water molecules seem to also be capable of storing and directing protons within proteins [42-44].

Water wires like those proposed in the Grotthuss mechanism play a key role in charge recombination in water, and even rather distant solvent molecules can play a role in autoionization and recombination, cauing what Chandler et al describe as "highly unusual fluctuation in proton potential" [45, 46]. The

pathways available to any given proton depend upon the solvent structure around the proton itself, which is extremely dynamic and in protic species often dominated by breaking and forming hydrogen bonds. The structure and dynamics adjacent to the proton are inherently intertwined and both contribute in significant ways to the entire process of proton transfer, mapping out the landscape over which the transport is possible.

Models of the Proton Potential

In the condensed phase, the solvation of charged particles involves many molecules, and thus it is difficult to identify one suitable reaction coordinate with which to describe proton transfer. Because of the relatively weak nature of the hydrogen bond, small solvation changes can nudge the energetics just enough to initiate a proton transfer solely through collective small motions of the surrounding molecular environment. In water, the prototypical protic solvent with both a high dielectric constant and an extensive and complex network of hydrogen bonds, the underlying structure is essential in both defining the rate of transfer and the reaction coordinate itself.

To cut through this molecular complexity, as early as the 1930s, chemists and physicists have pictured the schematic one dimensional potential experienced by the transferring or shared proton [47, 48]. These potential models have been refined and used to calculate bond energies, bond distances, and OH vibrational frequencies as a function of internuclear distances [49]. Recent studies have focused on one dimensional coordinates useful for describing and thinking about the transfer process, ranging from the geometric coordinates, such as the O-O distance for water or the change in the donor-acceptor center of mass, to coordinates such as the electric field, and all forms generally take the form of an asymmetric double well potential relating spatial position (x axis) to potential energy (y axis), shown schematically for the –OH stretch along the bond vector in water during a transfer event in Figure 3 [50-55]. When the proton is localized on either the donor or acceptor, this potential appears roughly Morse-like, and when symmetric there is a double well shape with a small barrier.

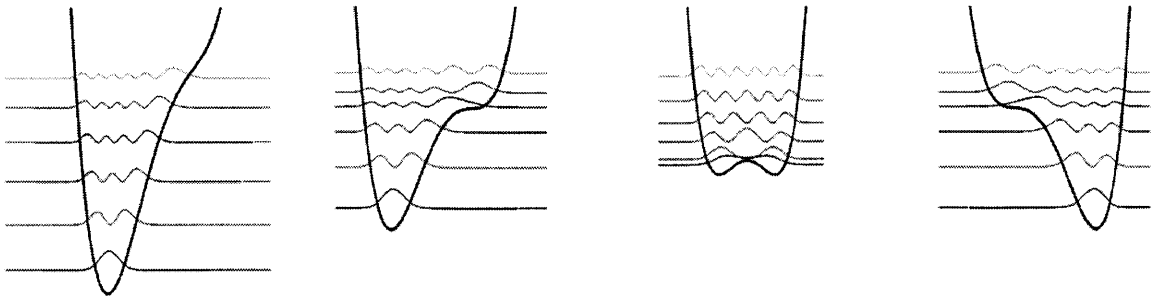

Figure 3: Double well potential model of proton transfer

In the simple 1D model, transfer of a proton is favored when the well becomes completely symmetric, which lowers the barrier such that the lowest vibrational eigenstate energies can become nearly degenerate, and the 0→1 stretching transition frequency drops significantly, while the higher energy transitions are also perturbed, hinting that changes in vibrational energy levels may serve as spectroscopic indicators of proton transfer events. In what Borgis and Hynes deem "adiabatic proton transfer," the stretching motion of the proton is much faster than the fluctuations of the surrounding solvent network (that is, the two motions are adiabatically decoupled due to their disparate timescales), such that any rearrangement of the solvent results in an essentially instantaneous adaptation of the potential governing the stretch, and efforts have been made to map the asymmetry of a model double well potential directly to the vibrational frequencies observed [32, 56, 57]. These sorts of effective proton potentials have been applied to systems ranging from the water dimer to ferroelectric materials [58-61].

Taking these one dimensional potentials as static, it is tempting to consider the effects of proton tunneling behavior through this barrier. Saykally is not the first and will certainly not be the last to claim that "one of the most fundamental, yet enigmatic, of all chemical processes is the transfer of protons in liquid water, which occurs via ultrafast quantum tunneling in the hydrogen bond network" [62]. But this is not the whole story. The potential experienced by the proton is itself dynamic, influenced by the large bath around it, and obsession with the tunneling proton neglects important realities of the proton potential. This overemphasized importance of proton tunneling to proton motion is all too commonplace, especially in the water literature, and oftentimes proton transfer is treated entirely nonadiabatically with a double well potential having a barrier height much higher than k_bT and the dominant contributor to transfer being tunneling [56, 63]. That is of course not to say that the proton does not behave quantum mechanically, as it most certainly does, but the structure of the barrier is such that tunneling is oftentimes the wrong picture [64].

Bernal and Fowler wrote in 1933 that "when two systems are in close contact as neighbors in the water... only a small barrier hill survives or the barrier may have almost totally disappeared, that that in either case the proton moves fairly freely from one system to the other during the period of this intimate contact" [65]. For many configurations, the potential energy surfaces have a low barrier at the shared state, which can easily be overcome when small solvent structural rearrangement occurs as the proton moves [66]. In fact, for low barrier potentials, quantum zero point motion alone can delocalize the proton, but it is largely a classical-like barrier crossing process [67]. In strong hydrogen bonding interactions, this barrier is effectively zero, and it is instead the small fluctuations in the proton environment which dictate proton dynamics [39, 68]. With this picture, Marx claims that "the picture of the 'tunneling proton in water', once obtained from oversimplified theoretical considerations, should finally be banished to the past" and that transfer of a proton occurs due to "mainly quantum mechanical zero-point vibrations—and not tunneling—in cooperation with 'appropriate fluctuations' of the hydrogen-bonded network in the vicinity of the excess charge" [69]. One recently used coordinate for these fluctuations driving proton transfer in a liquid is a "collective solvent coordinate" defined as the difference in energy of the stretching potential at the two proton minimum positions (on the "donor" and "acceptor"), such that when equally shared (a symmetric well) this value is zero [55, 70, 71].

While a useful conceptual model, this picture of simple potentials is complicated greatly when the solvent becomes part of the path of the proton as well, mediating the transfer process and connecting the acid and base through space, a situation we can depict for aqueous solutions schematically as:

$$DH \cdots (H_2O)_n \cdots A \rightarrow D^- \cdots H_3O^+(H_2O)_{n-1} \cdots A \rightarrow D^- \cdots (H_2O)_n \cdots AH^+$$

For such a scenario it is not clear whether the intervening water molecules accelerate the transfer, provide local minima which stall the proton in a stepwise or random-walk fashion, or introduce even more intricate dynamics. Water is a complex molecular network with a dynamic structure fluctuating and reorganizing on the order of 10fs to 10ps, breaking and forming hydrogen bonds and undergoing both collective and individual molecular motions. The interconnected pathways formed by this hydrogen-bonding structure dictate how energy and particles move through the solvent, and protons are guided and assisted by this underlying structure and rapid fluctuations so dramatically that even the inclusion of one or two water molecules greatly alters the fundamental proton transfer timescales and energies.

Reporting on H-Bonds and Proton Transfer

The effects of hydrogen bonding become apparent in a large variety of experimental methodologies, including microwave spectroscopy, nuclear magnetic resonance, infrared spectroscopy, x-ray absorption and emission, and both coherent and incoherent scattering [10, 21]. The electron density changes due to

this bonding can serve to deshield the shared hydrogen, leading to changes in the proton shielding tensor and thus altering NMR chemical shifts, anisotropies, and peak volumes, and nuclear couplings change quite noticeably when H-bonding is present [8]. It has also been shown that in some systems, NMR can even help to determine the shape of the proton potential [72-74].

For the same reasons that protons prone to hydrogen bonding can easily transfer to adjacent molecules, the stable hydrogen isotope deuterium, "^{2}H" or "D", can be easily exchanged with ^{1}H protons. Importantly, the extra neutron in the deuterium nucleus doubles the mass of the nucleus compared to that of a proton without changing the charge. The deuteron, being heavier, behaves more akin to a classical particle. Just due to its mass, D has a lower zero point energy and a narrower spatial extent of its nuclear wavefunction. With the extra uncharged neutron, the electronic structure of deuterium remains identical to that of the proton, so only spectroscopic properties which rely upon the nucleus in some way are altered. For example, the deuteron is a boson made of two spin ½ particles, thus having a nuclear spin of +1 and radically different NMR signatures from the spin ½ proton, but the visible absorption of deuterated compounds does not change considerably from the protonated species. The dynamics of deuterium motion are also significantly altered by the doubling of the mass, and everything from macroscopic diffusion to enzyme turnover rates changes upon deuteration. Because the substitution of deuterium for hydrogen is effectively nonperturbative to the geometry and electronic structure, deuteration provides a useful tool with which to examine the effect of mass upon the properties of the hydrogen bond and the nuclear potential surface. Recent theoretical work has hinted that nuclear quantum effects contribute meaningfully to the strength of the hydrogen bond itself due to modifications of bending and stretching potentials [67, 75].

IR SPECTROSCOPY

Infrared spectroscopy is perhaps the most informative technique for studying hydrogen bonds. Infrared spectra contain a wealth of information including both the dynamic electronic and nuclear components of bonding interactions, and it provides direct access to molecular motion. Modern spectroscopy in the IR region has been made simple and inexpensive by the proliferation of Fourier transform spectrometers (FTIR), and it has become one of the most commonly used methods of learning about condensed phase chemistry. IR spectroscopy has proven especially enlightening for hydrogen bonded systems, and by examining inter and intramolecular vibrations it is possible to obtain both geometrical and dynamical information on the nature of the bond.

THE STRETCH

Hydrogen stretching vibrations are particularly useful reporters on the local hydrogen bonding environment for a number of reasons. The stretch is classically the first motion in a full proton transfer, but exciting the hydrogen bonded stretch $\nu_s(XH\cdots)$ to the first excited state with laboratory-scale electric fields has been shown in general to not break the hydrogen bond [76]. IR spectroscopy of the stretch is in a sense supersensitive to hydrogen bonding because formation of the bond actually increases the absorption, as the changes in dipole due to polarization upon bond formation tend to increase the absorption intensities, so hydrogen bonded compounds are oftentimes easier to detect than unbound molecules.

Upon the formation of a hydrogen bonding interaction, most vibrational stretch bands red shift to lower frequencies as the X-H bond weakens, and the amount of red shift observed in the X-H stretch tends to correlate well with the strength of the hydrogen bonding interaction. Compared to the gas phase value, very strong hydrogen bonds can weaken the bond force constant enough to red shift the stretch well over 1000 cm^{-1}, while water, shifts a more moderate 300 cm^{-1} in the liquid phase [77-82]. In addition, the bond energy of H bond is also related to the stretching vibration intensity and the stretching frequency often correlates to the bond distance [83, 84]. Shared or transferring protons can demonstrate very dramatic changes in stretching frequency, and the shared proton in a water-hydroxide dimer exhibits strong IR absorption band as far down as 697 cm^{-1} in Ar, with a significantly enhanced transition moment (~1000x larger than a free OH stretch) [85]. Spectroscopic signatures of the shared proton in hydrogen bonded species of the form $[A\cdot H^+\cdot B]$ have been identified in the gas phase, but clear IR signatures of this intermolecular proton in the condensed phase are still difficult to classify [13].

IR spectroscopy does not directly measure geometric parameters, but spectroscopic observables are oftentimes closely related to the molecular geometry. Fecko et al. have shown that in simulations of liquid water, the stretching frequency can be nearly perfectly correlated to the projection of the sum total electric field along the OH bond at the proton position [86]. In addition, the energy of the proton stretch generally linearly increases as a function of equilibrium O···O distance R_{OO}. This goes in accordance with a trend often cited as "Badger's rule," first published in 1934, which relates the bond strength to the internuclear distance, thus connecting bond distance to vibrational frequency [87-89]. A similar study by Novak in 1974 on the IR spectra of hydrogen bonding in solids inspired many experiments to quantify R_{OO} distance fluctuations using the vibrational stretching frequency as a reporter [90]. This trend can be seen for over 135 different compounds containing OH···O hydrogen bonds in Figure 4:

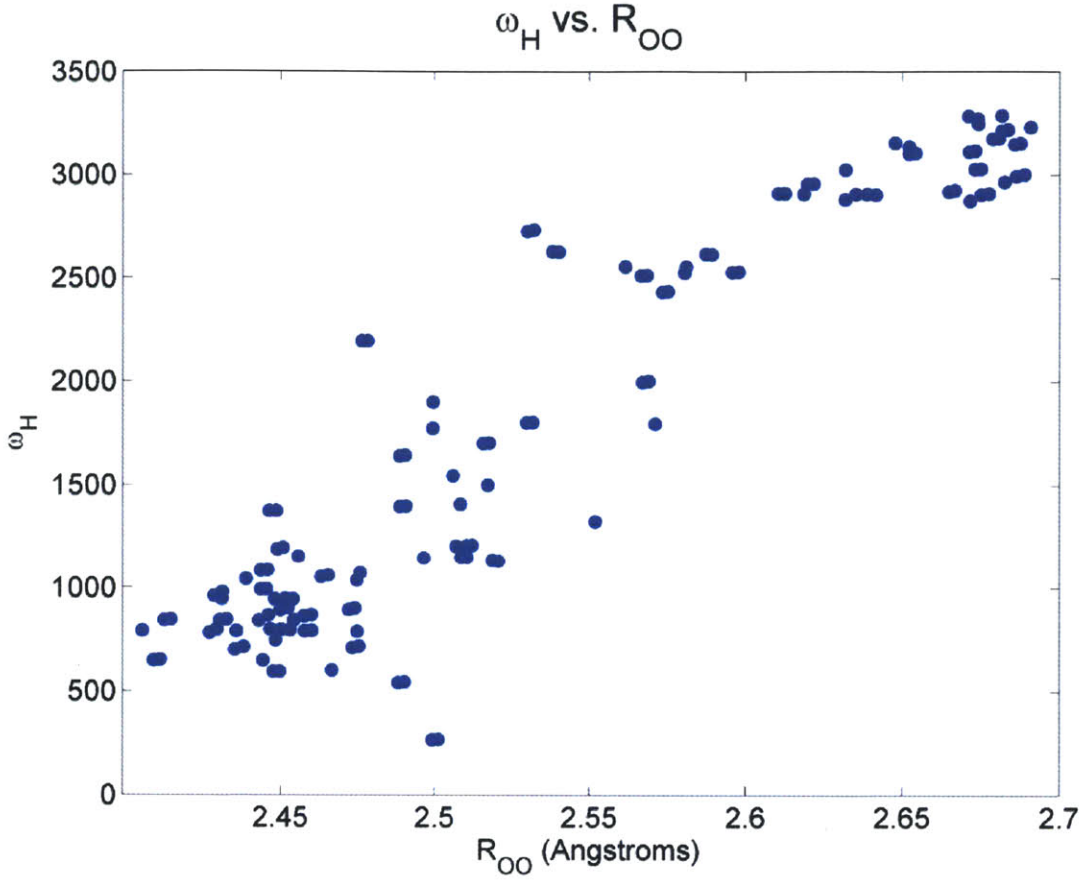

Figure 4: Stretching frequency vs. equilibrium internuclear distance. Data taken from Sokolov 1990 [81].

Because the substitution of hydrogen with deuterium changes the energy level structure within the vibrational potential, changes in the vibrational frequencies upon isotopic substitution can provide insight into the nature of the potential and thus the bonding environment. One can define the isotopic stretching frequency ratio of hydrogen to deuterium as [81]:

$$\gamma = \frac{\omega_{O-H}}{\omega_{O-D}} \tag{1.6}$$

The isotopic stretching frequency ratio is shown below as a function of R_{OO} for well over 100 different small molecule compounds containing a proton or deuteron shared between two oxygens.

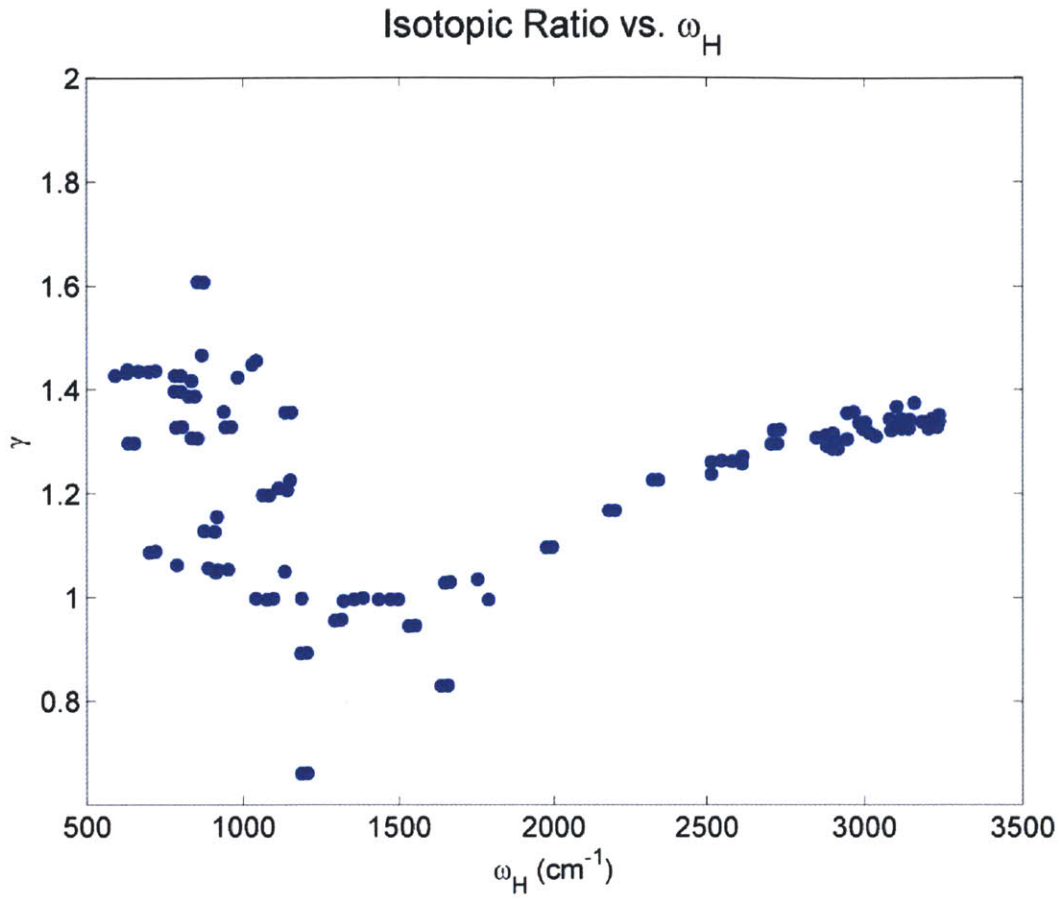

Figure 5: Isotopic stretching frequency ratio in O-H-O bonds as a function of hydrogen stretch. Data taken from Sokolov 1990 [81].

Although indirect, this change in stretching ratio is related to the shape of the proton potential which dictates the vibrational energy level structure, and if nothing else, the change in stretching frequency upon deuteration can also serve to shift specific protons of interest into a useful spectroscopic window. Some work has been made in connecting the shape of the proton potential to the IR spectrum in hydrogen bonded species for a more general case [91-94].

Strongly Hydrogen Bonded Systems

As a simple conceptual model of a strongly hydrogen bonded system, we can think of the normal mode vibrations of a dimer. Consider a complex involving two individual molecules, A and B, containing N_A and N_B atoms, respectively. Each molecule has $3(N_A)$-6 and $3(N_B)$-6 internal degrees of freedom and thus the same number of modes of motion. The AB dimer system, however, has $3(N_A+N_B)$-6 internal degrees

of freedom, and as a consequence six additional modes are obtained, stemming from possible intermolecular vibrations (for example, the A-B stretch or relative twisting).

A simple model for both inter- and intra- molecular vibrations is that of rigid bodies connected by classical springs. Houjou demonstrates this with a model consisting of the geometry $A_I - A_{II} \leftrightsquigarrow B_{II} - B_I$ with spring constants K_{inter} and K_{intra} [95]. For a total mass of molecule A of $m = m_{A_I} + m_{A_{II}}$ the lowest frequency eigenvalue of the system is

$$\omega^2 = \frac{2}{m}(K_{intra} + K_{inter} - \sqrt{K_{intra}^2 + K_{inter}^2})$$

where of course $\omega/2\pi = \nu$.

For simple harmonic motion, this frequency ν is related to the classical Hooke's law restoring force k and the reduced mass of the oscillator μ by $\nu = \frac{1}{2\pi}\sqrt{\frac{k}{\mu}}$ and since $\omega = 2\pi\nu$, $\omega = \sqrt{\frac{k}{\mu}}$. The quantum mechanical harmonic oscillator has energy $E_n = h\nu = h(n+\frac{1}{2})\frac{1}{2\pi}\sqrt{\frac{k}{m}}$ for a given vibrational quantum number n. The new vibrational modes which arise due to the dimerization lie low in energy - considering a sufficiently rigid small molecule dimer generally between 10-300 cm^{-1}. In contrast to the lower energy intermolecular motions, intramolecular stretching modes typically are observed between 400-4000 cm^{-1}, as stronger, covalent bonding interactions give a higher classical "spring constant."

If we suppose there is a low frequency intermolecular stretching mode (here subscript S) which changes the X···Y distance, the vibrational Hamiltonian becomes (following from (1.3)):

$$H(r, R_S) = \frac{p^2}{2m} + \frac{R_S}{2M_S} + \frac{1}{2}m\omega^2(R_S)(r - r_0)^2 + \frac{1}{2}M_S\Omega_S{}^2(R_S - R_0)^2 \qquad (1.7)$$

For a single intermolecular stretching motion changing the hydrogen bond distance, it is reasonable to truncate (1.5) at just the linear term, giving $\omega(R_s) = \omega R_s$. We can then consider the timescales of these two motions. The shorter, stronger XH bond will be fast and high frequency, while the intermolecular X···Y motion will be substantially slower. If we separate this fast X-H stretching motion (generally near 3000 cm^{-1} which is a vibrational frequency of 11.12fs) from the slower stretching motion (say, approximately 200 cm^{-1}, corresponding to a vibrational period of approximately 170fs) such that the fast stretch only

depends on the present value of R_s and not its dynamics (analogous to the Born-Oppenheimer approximation):

$$\phi_n^N(r,R_s) = \chi_n(r,R_S)\alpha_n^N(R_S) \tag{1.8}$$

Where $\chi_n(r,R_S)$ is the wavefunction for the fast XH stretch and the $\alpha_n^N(R_S)$ is the wavefunction of the slow mode when the fast stretch is excited to the n^{th} state. Again assuming $\omega(R_s)= \omega R_s$ we can solve for the energies allowed here [21, 82, 96]:

$$E_n^N = \left(n+\frac{1}{2}\right)\hbar\omega(R_0)+\left(N+\frac{1}{2}\right)\hbar\Omega_s - \left(n+\frac{1}{2}\right)^2 \frac{\hbar^2}{2M_s\Omega_S^2}\left(\frac{d\omega}{dR_S}\right)^2 \tag{1.9}$$

Given the observed trends of stretching frequency the term $\frac{d\omega}{dR}$ is positive, and this variation is mostly linear (see Figure 4). For even a linear dependence on R, additional transitions corresponding to excitations of the intermonomer mode become possible, and the stretch gains structure similar to the Franck-Condon progression observed in electronic spectroscopy which has been observed in many gas phase hydrogen bonded systems [93, 97, 98] In a liquid phase where these intermonomer vibrations can span a wide range of values the primary stretching lineshape can simply broaden out to a smooth distribution reflecting the many intermonomer distances accessible.

It is also worth noticing that at room temperature the Boltzmann population of a fast 3000 cm^{-1} stretch is $e^{\frac{-\hbar\omega}{k_BT}} \sim 10^{-7}$ while a slow low frequency motion at 200 cm^{-1} has the nontrivial thermal population of ~0.4 at 300K. As a result these low frequency modes modulating the internuclear distance are appreciably populated and there is constant fluctuation in these distances. This same sort of approach can be applied to more complex potentials as well, and has proven exceptionally useful for the Morse potential [99].

WATER

Water is the most ubiquitous and most intensely studied of hydrogen bonding molecules, and the one with which most people interact in their everyday lives. Water seems initially rather simple and uninteresting, as the water molecule contains only three small atoms and has no notable visible absorption. Because our daily lives revolve around floating ice cubes, easily poured liquid water, a high water boiling point, and beverages which maintain their temperatures for a relatively long time, we do not generally think that these properties are particularly peculiar, but for such a small molecule, water is a very unique liquid.

The interesting properties of the water molecule appear primarily to us in the condensed phase, which consists of a hyperdense hydrogen-bound network of molecules, with each molecule able to participate in four hydrogen bonds. At room temperature, a majority of the possible bonds are indeed present, and liquid water contains ~90% of the hydrogen bonds found in the familiar form of solid ice. As a result, the extended tetrahedral structure present in solid water is also a major feature in the liquid [24, 100]. Even with these structural similarities between the condensed phases of water, the charge distribution in the liquid phase of water is quite different, with a liquid phase dipole moment of 2.6-3.0 D, compared to the gas phase value of 1.85 D [100-102]. The compact nature of the liquid phase and the strong interaction between hydrogen bonding partners dictates much of the reactivity, and the fluctuating bonding network can significantly change what chemical processes take place, including proton transfer, charge separation, and even vibrational relaxation [103]. For example, the anomalously large diffusion of protons in water has been known for years, and at room temperature the diffusion constant of a proton in bulk water is ~9.3 x 10^{-5} cm^2/sec, over 4 times faster than any other cation in water [37, 104, 105].

Despite the reasonably well characterized average structure of water, these hydrogen bonds are extremely fluxional, and both collective and local motions can lead to bond breaking and forming. Pure water forms an extended and dense hydrogen bonding network, yet the relatively weak nature of these bonds allows them to rapidly break and form, creating temporary defects in the extending bonding structure and leading to unique dynamical properties as well. One cannot truly understand water without understanding these dynamics, which span timescales ranging from tens of femtoseconds to tens of picoseconds. Hindered rotations of water molecules occur on the 50fs timescale, bond stretches take place between 150-200fs, and bending motions occur on the longer 500fs timescale. Larger scale collective motions involving multiple water molecules such as translation or solvation can take many picoseconds. The wide range of possible bonding configurations which are sampled rapidly over very fast timescales lead to dynamic vibrational frequency fluctuations (spectral diffusion), which gives rise to broad absorptions in the infrared [22, 24, 77, 86, 106-113].

COOH DIMERS

Another interesting and historically important system for spectroscopy of strong hydrogen bonds is one containing to carboxylic acid moieties each donating and accepting one hydrogen bond as illustrated here:

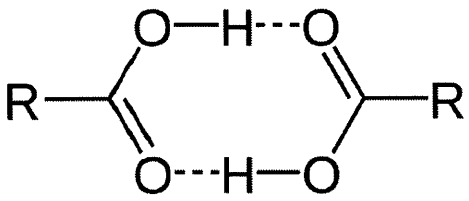

Figure 6: Carboxylic acid dimer structure

This cyclic hydrogen bonding interface allows for tautomerization by proton transfer, protonating each carbonyl C=O bond and simultaneously transferring electrons in such a way as to create no new charge separation [114]. In these systems, the OH stretch band is exceptionally broad with many structural features due to coupling to low frequency bending and stretching interdimer modes and with two carbonyl stretches as well. The simplest of these possible dimers are those containing two formic acid or acetic acid molecules, and these dimers are known to dominate much of the condensed phase structure [76, 115-121]. In these acetic acid dimers, the C=O and OH stretches show complicated band sub-structure due to anharmonic effects and coupling to intermolecular stretches and bends. Other dimers with similar cyclic interfaces have been studied, including 7-azaindole, a model for the hydrogen bonding interaction in DNA base pairs and a compound capable of rapid phototautomerization (the mechanism of which – stepwise or concerted – is still rather hotly contested) [122-125].

In order to understand and examine these unique molecular interactions, the next chapter will work to calculate spectroscopic observables for such systems and map these to potential reaction coordinates, working to answer questions regarding how transition frequencies and dipoles vary over the course of a proton transfer. From this static understanding of molecular quantities and a mapping of these in relation to one another, we will then be in place to develop dynamical models to calculate multidimensional spectroscopic experimental observables.

1. Gilli, G. and P. Gilli, *The nature of the hydrogen bond: outline of a comprehensive hydrogen bond theory*. 2009, Oxford ; New York: Oxford University Press. xi, 317 p.
2. Pimentel, G.C. and A.L. McClellan, *The Hydrogen Bond*. 1960, San Francisco,: W.H. Freeman; trade distributor: Reinhold Pub. Corp., New York. 475 p.
3. Lassettre, E.N., *The Hydrogen Bond and Association*. Chemical Reviews, 1937. **20**(2): p. 259-303.
4. Rodebush, W.H., *The Hydrogen Bond and Coordination*. Chemical Reviews, 1936. **19**(1): p. 59-65.
5. Latimer, W.M. and W.H. Rodebush, *Polarity and ionization from the standpoint of the lewis theory of valence*. Journal of the American Chemical Society, 1920. **42**(7): p. 1419-1433.
6. Pauling, L., *The nature of the chemical bond and the structure of molecules and crystals; an introduction to modern structural chemistry*. 3d ed. 1960, Ithaca, N.Y.,: Cornell University Press. 644 p.
7. Desiraju, G.R., *A Bond by Any Other Name*. Angewandte Chemie International Edition, 2011. **50**(1): p. 52-59.
8. Scheiner, S., *Hydrogen bonding : a theoretical perspective*. Topics in physical chemistry. 1997, New York: Oxford University Press. xix, 375 p.
9. Arunan, E., et al., *Defining the hydrogen bond: An account (IUPAC Technical Report)*. Pure and Applied Chemistry, 2011. **83**(8): p. 1619-1636.
10. Hadzi, D., *Theoretical treatments of hydrogen bonding*. 1997, Chichester, England ; New York: John Wiley. xiii, 318 p.
11. Gilli, P., et al., *Evidence for resonance-assisted hydrogen bonding. 4. Covalent nature of the strong homonuclear hydrogen bond. Study of the O-H--O system by crystal structure correlation methods*. Journal of the American Chemical Society, 1994. **116**(3): p. 909-915.
12. Sobczyk, L., S.J. Grabowski, and T.M. Krygowski, *Interrelation between H-Bond and Pi-Electron Delocalization*. Chemical Reviews, 2005. **105**(10): p. 3513-3560.
13. Roscioli, J.R., L.R. McCunn, and M.A. Johnson, *Quantum Structure of the Intermolecular Proton Bond*. Science, 2007. **316**(5822): p. 249-254.
14. Huggins, M.L., *50 Years of Hydrogen Bond Theory*. Angewandte Chemie International Edition in English, 1971. **10**(3): p. 147-152.
15. Weinhold, F., *Resonance Character of Hydrogen-bonding Interactions in Water and Other H-bonded Species*, in *Advances in Protein Chemistry*, L.B. Robert and B. David, Editors. 2005, Academic Press. p. 121-155.
16. Janoschek, R., et al., *Extremely high polarizability of hydrogen bonds*. Journal of the American Chemical Society, 1972. **94**(7): p. 2387-2396.
17. Goswami, M. and E. Arunan, *The hydrogen bond: a molecular beam microwave spectroscopist's view with a universal appeal*. Physical Chemistry Chemical Physics, 2009. **11**(40).
18. Steiner, T., *The hydrogen bond in the solid state*. Angewandte Chemie-International Edition, 2002. **41**(1): p. 48-76.
19. Desiraju, G.R. and T. Steiner, *The weak hydrogen bond in structural chemistry and biology*. 1999, Oxford ; New York: Oxford University Press. xiv, 507 p.
20. Millot, C. and A.J. Stone, *Towards an accurate intermolecular potential for water*. Molecular Physics, 1992. **77**(3): p. 439-462.
21. Maréchal, Y., *The hydrogen bond and the water molecule : the physics and chemistry of water, aqueous and bio media*. 1st ed. 2007, Amsterdam ; Boston: Elsevier. xiii, 318 p.
22. Kumar, R., J.R. Schmidt, and J.L. Skinner, *Hydrogen bonding definitions and dynamics in liquid water*. The Journal of Chemical Physics, 2007. **126**(20): p. 204107-12.
23. Matsumoto, M., *Relevance of hydrogen bond definitions in liquid water*. The Journal of Chemical Physics, 2007. **126**(5): p. 054503-6.
24. Eisenberg, D.S. and W. Kauzmann, *The structure and properties of water*. 1969, New York,: Oxford University Press. xii, 296 p.

25. Marcus, R.A., *Chemical and Electrochemical Electron-Transfer Theory.* Annual Review of Physical Chemistry, 1964. **15**(1): p. 155-196.
26. Marcus, R.A., *On the Theory of Oxidation-Reduction Reactions Involving Electron Transfer. I.* The Journal of Chemical Physics, 1956. **24**(5): p. 966-978.
27. Marcus, R.A. and N. Sutin, *Electron transfers in chemistry and biology.* Biochimica et Biophysica Acta (BBA) - Reviews on Bioenergetics, 1985. **811**(3): p. 265-322.
28. Nocera, D.G. and H.B. Gray, *Electron-transfer chemistry of the luminescent excited state of octachlorodirhenate(III).* Journal of the American Chemical Society, 1981. **103**(24): p. 7349-7350.
29. McCleskey, T.M., J.R. Winkler, and H.B. Gray, *Driving-force effects on the rates of bimolecular electron-transfer reactions.* Journal of the American Chemical Society, 1992. **114**(17): p. 6935-6937.
30. Mohammed, Omar F., et al., *Direct Femtosecond Observation of Tight and Loose Ion Pairs upon Photoinduced Bimolecular Electron Transfer.* Angewandte Chemie International Edition, 2008. **47**(47): p. 9044-9048.
31. Nitzan, A., *Chemical dynamics in condensed phases : relaxation, transfer and reactions in condensed molecular systems.* Oxford graduate texts. 2006, Oxford ; New York: Oxford University Press. xxii, 719 p.
32. Hynes, J.T., T.-H. Tran-Thi, and G. Granucci, *Intermolecular photochemical proton transfer in solution: new insights and perspectives.* Journal of Photochemistry and Photobiology A: Chemistry, 2002. **154**(1): p. 3-11.
33. Hynes, J.T., *Hydrogen-transfer reactions*. 2007, Weinheim: Wiley-VCH. 4 v. (xliv, 1559).
34. Golan, A., et al., *Ionization of dimethyluracil dimers leads to facile proton transfer in the absence of hydrogen bonds.* Nat Chem, 2012. **4**(4): p. 323-329.
35. Cukierman, S., *Et tu, Grotthuss! and other unfinished stories.* Biochimica et Biophysica Acta (BBA) - Bioenergetics, 2006. **1757**(8): p. 876.
36. de Grotthuss, C., *Sur la décomposition de l'eau et des corps qu'elle tient en dissolution à l'aide de l'électricité galvanique.* Ann. Chim, 1806. **58**: p. 54-74.
37. Agmon, N., *The Grotthuss mechanism.* Chemical Physics Letters, 1995. **244**(5-6): p. 456-462.
38. Danneel, H., *Notiz über ionengeschwindigkeiten.* Z. Elektrochem, 1905. **11**: p. 249-252.
39. Marx, D., et al., *The nature of the hydrated excess proton in water.* Nature, 1999. **397**(6720): p. 601-604.
40. Nagle, J.F. and H.J. Morowitz, *Molecular mechanisms for proton transport in membranes.* Proceedings of the National Academy of Sciences of the United States of America, 1978. **75**(1): p. 298-302.
41. Pomes, R. and B. Roux, *Theoretical Study of H+ Translocation along a Model Proton Wire.* The Journal of Physical Chemistry, 1996. **100**(7): p. 2519-2527.
42. Garczarek, F. and K. Gerwert, *Functional waters in intraprotein proton transfer monitored by FTIR difference spectroscopy.* Nature, 2006. **439**(7072): p. 109-112.
43. Mathias, G. and D. Marx, *Structures and spectral signatures of protonated water networks in bacteriorhodopsin.* Proceedings of the National Academy of Sciences, 2007. **104**(17): p. 6980-6985.
44. Phatak, P., et al., *Amino acids with an intermolecular proton bond as proton storage site in bacteriorhodopsin.* Proceedings of the National Academy of Sciences, 2008. **105**(50): p. 19672-19677.
45. Hassanali, A., et al., *On the recombination of hydronium and hydroxide ions in water.* Proceedings of the National Academy of Sciences, 2011. **108**(51): p. 20410-20415.
46. Chandler, D., C. Dellago, and P. Geissler, *Ion dynamics: Wired-up water.* Nat Chem, 2012. **4**(4): p. 245-247.
47. Huggins, M.L., *The Role of Hydrogen Bonds in Conduction by Hydrogen and Hydroxyl Ions.* Journal of the American Chemical Society, 1931. **53**(8): p. 3190-3191.

48. Huggins, M.L., *Hydrogen Bridges in Ice and Liquid Water.* The Journal of Physical Chemistry, 1935. **40**(6): p. 723-731.
49. Lippincott, E.R. and R. Schroeder, *One-Dimensional Model of the Hydrogen Bond.* The Journal of Chemical Physics, 1955. **23**(6): p. 1099-1106.
50. Geissler, P.L., et al., *Autoionization in Liquid Water.* Science, 2001. **291**(5511): p. 2121-2124.
51. Markovitch, O., et al., *Special Pair Dance and Partner Selection: Elementary Steps in Proton Transport in Liquid Water.* The Journal of Physical Chemistry B, 2008. **112**(31): p. 9456-9466.
52. Schuster, P., G. Zundel, and C. Sandorfy, *The Hydrogen bond: recent developments in theory and experiments*. 1976, Amsterdam: North-Holland.
53. Somorjai, R.L. and D.F. Hornig, *Double-Minimum Potentials in Hydrogen-Bonded Solids.* The Journal of Chemical Physics, 1962. **36**(8): p. 1980-1987.
54. Verguilla-Berdecia, L.A., *Tunneling in a quartic, symmetric, double well potential: A simple solution using a hermite basis.* Journal of Chemical Education, 1993. **70**(11): p. 928.
55. Ka, B.J. and W.H. Thompson, *Sampling the Proton Transfer Reaction Coordinate in Mixed Quantum-Classical Molecular Dynamics Simulations.* The Journal of Physical Chemistry A, 2011. **116**(2): p. 832-838.
56. Borgis, D. and J.T. Hynes, *Dynamical theory of proton tunneling transfer rates in solution: general formulation.* Chemical Physics, 1993. **170**(3): p. 315.
57. Cohen, B. and D. Huppert, *Evidence for a Continuous Transition from Nonadiabatic to Adiabatic Proton Transfer Dynamics in Protic Liquids.* The Journal of Physical Chemistry A, 2001. **105**(13): p. 2980-2988.
58. Scheiner, S., *AB Initio Studies of Hydrogen Bonds: The Water Dimer Paradigm.* Annual Review of Physical Chemistry, 1994. **45**(1): p. 23-56.
59. Totsuji, C. and T. Matsubara, *A simple model for 0-dimensional hydrogen-bonding ferroelectrics and antiferroelectrics.* Solid State Communications, 1994. **89**(8): p. 677-681.
60. Hiroto, T., *Dynamics of the vibrational mode-specific proton transfer reaction NH3+(v1) + NH3 → NH2 + NH4+: ab initio MO and classical trajectory studies.* Chemical Physics, 1996. **211**(1–3): p. 305-312.
61. Kearley, G.J., et al., *A New Look at Proton Transfer Dynamics Along the Hydrogen Bonds in Amides and Peptides.* Science, 1994. **264**(5163): p. 1285-1289.
62. Huneycutt, A.J. and R.J. Saykally, *Building Solutions--One Molecule at a Time.* Science, 2003. **299**(5611): p. 1329-1330.
63. Borgis, D. and J.T. Hynes, *Molecular-dynamics simulation for a model nonadiabatic proton transfer reaction in solution.* The Journal of Chemical Physics, 1991. **94**(5): p. 3619-3628.
64. Bell, R.P., *The Application of Quantum Mechanics to Chemical Kinetics.* Proceedings of the Royal Society of London. Series A, 1933. **139**(838): p. 466-474.
65. Bernal, J.D. and R.H. Fowler, *A Theory of Water and Ionic Solution, with Particular Reference to Hydrogen and Hydroxyl Ions.* The Journal of Chemical Physics, 1933. **1**(8): p. 515-548.
66. Komatsuzaki, T. and I. Ohmine, *Energetics of proton transfer in liquid water. I. Ab initio study for origin of many-body interaction and potential energy surfaces.* Chemical Physics, 1994. **180**(2–3): p. 239-269.
67. Tuckerman, M.E., et al., *On the Quantum Nature of the Shared Proton in Hydrogen Bonds.* Science, 1997. **275**(5301): p. 817-820.
68. Hynes, J.T., *Physical chemistry: The protean proton in water.* Nature, 1999. **397**(6720): p. 565-567.
69. Marx, D., *Proton Transfer 200 Years after von Grotthuss: Insights from Ab Initio Simulations.* ChemPhysChem, 2006. **7**(9): p. 1848-1870.
70. Roberts, S.T.S.T., *Hydrogen bond rearrangements and the motion of charge defects in water viewed using multidimensional ultrafast infrared spectroscopy*, in *Department of Chemistry.* 2010, Massachusetts Institute of Technology. : Cambridge, MA.

71. Schenter, G.K., B.C. Garrett, and D.G. Truhlar, *The Role of Collective Solvent Coordinates and Nonequilibrium Solvation in Charge-Transfer Reactions.* The Journal of Physical Chemistry B, 2001. **105**(40): p. 9672-9685.
72. Perrin, C.L., *Symmetries of Hydrogen Bonds in Solution.* Science, 1994. **266**(5191): p. 1665-1668.
73. Harris, T.K. and A.S. Mildvan, *High-Precision Measurement of Hydrogen Bond Lengths in Proteins by Nuclear Magnetic Resonance Methods.* Proteins: Structure, Function, and Bioinformatics, 1999. **35**(3): p. 275-282.
74. Kreevoy, M.M. and T.M. Liang, *Structures and isotopic fractionation factors of complexes, A1HA2.* Journal of the American Chemical Society, 1980. **102**(10): p. 3315-3322.
75. Li, X.-Z., B. Walker, and A. Michaelides, *Quantum nature of the hydrogen bond.* Proceedings of the National Academy of Sciences, 2011. **108**(16): p. 6369-6373.
76. Heyne, K., et al., *Coherent low-frequency motions of hydrogen bonded acetic acid dimers in the liquid phase.* The Journal of Chemical Physics, 2004. **121**(2): p. 902-913.
77. Auer, B., et al., *Hydrogen bonding and Raman, IR, and 2D-IR spectroscopy of dilute HOD in liquid D2O.* Proceedings of the National Academy of Sciences, 2007. **104**(36): p. 14215-14220.
78. Feyereisen, M.W., D. Feller, and D.A. Dixon, *Hydrogen Bond Energy of the Water Dimer.* The Journal of Physical Chemistry, 1996. **100**(8): p. 2993-2997.
79. Guissani, Y. and H. Ratajczak, *Theoritical study on an anomalous isotopic effect on the position and integrated intensity of the ir stretching vibration band for medium-strong and strong hydrogen bonds.* Chemical Physics, 1981. **62**(3): p. 319-331.
80. Henri-Rousseau, O. and P. Blaise, *The Infrared Spectral Density of Weak Hydrogen Bonds within the Linear Response Theory*, in *Advances in Chemical Physics*. 2007, John Wiley & Sons, Inc. p. 1-186.
81. Sokolov, N.D., M.V. Vener, and V.A. Savel'ev, *Tentative study of strong hydrogen bond dynamics: Part II. Vibrational frequency considerations.* Journal of Molecular Structure, 1990. **222**(3–4): p. 365-386.
82. Witkowski, A. and M. Wójcik, *Infrared spectra of hydrogen bond a general theoretical model.* Chemical Physics, 1973. **1**(1): p. 9-16.
83. Iogansen, A.V., *Direct proportionality of the hydrogen bonding energy and the intensification of the stretching v(XH) vibration in infrared spectra.* Spectrochimica Acta Part A: Molecular and Biomolecular Spectroscopy, 1999. **55**(7–8): p. 1585-1612.
84. Pimentel, G.C. and C.H. Sederholm, *Correlation of Infrared Stretching Frequencies and Hydrogen Bond Distances in Crystals.* The Journal of Chemical Physics, 1956. **24**(4): p. 639-641.
85. Diken, E.G., et al., *Fundamental Excitations of the Shared Proton in the H3O2- and H5O2+ Complexes.* The Journal of Physical Chemistry A, 2005. **109**(8): p. 1487-1490.
86. Fecko, C.J., et al., *Ultrafast Hydrogen-Bond Dynamics in the Infrared Spectroscopy of Water.* Science, 2003. **301**(5640): p. 1698-1702.
87. Badger, R.M., *A Relation Between Internuclear Distances and Bond Force Constants.* The Journal of Chemical Physics, 1934. **2**(3): p. 128-131.
88. Jerzy, G. Liu, and R.A. Mosquera Castro, *Badger's rule revisited.* Chemical Physics Letters, 2000. **331**(5–6): p. 497-501.
89. Badger, R.M., *The Relation Between the Internuclear Distances and Force Constants of Molecules and Its Application to Polyatomic Molecules.* The Journal of Chemical Physics, 1935. **3**(11): p. 710-714.
90. Novak, A., *Hydrogen bonding in solids correlation of spectroscopic and crystallographic data* *Large Molecules*. 1974, Springer Berlin / Heidelberg. p. 177-216.
91. Wood, J.L., *The proton potential in complex hydrogen bonded cations.* Journal of Molecular Structure, 1973. **17**(2): p. 307-328.
92. Gorbaty, Y.E. and A.G. Kalinichev, *Hydrogen Bonding in Supercritical Water. 1. Experimental Results.* The Journal of Physical Chemistry, 1995. **99**(15): p. 5336-5340.

93. Legon, A.C. and D.J. Millen, *Gas-phase spectroscopy and the properties of hydrogen-bonded dimers. HCN.cntdot..cntdot..cntdot.HF as the spectroscopic prototype.* Chemical Reviews, 1986. **86**(3): p. 635-657.
94. Legon, A.C. and D.J. Millen, *Directional character, strength, and nature of the hydrogen bond in gas-phase dimers.* Accounts of Chemical Research, 1987. **20**(1): p. 39-46.
95. Houjou, H., *Evaluation of coupling terms between intra- and intermolecular vibrations in coarse-grained normal-mode analysis: Does a stronger acid make a stiffer hydrogen bond?* The Journal of Chemical Physics, 2011. **135**(15): p. 154111-9.
96. Marechal, Y. and A. Witkowski, *Infrared Spectra of H-Bonded Systems.* The Journal of Chemical Physics, 1968. **48**(8): p. 3697-3705.
97. Bertie, J.E. and D.J. Millen, *79. Hydrogen bonding in gaseous mixtures. Part I. Infrared spectra of ether-hydrogen chloride systems.* Journal of the Chemical Society (Resumed), 1965: p. 497-503.
98. Millen, D.J., *Vibrational spectra and vibrational states of simple gas-phase hydrogen-bonded dimers.* Journal of Molecular Structure, 1983. **100**(0): p. 351-377.
99. Belhayara, K., D. Chamma, and O. Henri-Rousseau, *Infrared spectra of weak H-bonds: Fermi resonances and intrinsic anharmonicity of the H-bond bridge.* Journal of Molecular Structure, 2003. **648**(1–2): p. 93-106.
100. Head-Gordon, T. and G. Hura, *Water Structure from Scattering Experiments and Simulation.* Chemical Reviews, 2002. **102**(8): p. 2651-2670.
101. Clough, S.A., et al., *Dipole moment of water from Stark measurements of H[sub 2]O, HDO, and D[sub 2]O.* The Journal of Chemical Physics, 1973. **59**(5): p. 2254-2259.
102. Silvestrelli, P.L. and M. Parrinello, *Structural, electronic, and bonding properties of liquid water from first principles.* The Journal of Chemical Physics, 1999. **111**(8): p. 3572-3580.
103. Yarwood, J., R. Ackroyd, and G.N. Robertson, *Vibrational relaxation of hydrogen-bonded species in solution: analysis of the vσ(OHiN) vibration of phenol-pyridine.* Chemical Physics Letters, 1981. **78**(3): p. 614-617.
104. Robinson, G.W., *Proton charge transfer involving the water solvent.* The Journal of Physical Chemistry, 1991. **95**(25): p. 10386-10391.
105. Robinson, R. and R. Stokes, *Electrolyte solutions*. 2002: Dover Pubns.
106. Corcelli, S.A. and J.L. Skinner, *Infrared and Raman Line Shapes of Dilute HOD in Liquid H2O and D2O from 10 to 90 °C.* The Journal of Physical Chemistry A, 2005. **109**(28): p. 6154-6165.
107. Cho, M., et al., *Instantaneous normal mode analysis of liquid water.* The Journal of Chemical Physics, 1994. **100**(9): p. 6672-6683.
108. Eaves, J.D., et al., *Hydrogen bonds in liquid water are broken only fleetingly.* Proceedings of the National Academy of Sciences of the United States of America, 2005. **102**(37): p. 13019-13022.
109. Fecko, C.J., et al., *Local hydrogen bonding dynamics and collective reorganization in water: Ultrafast infrared spectroscopy of HOD/D[sub 2]O.* The Journal of Chemical Physics, 2005. **122**(5): p. 054506-18.
110. Gale, G.M., et al., *Femtosecond Dynamics of Hydrogen Bonds in Liquid Water: A Real Time Study.* Physical Review Letters, 1999. **82**(5): p. 1068-1071.
111. Lawrence, C.P. and J.L. Skinner, *Vibrational spectroscopy of HOD in liquid D[sub 2]O. I. Vibrational energy relaxation.* The Journal of Chemical Physics, 2002. **117**(12): p. 5827-5838.
112. Lawrence, C.P. and J.L. Skinner, *Vibrational spectroscopy of HOD in liquid D[sub 2]O. II. Infrared line shapes and vibrational Stokes shift.* The Journal of Chemical Physics, 2002. **117**(19): p. 8847-8854.
113. Roberts, S.T., K. Ramasesha, and A. Tokmakoff, *Structural Rearrangements in Water Viewed Through Two-Dimensional Infrared Spectroscopy.* Accounts of Chemical Research, 2009. **42**(9): p. 1239-1249.
114. Bournay, J. and Y. Marechal, *Dynamics of Protons in Hydrogen-Bonded Systems: Propynoic and Acrylic Acid Dimers.* The Journal of Chemical Physics, 1971. **55**(3): p. 1230-1235.

115. Karsten, H., et al., *Coherent vibrational dynamics of intermolecular hydrogen bonds in acetic acid dimers studied by ultrafast mid-infrared spectroscopy.* Journal of Physics: Condensed Matter, 2003. **15**(1): p. S129.
116. Elsaesser, T., *Coherent Dynamics of Hydrogen Bonds in Liquids Studied by Femtosecond Vibrational Spectroscopy*, in *Coherent Vibrational Dynamics*. 2007, CRC Press. p. 49-91.
117. Dreyer, J., *Density functional theory simulations of two-dimensional infrared spectra for hydrogen-bonded acetic acid dimers.* International Journal of Quantum Chemistry, 2005. **104**(5): p. 782-793.
118. Heyne, K., et al., *Ultrafast coherent nuclear motions of hydrogen bonded carboxylic acid dimers.* Chemical Physics Letters, 2003. **369**(5–6): p. 591-596.
119. Heyne, K., et al., *Ultrafast relaxation and anharmonic coupling of O–H stretching and bending excitations in cyclic acetic acid dimers.* Chemical Physics Letters, 2003. **382**(1–2): p. 19-25.
120. Seifert, G., T. Patzlaff, and H. Graener, *Ultrafast vibrational dynamics of doubly hydrogen bonded acetic acid dimers in liquid solution.* Chemical Physics Letters, 2001. **333**(3–4): p. 248-254.
121. Florio, G.M., et al., *Theoretical modeling of the OH stretch infrared spectrum of carboxylic acid dimers based on first-principles anharmonic couplings.* The Journal of Chemical Physics, 2003. **118**(4): p. 1735-1746.
122. Petersen, P.B., et al., *Ultrafast N−H Vibrational Dynamics of Cyclic Doubly Hydrogen-Bonded Homo- and Heterodimers.* The Journal of Physical Chemistry B, 2008. **112**(42): p. 13167-13171.
123. Catalán, J., et al., *The concerted mechanism of photo-induced biprotonic transfer in 7-azaindole dimers: A model for the secondary evolution of the classic C2h dimer and comparison of four mechanisms.* Proceedings of the National Academy of Sciences of the United States of America, 2002. **99**(9): p. 5799-5803.
124. Sekiya, H. and K. Sakota, *Excited-state double-proton transfer in a model DNA base pair: Resolution for stepwise and concerted mechanism controversy in the 7-azaindole dimer revealed by frequency- and time-resolved spectroscopy.* Journal of Photochemistry and Photobiology C: Photochemistry Reviews, 2008. **9**(2): p. 81-91.
125. Kwon, O.-H. and A.H. Zewail, *Double proton transfer dynamics of model DNA base pairs in the condensed phase.* Proceedings of the National Academy of Sciences, 2007. **104**(21): p. 8703-8708.

Chapter 2 : MAPPING SPECTROSCOPIC VARIABLES: THE SYSTEM

In this chapter I discuss methodologies for evaluating and describing the relationships between static spectroscopic variables, such as the instantaneous vibrational frequency or the transition dipole moment. First I will review the concept of correlation functions as a means of describing the properties of a general classical or quantum observable. Then the discussion will turn to quantum mechanical observables useful for describing and modeling spectroscopy, first reviewing quantum mechanical formalisms often applied to spectroscopic systems along with the material response to applied electric fields. Finally this chapter will show methods for mapping static values for the vibrational frequency and transition dipoles utilizing a variety of models and methodologies, demonstrating the basic principles on simple hydrogen-bonded systems.

CORRELATION FUNCTIONS

For an observable A and its equilibrium ensemble average at thermal equilibrium, classically we calculate the expectation value

$$\langle A \rangle = \int dp \int dq A(p,q;t)\rho(p,q) \tag{2.1}$$

Where we use the partition function to obtain the canonical probability distribution

$$\rho = \frac{e^{-\beta H}}{Z} \tag{2.2}$$

Quantum mechanically this expectation value is

$$\langle A \rangle = \sum_n p_n \langle n | A | n \rangle \tag{2.3}$$

where

$$p_n = \frac{e^{-\beta E_n}}{Z} \tag{2.4}$$

Just as random single variables are described by moments of their distributions; stochastic processes are characterized by time correlation functions, a relationship which will be further developed in a later section. We can define the correlation function (covariance) as

$$C_{AB} = \langle AB \rangle - \langle A \rangle \langle B \rangle \tag{2.5}$$

$$C_{AB}(t,t') \equiv \langle A(t)B(t') \rangle \tag{2.6}$$

From this and equation (2.1) we can write the classical correlation function

$$C_{AB}(t,t') = \int dp \int dq A(p,q;t)B(p,q;t')\rho(p,q) \tag{2.7}$$

and the quantum correlation function from (2.6) and (2.3)

$$C_{AB}(t,t') = \sum_n p_n \langle n | A(t)B(t') | n \rangle \tag{2.8}$$

Classical correlation functions are real and even in time [1, 2]

$$\langle A(t)A(t') \rangle = \langle A(t')A(t) \rangle \tag{2.9}$$

$$C_{AA}(t) = C_{AA}(-t) \tag{2.10}$$

while quantum correlation functions are complex and have the property that [3]

$$C_{AA}^{*}(t) = C_{AA}(-t) = C_{AA}(t - i\beta\hbar) \tag{2.11}$$

The first equality following from the properties of the quantum time propagator U

$$\langle A(t)A(0) \rangle^{*} = \langle U^{\dagger}AUA(0) \rangle^{*} = \langle A(0)U^{\dagger}AU \rangle = \langle A(0)A(t) \rangle \tag{2.12}$$

$$\langle A(0)A(t) \rangle = \langle A(0)U^{\dagger}AU \rangle = \langle UAU^{\dagger}A(0) \rangle = \langle A(-t)A(0) \rangle \tag{2.13}$$

Because these quantum correlation functions are complex quantities, it is often useful to break them up into two real functions: the symmetric real and asymmetric imaginary components

$$C_{AA}(t) = C'_{AA}(t) + iC''_{AA}(t) \tag{2.14}$$

We will also be interested in the Fourier transform of time correlation functions given by

$$\tilde{C}_{AA}(\omega) = \int_{-\infty}^{\infty} dt e^{i\omega t} C_{AA}(t) \tag{2.15}$$

which according to the time symmetries results in a real valued quantity $\hat{C}_{AA}(\omega) \geq 0$. For the quantum time correlation function detailed balance also results in the condition [3]

$$\tilde{C}_{AA}(-\omega) = e^{-\beta\hbar\omega}\tilde{C}_{AA}(\omega) \tag{2.16}$$

Taking the real and imaginary parts defined in (2.14) and this detailed balance condition (2.16) we can obtain the result

$$\begin{aligned} \tilde{C}_{AA,S}(\omega) &= \int_{-\infty}^{\infty} dt e^{i\omega t} C'_{AA}(t) \\ \tilde{C}_{AA,A}(\omega) &= i\int_{-\infty}^{\infty} dt e^{i\omega t} C''_{AA}(t) \end{aligned} \tag{2.17}$$

$$\tilde{C}_{AA,A}(\omega) = \tilde{C}_{AA,S}(\omega)\tanh(\beta\hbar\omega/2) \tag{2.18}$$

where S and A stand for symmetric and asymmetric, respectively. Likewise in the time domain then we can obtain, by term by term inverse Fourier transform [4]

$$\sin\left(\frac{\beta\hbar}{2}\frac{\partial}{\partial t}\right)C'_{AA}(t) = -\cos\left(\frac{\beta\hbar}{2}\frac{\partial}{\partial t}\right)C''_{AA}(t) \tag{2.19}$$

where sin and cos of operators are defined by their series expansions. With this the full correlation function can be expressed in terms of just its imaginary part

$$C_{AA}(t) = \int_{-\infty}^{\infty} d\omega \cos(\omega t)\coth\left(\frac{\beta\hbar\omega}{2}\right)\tilde{C}''(\omega) - i\int_{-\infty}^{\infty} d\omega \sin(\omega t)\tilde{C}''(\omega) \tag{2.20}$$

or its real part via substitution of (2.18) into (2.20). This implies equivalence between the information contained in both parts of the correlation function in the time and frequency domain representations. Notice that these results do return the expected behavior in the classical limit where $\hbar \to 0$, as in this limit the imaginary part $C''_{AA}(t) \to 0$ from (2.19) and from (2.16) the classical correlation function in the frequency domain is even as $\tilde{C}_{AA}(-\omega) = \tilde{C}_{AA}(\omega)$.

A consequence of the properties in (2.10) and (2.11) is that we cannot directly equate quantum and classical correlation functions, which will become important in the application of the classical Langevin description to fully quantum systems. Oftentimes one is able to compute a classical time correlation function either analytically or through molecular dynamics, but determining a corresponding approximate effective quantum correlation function from this is a topic of ongoing interest - for instance see Egorov et al. for a comparison of four of these schemes [5].

Input for Calculating Spectroscopy

The most common description of spectroscopy starts with a simple matter-field Hamiltonian of the form

$$H = H_0 + V(t) \tag{2.21}$$

where H_0 is the matter Hamiltonian which describes the system when it is not interacting with light and is thus time independent, and V(t) describes the time dependant electric field **E** which can interact with the matter through the quantum mechanical dipole operator $\boldsymbol{\mu}$ [1, 6]. It is oftentimes expedient to focus specifically on the degrees of freedom of the system which interact with the perturbation by partitioning the matter Hamiltonian into a "system" which contains variables **P** and **Q** resonant with the **E** field, a "bath" which contains the remaining variables **p** and **q**, and an additional term describing the interaction between the "system" and "bath" as follows:

$$H_0 = H_S + H_B + H_{SB} \tag{2.22}$$

The dynamics of any system (with general coordinates **q** here) are described in how the wavefunction evolves according to the time dependant Schrodinger equation

$$\frac{\partial}{\partial t}\psi(\mathbf{q},t) = \frac{1}{i\hbar}H(\mathbf{q},t)\psi(\mathbf{q},t) \tag{2.23}$$

The time evolution under the time independent Hamiltonian H_0 is rather trivially solved by directly integrating (2.23), giving for initial time t_0 and time t

$$\psi(\mathbf{q},t) = \exp\left(\frac{1}{i\hbar}H_0(t-t_0)\right)\psi(\mathbf{q},t_0) \tag{2.24}$$

We can define this first term as the time-evolution operator, an exponential operator which can be applied term by term according to its Taylor expansion

$$U(t,t_0) \equiv \exp\left(\frac{1}{i\hbar} H_0(t-t_0)\right) \tag{2.25}$$

which acts to propagate the wavefunction in time under the time-independent Hamiltonian. We can also then propagate a wavefunction backwards in time under this Hamiltonian using the relation

$$\begin{aligned} \psi(t_0) &= \exp\left(-\frac{1}{i\hbar} H_0(t-t_0)\right)\psi(t) \\ &= U^{\dagger}(t,t_0)\psi(t) \end{aligned} \tag{2.26}$$

It is oftentimes useful to utilize the interaction representation, where the time evolution under this trivial time independent Hamiltonian is incorporated into the operators as

$$\begin{aligned} A_I(t) &= \exp\left(-\frac{1}{i\hbar} H_0(t-t_0)\right) A(t) \exp\left(+\frac{1}{i\hbar} H_0(t-t_0)\right) \\ &= U^{\dagger}(t,t_0) A(t) U(t,t_0) \end{aligned} \tag{2.27}$$

This is technically an application of a general unitary transformation on the Hilbert space. Without an external time dependant perturbation (that is, when $H = H_0$), the operators in this picture are the same as those in the Heisenberg picture, with a time constant wavefunction and operators which evolve with time. Utilizing (2.27) we can we can then rewrite (2.23) as

$$\frac{\partial}{\partial t}\psi_I(t) = \frac{1}{i\hbar} V_I(t)\psi_I(t) \tag{2.28}$$

It is worth noting that here $V_I(t)$ acts as an effective Hamiltonian [6].

We can iteratively solve (2.28) by formally integrating it

$$\psi_I(t) = \psi_I(t_0) + \frac{1}{i\hbar}\int_{t_0}^{t} d\tau V_I(\tau)\psi_I(\tau) \tag{2.29}$$

Then upon repeated substitution of (2.29) into itself we obtain

$$\psi_I(t) = \psi_I(t_0) + \sum_{n=1}^{\infty}\left(\frac{1}{i\hbar}\right)^n \int_{t_0}^{t} d\tau_n \int_{t_0}^{\tau_n} d\tau_{n-1} \cdots \int_{t_0}^{\tau_2} d\tau_1 V_I(\tau_n) V_I(\tau_{n-1}) \cdots V_I(\tau_1)\psi_I(t_0) \tag{2.30}$$

Which if desired can be truncated at m^{th} order:

$$\psi_I(t) = \psi_I(t_0) + \sum_{n=1}^{m-1}\left(\frac{1}{i\hbar}\right)^n \int_{t_0}^{t} d\tau_n \int_{t_0}^{\tau_n} d\tau_{n-1} \cdots \int_{t_0}^{\tau_2} d\tau_1 V_I(\tau_n) V_I(\tau_{n-1}) \cdots V_I(\tau_1)\psi_I(t_0)$$
$$+\left(\frac{1}{i\hbar}\right)^m \int_{t_0}^{t} d\tau_m \int_{t_0}^{\tau_n} d\tau_{m-1} \cdots \int_{t_0}^{\tau_2} d\tau_1 V_I(\tau_m) V_I(\tau_{m-1}) \cdots V_I(\tau_1)\psi_I(\tau_1) \tag{2.31}$$

This perturbative expansion approach allows us to make use of the fact that interactions with an external potential (say, the electric field) are generally much weaker than molecular interactions, and thus we can expand about the unperturbed molecular wavefunction in powers of this much weaker interaction.

Here it is useful to introduce another formalism which more easily incorporates some of the phenomena we wish to describe. Consider a quantum system with spatial coordinates **q**. The wavefunction of this can be expanded onto a properly chosen orthonormal basis set of functions φ_n

$$\psi(\mathbf{q},t) = \sum_{n=1}^{N} c_n(t)\phi_n(\mathbf{q}) \tag{2.32}$$

or in somewhat sloppy Dirac notation

$$|\psi\rangle = \sum_{n=1}^{N} c_n(t)|\phi_n\rangle \tag{2.33}$$

With this we can define the complex, Hermitian density matrix as the $N \times N$ matrix with elements

$$\rho_{nm}(t) = c_n(t)c_m^*(t) \tag{2.34}$$

The nomenclature here is chosen for compliance with the historical literature, but the terminology "density matrix" has an unfortunate side effect of adherence to this framework – the "matrix" is in fact best defined as an operator, but it is commonly still referred to as a "matrix" thus leading to the exceptionally awkward phrases such as "the matrix elements of the density matrix" [7]. These matrix elements are produced by the Hermitian density operator

$$\hat{\rho} \equiv |\psi(t)\rangle\langle\psi(t)| \tag{2.35}$$

Which is the projector onto the ket $|\psi(t)\rangle$ such that

$$\begin{aligned}\rho_{nm}(t) &= \langle m|\hat{\rho}(t)|n\rangle \\ &= c_m^*(t)c_n(t)\end{aligned} \tag{2.36}$$

In a coherent superposition this matrix contains only diagonal elements, while in statistical mixtures this matrix contains off-diagonal terms. Of course, the distinction here between a coherence or a population depends upon the basis chosen for the state space, and because the density matrix operator is Hermitian, it is always possible to find an orthonormal basis $\{|\chi_l\rangle\}$ over which it is diagonal, in which case the density matrix describes a statistical mixture with no coherences of the states $|\chi_l\rangle$ [8].

This notation is particularly useful because we can easily extend it to a system which may be in a statistical mixture of states. Consider a system where for a finite dimensional function space the state has a probability p_k of being in the pure state $|\psi_k\rangle$. This system cannot be represented with a single wavefunction as a puse state can. As before we can define as the density operator this time as a sum over the projection operators of each state weighted by a probability

$$\begin{aligned}\hat{\rho} &\equiv \sum_k p_k |\psi_k\rangle\langle\psi_k| \\ &= \sum_k p_k \rho_k(t)\end{aligned} \tag{2.37}$$

This in principle can be extended to an infinite yet countable space with the careful introduction of integrals in place of some sums, but for our purposes the dimensionality of the function space is of minimal importance [9-12]. The quantum system is them completely described by the time evolution of the matrix elements of this operator, $\hat{\rho}(t)$, and the expectation value of operator A corresponding to matrix **A** with element $A_{nm} = \langle n|\hat{A}|m\rangle$ is

$$\langle \hat{A} \rangle = Tr(\hat{\rho}\hat{A}) \tag{2.38}$$

The time evolution of this density matrix then can be described by the Liouville-von Neumann equation, equivalent to (2.23) [8]

$$\frac{d}{dt}\hat{\rho} = \frac{1}{i\hbar}\left[\hat{H}, \hat{\rho}\right] \tag{2.39}$$

Sometimes written in terms of the Liouville superoperator $\mathcal{L}$ which forms the commutator (or Poisson bracket, depending) between the Hamiltonian and the operator being acted upon

$$\frac{d}{dt}\hat{\rho} = \frac{1}{i\hbar}\mathcal{L}\hat{\rho} \tag{2.40}$$

Because we can think of the density matrix as a combination of Schrodinger kets and bras as illustrated in (2.37), for a time-independent Hamiltonian the density matrix can be acted upon by the time propagator (2.25):

$$\begin{aligned}\hat{\rho}(t) &= \exp\left(\frac{1}{i\hbar}H_0(t-t_0)\right)\hat{\rho}(0)\exp\left(-\frac{1}{i\hbar}H_0(t-t_0)\right) \\ &= U(t,t_0)\hat{\rho}(0)U^{\dagger}(t,t_0)\end{aligned} \tag{2.41}$$

As with the wavefunction, we can define the density matrix in the interaction picture, utilizing the time propagators

$$\begin{aligned}\hat{\rho}_I &= \sum_k p_k \left|\psi_{I,k}\right\rangle\left\langle\psi_{I,k}\right| \\ &= \sum_k p_k \exp\left(-\frac{1}{i\hbar}\hat{H}_0(t-t_0)\right)\left|\psi_k(t)\right\rangle\left\langle\psi_k(t)\right|\exp\left(+\frac{1}{i\hbar}\hat{H}_0(t-t_0)\right) \\ &= U^{\dagger}(t,t_0)\hat{\rho}(t)U(t,t_0)\end{aligned} \tag{2.42}$$

This allows us to transform the von Neumann equation (2.39) into the interaction picture for a Hamiltonian of the form (2.21) to obtain

$$\frac{d}{dt}\hat{\rho}_I(t) = \frac{1}{i\hbar}\left[\hat{V}_I(t),\hat{\rho}_I(t)\right] \tag{2.43}$$

An in the same manner as equation (2.30), formal integration and self substitution yields

$$\rho_I(t) = \rho_I(t_0) + \sum_{n=1}^{\infty}\left(\frac{1}{i\hbar}\right)^n \int_{t_0}^{t} d\tau_n \int_{t_0}^{\tau_n} d\tau_{n-1}\cdots\int_{t_0}^{\tau_2} d\tau_1 \left[\hat{V}_I(\tau_n),\left[\hat{V}_I(\tau_{n-1}),\cdots\left[\hat{V}_I(\tau_1),\rho_I(t_0)\right]\cdots\right]\right] \tag{2.44}$$

And then going back to the Schrodinger picture from the interaction picture using $\hat{\rho}(t) = U(t,t_0)A(t)U^{\dagger}(t,t_0)$:

$$\begin{aligned}\rho(t) = \rho^{(0)}(t) + \sum_{n=1}^{\infty}\left(\frac{1}{i\hbar}\right)^n \int_{t_0}^{t} d\tau_n \int_{t_0}^{\tau_n} d\tau_{n-1}\cdots\int_{t_0}^{\tau_2} d\tau_1 \\ U(t,t_0)\left[\hat{V}_I(\tau_n),\left[\hat{V}_I(\tau_{n-1}),\cdots\left[\hat{V}_I(\tau_1),\rho_I(t_0)\right]\cdots\right]\right]U^{\dagger}(t,t_0)\end{aligned} \tag{2.45}$$

Or alternatively we can define this in terms of n^{th} order density matrices:

$$\rho(t) = \rho^{(0)}(t) + \sum_{n=1}^{\infty} \rho^{(n)}(t) \tag{2.46}$$

Where obviously

$$\begin{aligned} \rho^{(n)}(t) = \left(\frac{1}{i\hbar}\right)^n \int_{t_0}^{t} d\tau_n \int_{t_0}^{\tau_n} d\tau_{n-1} \cdots \int_{t_0}^{\tau_2} d\tau_1 \\ U(t,t_0)\left[\hat{V}_I(\tau_n),\left[\hat{V}_I(\tau_{n-1}),\cdots\left[\hat{V}_I(\tau_1),\rho_I(t_0)\right]\cdots\right]\right]U^{\dagger}(t,t_0) \end{aligned} \tag{2.47}$$

For spectroscopy, the time dependant perturbation is the interaction between a system and an applied external electric field from the light. This interaction can be written as an expansion in powers of the applied field utilizing transition tensors of increasing rank

$$V_I = \boldsymbol{\mu}_1 \cdot \mathbf{E}(\mathbf{r},t) + \boldsymbol{\alpha}_1 : \mathbf{E}(\mathbf{r},t)\mathbf{E}(\mathbf{r},t) + \cdots \tag{2.48}$$

Where given (2.27) the dipole operator in the interaction picture is

$$\hat{\mu}_I(t) = U^{\dagger}(t,t_0)\hat{\mu}U(t,t_0) \tag{2.49}$$

Because the time dependence of this transition dipole operator only emerges in the interaction picture, oftentimes the subscript I is dropped, as if there is any time dependence to this operator, it is in the interaction picture, and if not, it is in the Schrodinger representation.

For vibrational spectroscopy the field-matter interaction occurs between molecular bonds and dipoles on the order of angstroms while the radiation wavelength is on the order of a few microns, and thus it is valid to make the "dipole approximation" where each molecule is approximated as a point dipole and the only pertinent quantity for which we must take account is the transition dipoles. We can assume the major contribution to the perturbative interaction is just the first term

$$V_I(t) \approx -\hat{\mu}_I(t)\mathbf{E}(t) \tag{2.50}$$

What we measure for nonlinear spectroscopy is the macroscopic polarization in the sample generated from the interaction with a series of external electric fields. This induced nonlinear polarization comes classically from Maxwell's equations, which when in a source free ($\nabla \cdot \mathbf{E} = 0$) isotropic medium tell us:

$$\begin{aligned}\nabla\times\mathbf{E} &= -\frac{\partial}{\partial t}\mathbf{B} \\ &= -\frac{\partial}{\partial t}\mu_0\mathbf{H}\end{aligned} \tag{2.51}$$

And allowing the material to be nonlinear such that the constitutive relation for the displacement current is $\mathbf{D} = \varepsilon\mathbf{E} = \varepsilon_0\mathbf{E} + \mathbf{P}(\mathbf{E})$

$$\begin{aligned}\nabla\times\mathbf{H} &= \mathbf{J} + \frac{\partial}{\partial t}\mathbf{D} \\ &= J + \frac{\partial}{\partial t}\varepsilon\mathbf{E} + \frac{\partial}{\partial t}\mathbf{P}\end{aligned} \tag{2.52}$$

The nonlinear polarization density term $\mathbf{P}$ in (2.52) can be found to act as a source by arriving at the wave equation the usual way - combining these two equations and assuming the region of space of interest contains no free currents so $\mathbf{J} = 0$ [13-15]:

$$\left(\nabla^2 - \frac{n^2}{c^2}\frac{\partial^2}{\partial t^2}\right)\mathbf{E} = \mu_0\frac{\partial^2}{\partial t^2}\mathbf{P} \tag{2.53}$$

Nonlinear material polarization is oftentimes described by expanding the polarization as a power series in the field, introducing the susceptibility tensors χ. For the pure electric dipole case this looks like [16]:

$$\mathbf{P} = \chi\cdot\mathbf{E} + \chi:\mathbf{EE} + \chi\vdots\mathbf{EEE} + \cdots \tag{2.54}$$

In the language of quantum mechanics (and dropping the bold notation), the total polarization of the sample is the expectation value of the dipole operator:

$$P(t) = Tr\left(\hat{\mu}(t)\rho(t)\right) \tag{2.55}$$

which may also have spatial dependence. Utilizing the perturbative expansion of the density matrix in (2.46) we can obtain a perturbative expansion of the polarization where similarly to (2.54) the nth term describes n matter-field interactions:

$$P(t) = \sum_{n=1}^{\infty} Tr\left(\hat{\mu}(t)\rho^{(n)}(t)\right) \tag{2.56}$$

Utilizing the dipole approximation for the perturbation term (2.50) we then obtain for the nth order polarization:

$$P^{(n)}(t) = -\left(\frac{1}{i\hbar}\right)^n \int_{t_0}^{t} d\tau_n \int_{t_0}^{\tau_n} d\tau_{n-1} \cdots \int_{t_0}^{\tau_2} d\tau_1 E(\tau_n)E(\tau_{n-1})\cdots E(\tau_1) \\ Tr\left(\hat{\mu}(t)\left[\hat{\mu}(\tau_n),\left[\hat{\mu}(\tau_{n-1}),\cdots\left[\hat{\mu}(\tau_1),\rho(t_0)\right]\cdots\right]\right]\right) \tag{2.57}$$

where the disappearance of the time evolution operators comes from the property that the trace is invariant with respect to cyclic permutation of elements and the added presence of this last interaction $\hat{\mu}(t)$ which is not part of the commutators. To agree with the literature, we change the time variables here according to times τ_n and time gaps defined according to Mukamel [17]:

$$t_1 \equiv \tau_2 - \tau_1, \quad t_2 \equiv \tau_3 - \tau_2, \quad \cdots, \quad t_n \equiv t - \tau_n \tag{2.58}$$

Allowing us to rewrite the polarization in (2.57) as:

$$P^{(n)}(t) = -\left(\frac{1}{i\hbar}\right)^n \int_0^{\infty} dt_n \int_0^{\infty} dt_{n-1} \cdots \int_0^{\infty} dt_1 \\ E(t-t_n)E(t-t_n-t_{n-1})\cdots E(t-t_n-t_{n-1}-\cdots-t_1) \\ Tr\left(\hat{\mu}(t+t_n+t_{n-1}+\cdots+t_1)\left[\hat{\mu}(t_{n-1}+\cdots+t_1),\cdots\left[\hat{\mu}(\tau_1),\rho(t_0)\right]\cdots\right]\right) \tag{2.59}$$

The general description of the n^{th} order polarization introduces an nth order response function, $R^{(n)}$, a rank n+1 tensor which is a function of the n time variables $\tau_1, \ldots, \tau_n$ which describes how the system responds to n separate matter-field interactions. The n^{th} order polarization is expressed as a convolution of this response tensor with the n input electric fields:

$$P^{(n)}(t) = \int_0^{\infty} dt_n \int_0^{\infty} dt_{n-1} \cdots \int_0^{\infty} dt_1 \\ E(t-t_n)E(t-t_n-t_{n-1})\cdots E(t-t_n-\cdots-t_1)R^{(n)}(t_n,\ldots,t_1) \tag{2.60}$$

Where the response function is

$$R^{(n)}(t_n,\ldots,t_1) = -\left(\frac{1}{i\hbar}\right)^n \theta(t_1)\theta(t_2)\cdots\theta(t_n) \\ Tr\left(\hat{\mu}(t+t_n+t_{n-1}+\cdots+t_1)\left[\hat{\mu}(t_{n-1}+\cdots+t_1),\cdots\left[\hat{\mu}(\tau_1),\rho(t_0)\right]\cdots\right]\right) \tag{2.61}$$

With the Heaviside step functions introduced to allow integration from -∞ to ∞. Due to the invariance of the trace under cyclic permutation, the set of commutators here can be written in a variety of orders. In the frequency domain, the Fourier transform of the response function gives the frequency susceptibility

$$\chi(\omega) = \int_{-\infty}^{\infty} R(t) e^{i\omega t} dt \tag{2.62}$$

This n^{th} order response function contains within it all the molecular information necessary to predict the material polarization response to applied electric fields. Looking at (2.59) it becomes obvious that this response function is, in the dipole approximation, related directly to the time evolution of the dipole matrix elements. Although it should not come as a surprise that the molecular dipoles dictate the response to an applied electric field, this cannot be stressed enough. The dynamics of the time dependent quantum mechanical dipole operator dictate how the system polarization responds and thus any nonlinear signals emitted.

QUANTUM DYNAMICS

If we consider a general non-Hermitian quantum operator A, the time dependence of this operator in the Heisenberg framework is, under Hamiltonian H [6]

$$\hat{A}(t) = e^{\frac{\hat{H}t}{i\hbar}} \hat{A} e^{\frac{\hat{H}t}{i\hbar}} \tag{2.63}$$

And the expectation value / ensemble average of this is obtained via the traces

$$\langle A \rangle = \frac{Tr\left[e^{-\beta H} A\right]}{Tr\left[e^{-\beta H}\right]} \tag{2.64}$$

The evolution of a quantum system over time is often modeled in the framework of time correlation functions, as many important physical observables can be described in this language – for instance, the velocity-velocity autocorrelation function is related to the bulk diffusion constant, and the time autocorrelation function of the dipole moment operator is directly related to the absorption spectrum [1, 2, 6, 18]:

$$\sigma(\omega) \propto \int_{-\infty}^{\infty} dt e^{-i\omega t} \left\langle \hat{\varepsilon} \cdot \mu_I(0) \hat{\varepsilon} \cdot \mu_I(t) \right\rangle \tag{2.65}$$

Combining (2.27) with (2.38) and (2.6) we can write out the time correlation function for two operators with of a pure state $\hat{\rho}_0$ as

$$C_{AB}(t,t_0) = Tr\left(\hat{\rho}_0 \hat{A} U^{\dagger}(t,t_0)\hat{B}U(t,t_0)\right) \tag{2.66}$$

This full operator time evolution is, unfortunately, a quantity which is exceptionally difficult to compute. Obtaining complete and exact knowledge of the full quantum dynamics of any system is a computational challenge, and for condensed phase systems this is effectively impossible with current computational methods beyond anything larger than a few tens of atoms. So in order to actually deal with this dynamic evolution, we will have to make a number of approximations.

LINEAR RESPONSE

As we cans see from (2.61), the response function depends upon the time evolution of the dipole operator. Oftentimes this is expressed in terms of correlation functions in μ. For the case of linear response, we can write out the response function by expanding the commutator:

$$\begin{aligned} R^{(1)}(t) &= -\left(\frac{1}{i\hbar}\right)\theta(t)Tr\left(\hat{\mu}(t)\left[\hat{\mu}(\tau_1), \rho(t_0)\right]\right) \\ &= -\left(\frac{1}{i\hbar}\right)\theta(t)Tr\left(\hat{\mu}(t)\hat{\mu}(\tau_1)\rho(t_0) - \hat{\mu}(t)\rho(t_0)\hat{\mu}(\tau_1)\right) \end{aligned} \tag{2.67}$$

Defining time τ_1 as 0 and assuming that $\rho(t_0) = \rho(-\infty) = \rho_{eq}$ (that is, the density matrix is at equilibrium until perturbed) we can then use the definition of the correlation function (2.8) and the definition of the density matrix (2.37) along with the fact that the expectation value of an operator is given by (2.38) to rewrite this as:

$$R^{(1)}(t) = -\left(\frac{1}{i\hbar}\right)\theta(t)\left(\left\langle\hat{\mu}(t)\hat{\mu}(0)\right\rangle - \left\langle\hat{\mu}(0)\hat{\mu}(t)\right\rangle\right) \tag{2.68}$$

We can explicitly expand this out in terms of system eigenstates if we realize that the dipole operator in an arbitrary basis (for which the basis functions evolve over time and thus are time propagated under the unperturbed Hamiltonian H_0) can be written as:

$$\begin{aligned} \hat{\mu}(t) &= \sum_{a,b}\left|\psi_a(t)\right\rangle\left\langle\psi_a(t)\right|\hat{\mu}(t)\left|\psi_b(t)\right\rangle\left\langle\psi_b(t)\right| \\ &= \sum_{a,b}\left|\psi_a(t)\right\rangle\mu_{ab}(t)\left\langle\psi_b(t)\right| \\ &= \sum_{a,b}U^{\dagger}(t,0)\left|a\right\rangle\mu_{ab}(t)\left\langle b\right|U(t,0) \\ &= \sum_{a,b}\exp\left(-\frac{1}{i\hbar}H_0 t\right)\left|a\right\rangle\mu_{ab}(t)\left\langle b\right|\exp\left(\frac{1}{i\hbar}H_0 t\right) \end{aligned} \tag{2.69}$$

We then get for the first term in the expansion of the commutator from (2.67)

$$Tr\left(\hat{\mu}(t)\hat{\mu}(0)\rho_{eq}\right)=Tr\left(\sum_{a,b}\mathrm{e}^{-\frac{1}{i\hbar}H_0 t}\left|a\right\rangle\mu_{ab}(t)\left\langle b\right|\mathrm{e}^{\frac{1}{i\hbar}H_0 t}\left|b\right\rangle\mu_{ba}(0)\left\langle a\right|\rho_{eq}\right) \tag{2.70}$$

We can then make use of the operator

$$e^{\frac{1}{i\hbar}H_a t}e^{-\frac{1}{i\hbar}H_b t}=\exp_{+}\left[\frac{1}{i\hbar}\int_0^t d\tau H_{ab}(\tau)\right] \tag{2.71}$$

With the + subscript indicating a time ordered exponential series, describing in practice how this operator is applied:

$$\exp_{+}\left[\int_0^t d\tau A(\tau)\right]=1+\sum_{n=1}^{\infty}\int_0^t d\tau_n\int_0^{\tau_n}d\tau_{n-1}\ldots\int_0^{\tau_2}d\tau_1 A(\tau_n)A(\tau_{n-1})\ldots A(\tau_1) \tag{2.72}$$

It is also useful to utilize the identity:

$$e^{\frac{1}{i\hbar}H_a t}e^{-\frac{1}{i\hbar}H_a t}=1 \tag{2.73}$$

The time dependant transition energy of the system for which the unperturbed Hamiltonian takes the form $H_0 = H_s + H_B + H_{SB}$ as in (2.22) is given by the difference in energies of two system states averaged over the bath degrees of freedom:

$$\omega_{ab}(t)=\frac{\langle a|H_S+H_{SB}|a\rangle}{\hbar}-\frac{\langle b|H_S+H_{SB}|b\rangle}{\hbar} \tag{2.74}$$

All this allows us to rewrite the first term in the expansion of the linear response commutator (2.70)

$$Tr\left(\hat{\mu}(t)\hat{\mu}(0)\rho_{eq}\right)=Tr\left(\sum_{a,b}\mu_{ab}(t)\mu_{ab}(0)\exp_{+}\left[-i\int_0^t d\tau\omega_{ab}(\tau)\right]\rho_{eq}\right) \tag{2.75}$$

This is actually the only term we need to calculate the full linear response, as the second part of (2.67) is the conjugate (technically the Hermitian adjoint) of this term.

What we see here is that the pertinent variables for calculating the response are

1) The values of the transition dipoles over time, $\mu_{ab}(t)$

2) The full dynamics of the transition frequencies $\omega_{ab}(t)$

This provides a key physical picture to how one predicts the response of a molecular system to an external electric field - if we can calculate trajectories describing how both μ and ω evolve in time, we then we are able to calculate the full response.

FREQUENCY RELATIONSHIPS

The overtone transition ω_{12} is, in most molecular potentials, slightly lower energy than the fundamental ω_{01} transition, a trend which can be characterized by an "anharmonicity"

$$\Delta \equiv \omega_{01} - \omega_{12} \tag{2.76}$$

So named because in a harmonic potential the energy gap is constant and $\omega_{12} = \omega_{01}$. Correlation between the anharmonicity and fundamental frequency ω_{01} for the water –OH stretch can be mapped empirically from general trends in calculations, for example something entirely phenomenological based upon experimental observations, such as [19]:

$$\omega_{12}(t) \approx \frac{137}{126}\omega_{01}(t) - 472 \tag{2.77}$$

or the anharmonicity can be assumed to be constant across the entire stretching band.

DIPOLE RELATIONSHIPS

The so-called Condon approximation is used to adiabatically separate "fast" and "slow" coordinates, much like the familiar Born-Oppenheimer separation. In gas phase spectroscopy, this oftentimes is used to separate the electronic transition dipole moment from vibrational coordinates and treat the two independently. It is common in ultrafast condensed phase work to utilize a similar framework and treat the vibrational transition dipole as independent of the other degrees of freedom, such as rotational and translational coordinates. As a result, this means that people commonly assumes that a vibrational transition dipole is independent of the solvent degrees of freedom and thus constant across a given vibrational band [20, 21]. This breaks down dramatically in strongly hydrogen bonded systems, where it is known that the hydrogen bond greatly enhances stretch absorptions and different hydrogen bonding environments lead to different absorption intensities, and thus a variation in transition dipole across band [20, 22-27].

When the transition dipole is treated as a constant, dipoles can be generated from one of the many experimentally motivated empirical mappings, for instance, in water Roberts has utilized [28]

$$\mu_{01} = 1.8336 - 1.2973\times10^{-3}\omega_{01} + 4.7136\times10^{-7}\omega_{01}^2 - 6.8016\times10^{-11}\omega_{01}^3 \quad (2.78)$$

with frequencies in cm^{-1} and dipole moments in Debye. With the fundamental transition evaluated, higher transition dipoles can be generated from harmonic scaling

$$\mu_{01} = \sqrt{2}\mu_{12} \quad (2.79)$$

or through other empirical mappings. Dipoles can also be directly calculated from numerically solving the Schrodinger equation for the potentials, as will be demonstrated shortly.

Model Potentials for Proton Transfer

A particularly useful schematic tool for considering the motion of a proton along a hydrogen bond is picturing the actual potential experienced by the proton along which it may move. In the simplest case, this can be modeled by an effective 1D potential, which, considering the strong directionality of the hydrogen bond, is a reasonable approximation for the full potential energy surface. This generally takes the form of a double well potential, as discussed in Chapter 1, with energetic minima for the proton residing on both the donor and acceptor at an appropriate bond distance [29]. When the hydrogen bond is short and strong, the proton is essentially shared between the two larger nuclei, and this potential becomes a single well in shape with only one clear symmetric minimum [30]. When the internuclear distance is large, the hydrogen bond is weak and the potential should look very much like two separated harmonic or Morse potentials. The surrounding solvent fluctuations can further alter this potential, in a manner analogous to reorganization terms in electron transfer theory – sometimes favoring localization of the proton on the donor or acceptor by shifting the energetic potential minimum.

Such highly anharmonic potentials pose a number of extra challenges for calculations and experimental observation, including large non-Condon effects for which the transition dipole moments change greatly depending upon the bond energy and length, relaxation of the restrictions imposed upon direct 0-2 transitions which are harmonically forbidden, large changes in transition energy gaps allowing transitions to move in and out of a spectroscopic experimentally accessible range, and possible negative anharmonicities where $\omega_{12} > \omega_{01}$. With these sorts of potentials, the chemist's ingrained harmonic oscillator intuition can fail spectacularly.

With the proton potential in hand, it is possible to solve the nuclear Schrödinger equation to determine the vibrational energies and transition dipoles. This is done numerically for an arbitrary potential through the implementation of Colbert and Miller's discrete variable representation (DVR) [31]. Briefly, this approach allows for numerical solutions to the Schrödinger equation in an arbitrary number of dimensions

without explicit integration through a grid point representation to create a tractable linear algebra problem. A sparse Hamiltonian is constructed by creating a diagonal potential energy matrix and an infinite order finite difference approximation based construction of the kinetic energy component on the grid. This approach has been shown to be a more accurate method of the computation of anharmonic frequencies than fitting to a Morse potential or harmonic approximations for proton transfer scenarios in liquid water [32].

For a model asymmetric double well proton potential we can then obtain the vibrational energy levels and wavefunctions. Using these wavefunctions, we can also calculate the transition dipole element, as the transition dipole element is, for displacement vector $\hat{d}$ pointing from positive charge +q to negative charge -q:

$$\begin{aligned} \mu_{ab} &= \langle \psi_a | \hat{\mu} | \psi_b \rangle \\ &= \langle \psi_a | q \cdot \hat{d} | \psi_b \rangle \\ &= q \langle \psi_a | \hat{d} | \psi_b \rangle \end{aligned} \tag{2.80}$$

Here for our one dimensional potential this displacement vector is related to the 1D position coordinate and thus we can compute the 1D wavefunction position overlap integral for each set of wavefunctions.

The potential model used contains an asymmetry term A which is linear in position, shifting the double well such that when "asymmetry" = 0 the well is symmetric with minima at $x = \pm\sqrt{\frac{\beta}{2\alpha}}$ and a barrier height of $\frac{\beta^2}{4\alpha}$:

$$V(x) = \alpha x^4 - \beta x^2 + Ax + \frac{\beta^2}{4\alpha} \tag{2.81}$$

The parameters alpha and beta are given an additional constraint such that they give minima corresponding to the water dimer, which has an average O-O distance of approximately 2.7Å. These potentials can then be plotted and the corresponding proton wavefunctions and energy levels solved for. For example, when the well is very asymmetric, corresponding to a proton localized on a single water molecule, we see a potential which appears somewhat Morse-like for lower energies and harmonic for higher energy levels:

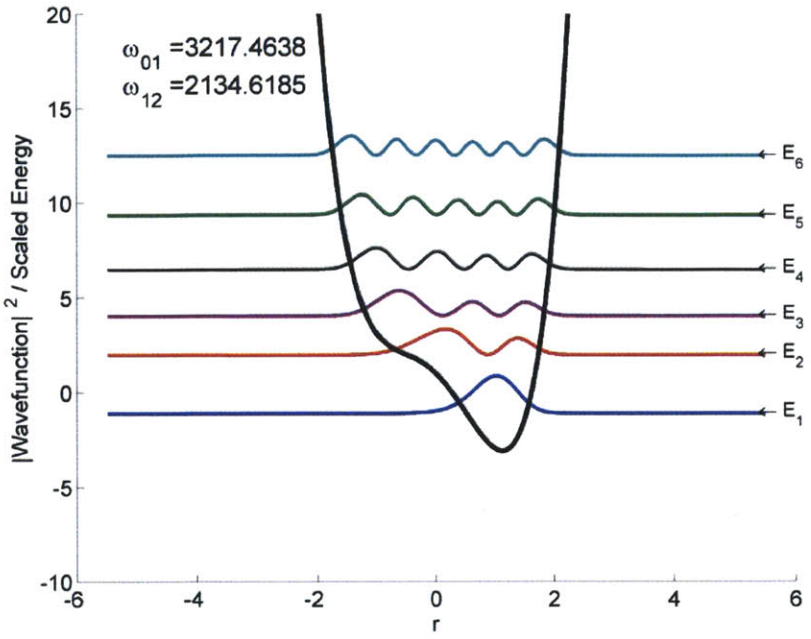

Figure 7: Asymmetric model double well potential

While when the potential is perfectly symmetric the resulting wavefunctions and energy levels are:

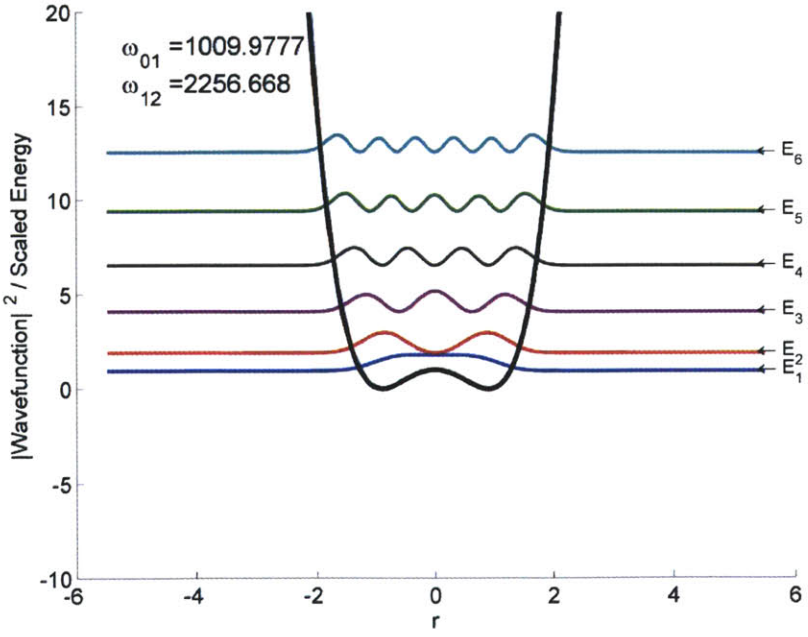

Figure 8: Symmetric model double well potential

We can then vary the value of the asymmetry A and calculate the transition frequencies and transition dipoles for a range of possible potentials. In a condensed phase system such as liquid water, the surrounding solvent environment can cause the proton potential and thus these values to rapidly fluctuate. For this potential, varying the asymmetry from -5 to 5 (corresponding to a proton localized on one oxygen and then moving to be localized on the other, passing through an equally shared state A=0) we can map out the transition frequencies:

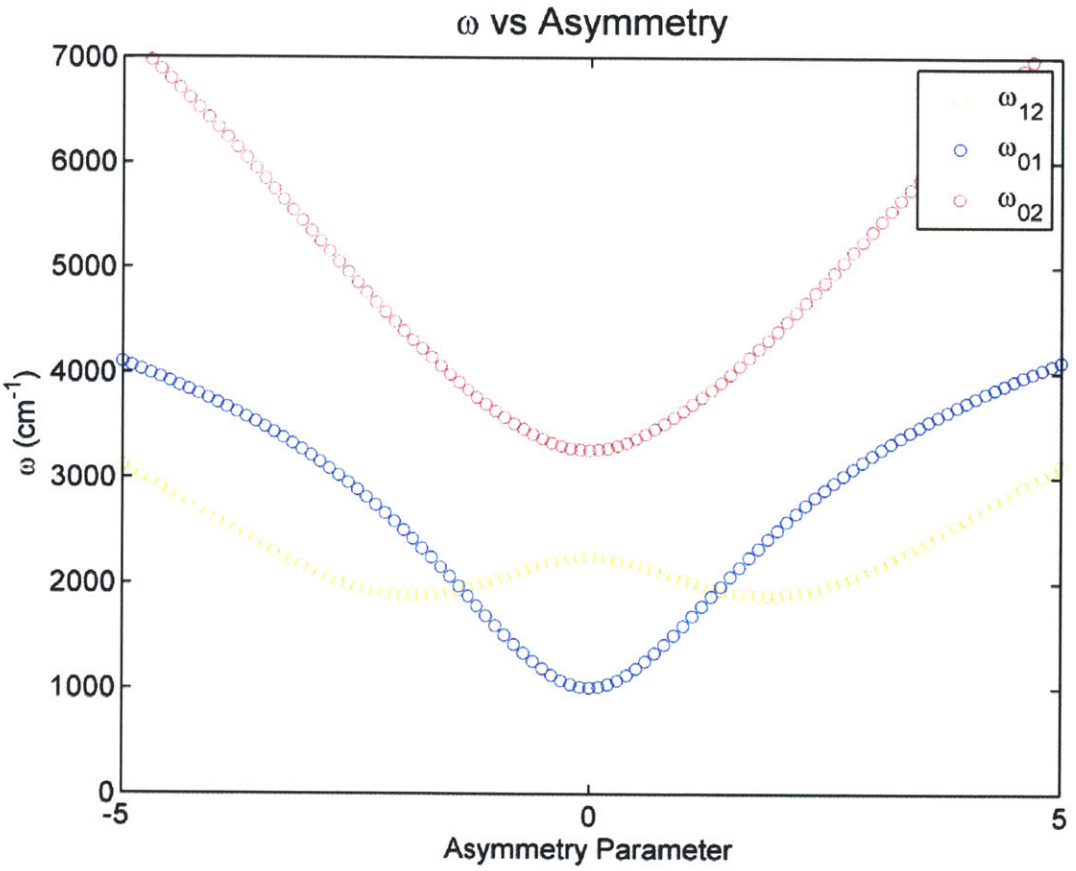

Figure 9: Transition frequencies vs. double well asymmetry

The vibrational energy level structure changes considerably as the potential moves to completely symmetric and back, and near the symmetric state there is a negative anharmonicity for the ω_{12} transition, actually moving higher in energy than the fundamental. In addition, the weakly allowed ω_{02} transition drops significantly down into the same frequency regime as that of the fundamental for the localized proton. Plotting the transition dipole magnitudes we see similar dramatic changes near the completely symmetric potential shape where the proton is shared, including clear non-Condon dipole scaling:

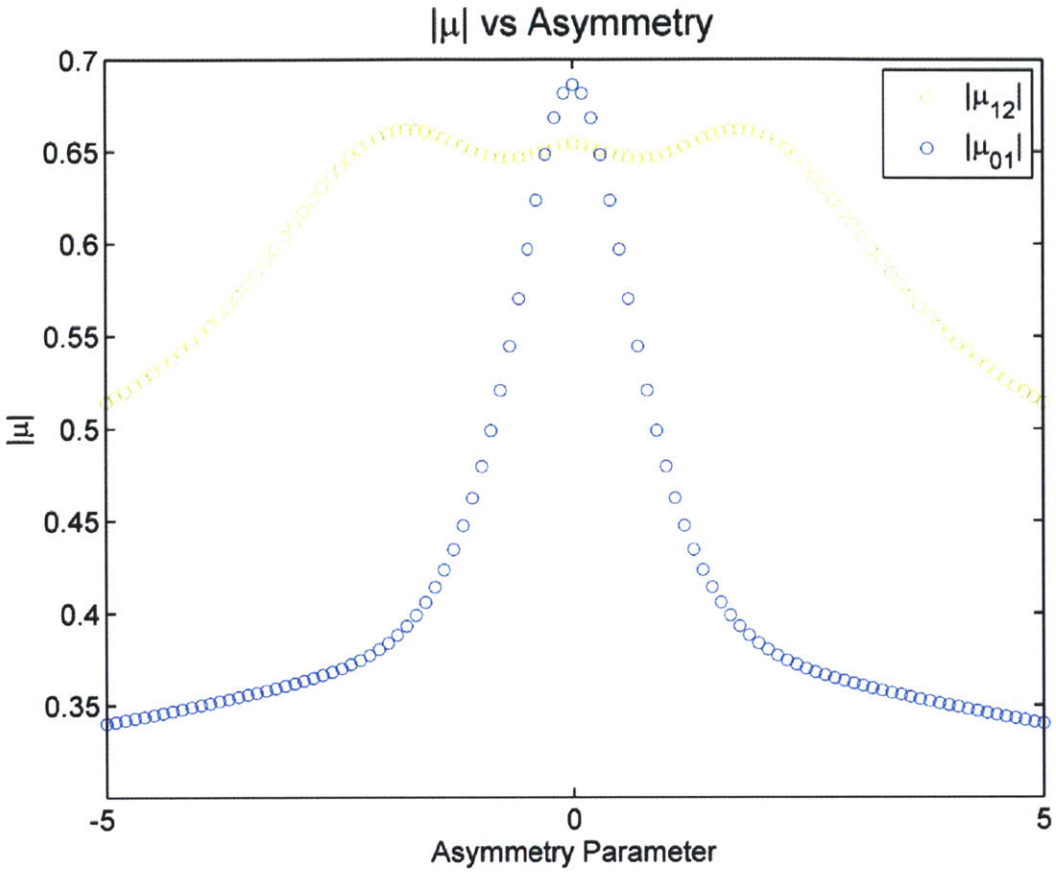

Figure 10: Transition dipoles vs. double well asymmetry

AB INITIO APPROACHES

The calculation of both the structure and interaction energies of hydrogen bonded species presents a number of challenges for even modern numerical quantum chemistry techniques. Many of these challenges arise from the unique nature of the hydrogen bond interaction itself, including the important contributions of computationally challenging effects such as polarizability, induction, dispersion interactions, nonadditivity, and small exchange repulsion energies [33]. In addition, for bonds on the order of only 5 kcal/mol, small errors in absolute energies lead to predictions of very different physical properties.

Density functional theory and wavefunction-based methods both can provide reasonably accurate geometries, dipole moments, polarizabilities, and binding energies for small molecules (for example, $(H_2O)_2$), but quantum chemical calculations tend to be significantly less reliable in predicting intra- and intermolecular vibrations in these hydrogen bonded species, in part because modern vibrational energy

calculation schemes cannot properly account for strongly anharmonic vibrational potentials [34-37]. For hydrogen bonding interactions, large and polarizable basis sets are required and nonlocal corrections to exchange with electron correlation effects must be carefully incorporated as well [38]. For anything beyond qualitative level predictions of hydrogen bonded systems, ab-initio methods are often required. These are commonly implemented utilizing electronic structure software packages such as Gaussian and Q-Chem [39, 40].

To highlight the challenges still faced in quantum chemical calculations of hydrogen bonding parameters, it has been shown that for no-CP SCF-MP2 work a basis set as large as aug-cc-pVQZ (348 functions!) is required for even medium accuracy agreement with absolute experimental values and isomer stability predictions [41, 42]. One must be exceptionally careful in choice of basis sets and initial unoptimized geometries in expecting computational chemistry packages to converge upon an energy minimizing hydrogen bond interaction, as even the water dimer does not necessarily converge to a bonding type interaction at the SCF level. The hybrid functional B3LYP has been shown to produce results, at least for the water dimer, comparable to the more expensive MP2 level [43-45].

One major difficulty in obtaining accurate quantum chemical vibrational energy calculations for these systems is that usually the potential energy is truncated to only include second order terms, thus creating a harmonic potential [46]. One of the characteristic features of hydrogen bonds is a very anharmonic potential, and thus the typical approaches to vibrational frequency calculation in quantum chemical software packages often does not give reasonable results. Instead of making the harmonic approximation and calculating vibrational energies from the Hessian matrix, I will map out the proton potential for a strongly hydrogen bonded system through a series of single point energy calculations corresponding to different small steps in proton position over a range of internuclear separations and solvent configurations. The different total energies obtained for each scan of proton position allows us to construct a one dimensional proton potential. This then allows us to assemble a Hamiltonian over which the Schrödinger equation may be solved, and utilizing the same DVR approach discussed previously, we can obtain vibrational energy levels and transition dipole moments.

Due to the relatively weak interaction energy of the hydrogen bond, it should be emphasized that the assumption of a single equilibrium geometry is of limited utility. Because bonds can break and form quickly and only persist for a limited amount of time at room temperature, the dynamics of bonding are as important if not more than the energetics. The purpose here is to map out static trends in observables upon which can later be imposed dynamics. For HF, some excellent work has been proton potentials have been mapped for the water dimer as well [47, 48]. Recent developments in full quantum treatments of water,

generally relying density functional theory utilizing the local density approximation, have proven useful and exiting for small numbers of water molecules (O(100)), and with computational advances it is becoming possible to come close to simulations adequate to describe the condensed phase, including mixed QM/MM simulations to study dynamics [49-54].

As an example of this static mapping, we can consider the simple acid-base system of a protonated water-ammonia dimer, $[H_2O\text{-}H\text{-}NH_3]^+$ [55-58]. For a given fixed ON distance (R_{ON}) a constrained geometry optimization is performed to calculate the molecular configuration of lowest energy. The shared proton is then scanned in small steps and the resulting single point energy is calculated. The single point energy is then plotted as a function of the proton position to approximate the proton potential at any given point in space. This can also be done with optimization of the peripheral atoms allowed (with a fixed ON distance and fixed proton position), but assuming a separation of timescales between proton motion and motion for the rest of the molecular degrees of freedom, the following results do not allow for geometry reoptimization during the scan.

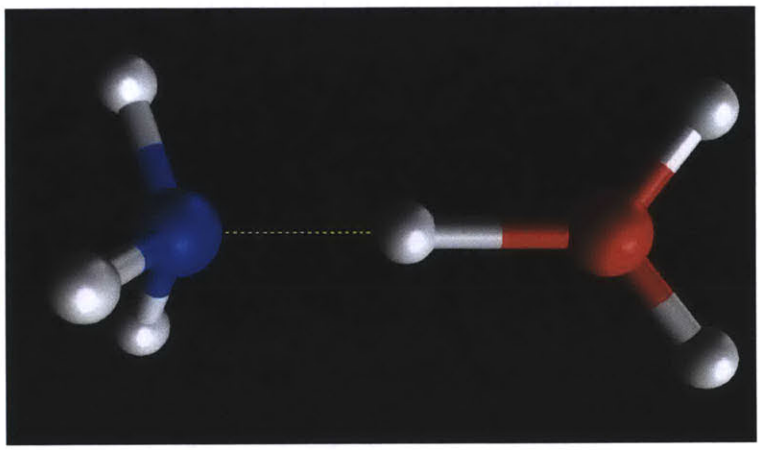

Figure 11: Acid-base proton transfer geometry in $[H_2O\text{-}H\text{-}NH_3]^+$

Using the hybrid B3LYP/6-31G(d) model in the Gaussian 03 software package, the geometry was optimized for a fixed internuclear distance, and then the shared proton was scanned along the O-O internuclear coordinate vector [39]. Figure 12 and Figure 13 illustrate the results of this approach for two different fixed values of R_{ON}:

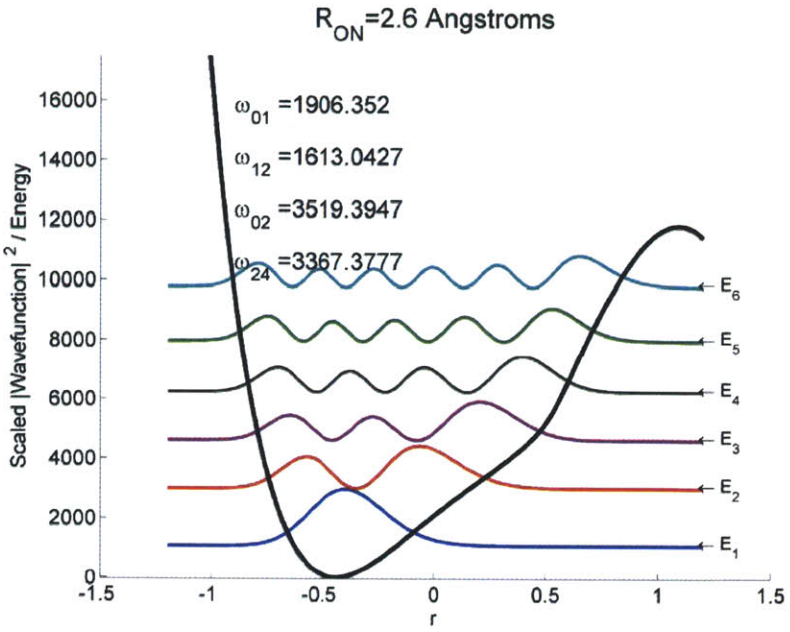

Figure 12: Calculated proton potential for $[H_2O\text{-}H\text{-}NH_3]^+$ with an ON distance of 2.6 Angstroms

If the intermolecular separation is increased, the potential begins to more clearly gain two separate minima

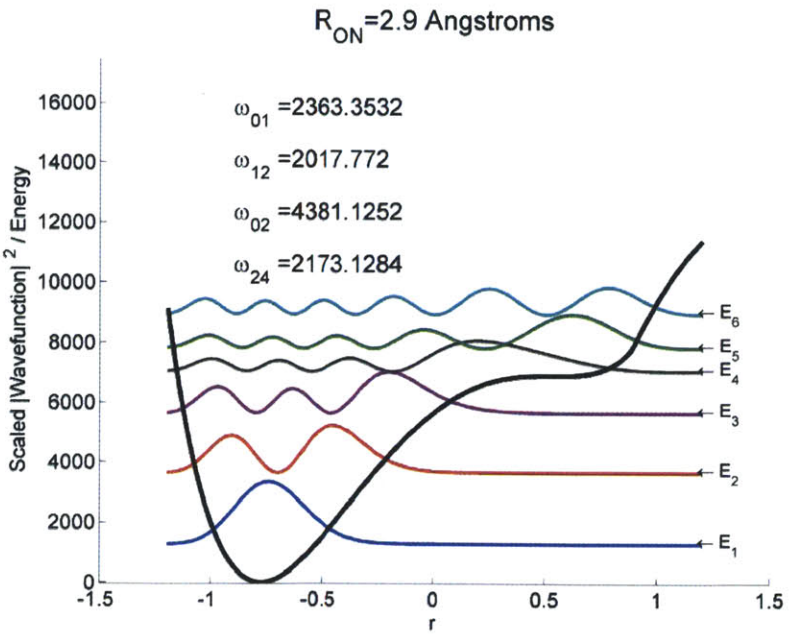

Figure 13: Calculated proton potential for $[H_2O\text{-}H\text{-}NH_3]^+$ with an ON distance of 2.9 Angstroms

There are a few key things to notice here. First, this heterodimer expectedly produces an asymmetric potential, and as a result the proton is clearly more likely to reside on the nitrogen. Second, we notice that when close together, the barrier is very low, and the potential looks quite Morse-like, while as we increase the interdimer distance, the two minima more clearly appear. This general method can be applied to other heterodimer systems, and explicit solvent molecules in various configurations can also be included, although the simple gas phase dimer is demonstrated here to simply examine the resulting trends.

Plotting the calculated vibrational frequencies from these potentials we see the effects of internuclear distance upon the energy level structure, here shown without any correction directly from the calculated potentials:

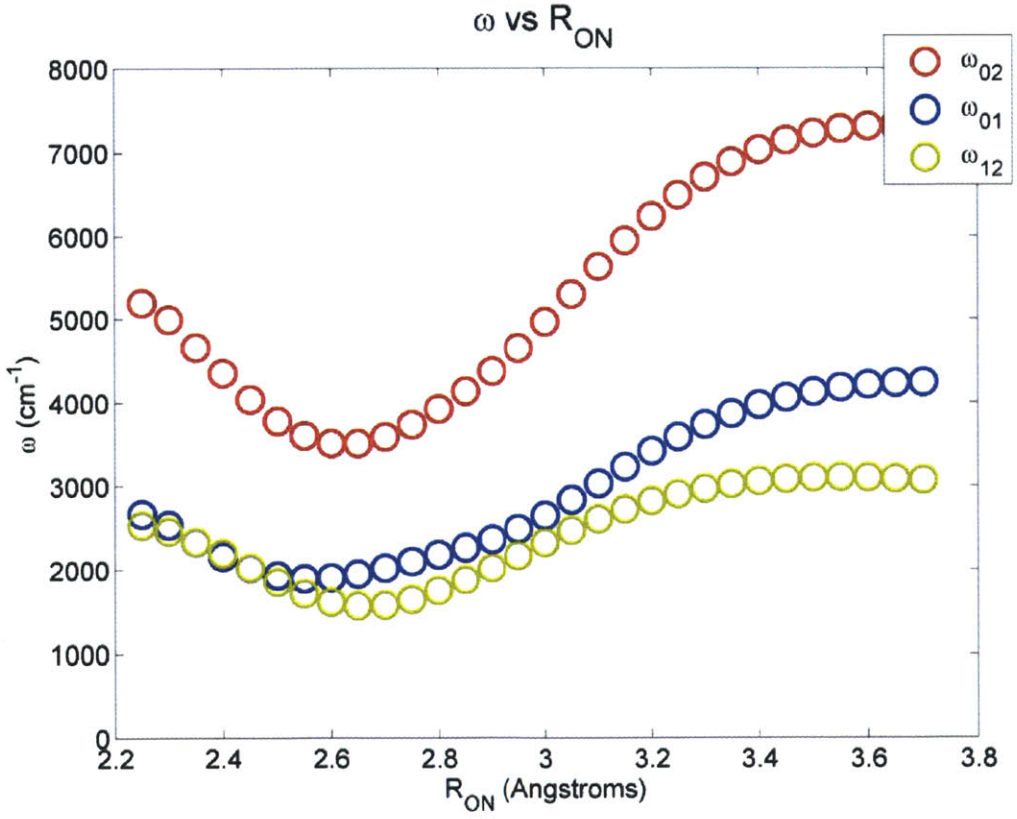

Figure 14: Calculated vibrational frequencies for $[H_2O\text{-}H\text{-}NH_3]^+$ as a function of ON distance

The dipole moment trends reflect the extra polarization due to hydrogen bond formation, and single quantum transition dipole intensities increase for distances where the proton takes part in a strong hydrogen bond:

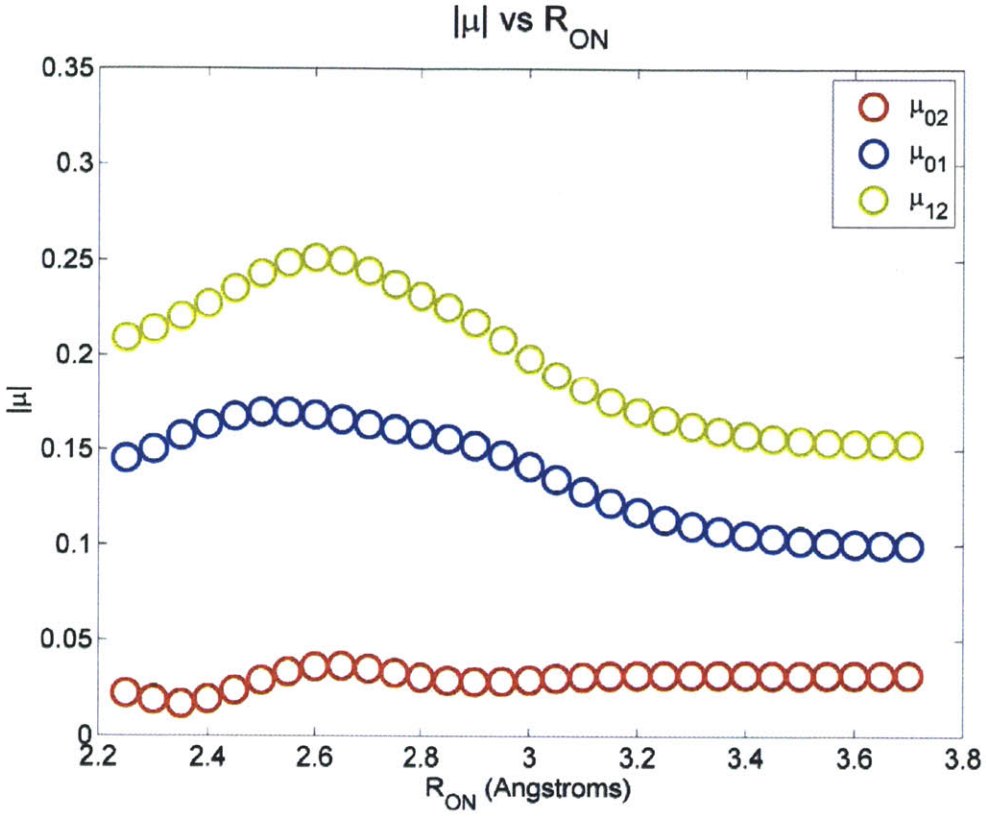

Figure 15: Calculated transition dipoles for $[H_2O\text{-}H\text{-}NH_3]^+$ as a function of ON distance

The calculations here reproduce many traits which we would classically expect for a traditional harmonic or Morse potential. The 0⟶2 transition is forbidden in a harmonic potential, and here we see a very low transition dipole for this as well. In addition the 1⟶2 transition in the harmonic potential should scale as $\mu_{12} = \sqrt{2}\mu_{01}$, and for this system the ratio $\frac{\mu_{12}}{\mu_{01}}$ remains between 1.39 and 1.53 across the range of R_{ON} internuclear distances scanned.

Similarly we can also consider the very simple case of the shared proton in the water-hydroxide ion dimer $H_3O_2^-$, shown in Figure 16:

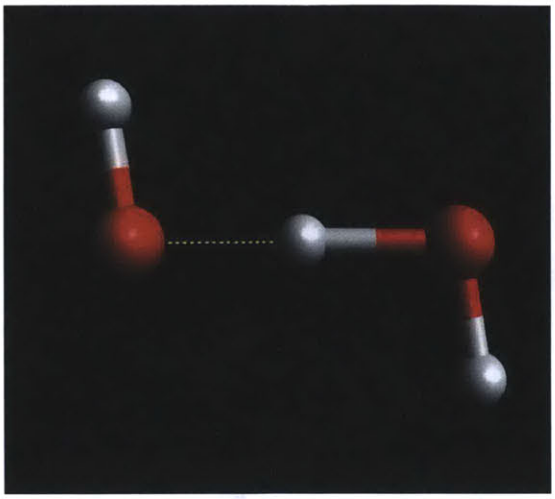

Figure 16: $H_3O_2^-$ equilibrium geometry

Solvation of a real hydroxide in the condensed phase is significantly more complicated and requires a large number of water molecules, and it is only for illustrative purposes that two molecules are shown – one can also perform this same sort of calculation for geometries obtained from snapshots of molecular dynamics trajectories, which tend to be dominated by three and four coordinate hydroxide species [28, 59]. The shared proton in these sorts of water-hydroxide complex has been shown to absorb strongly as low as 700 cm^{-1}, with a large enhancement in the dipole compared to pure water [60]. This same sort of low frequency absorption and transition dipole enhancement manifests itself in the results obtained through the calculation of the proton potential. For the case of hydroxide, the potential is symmetric and thus has some degeneracy, as can be seen for R_{OO} distance of 2.9Å, for which the two lowest energy levels are effectively equal, a trend observed in other symmetric proton transfers as well [61].

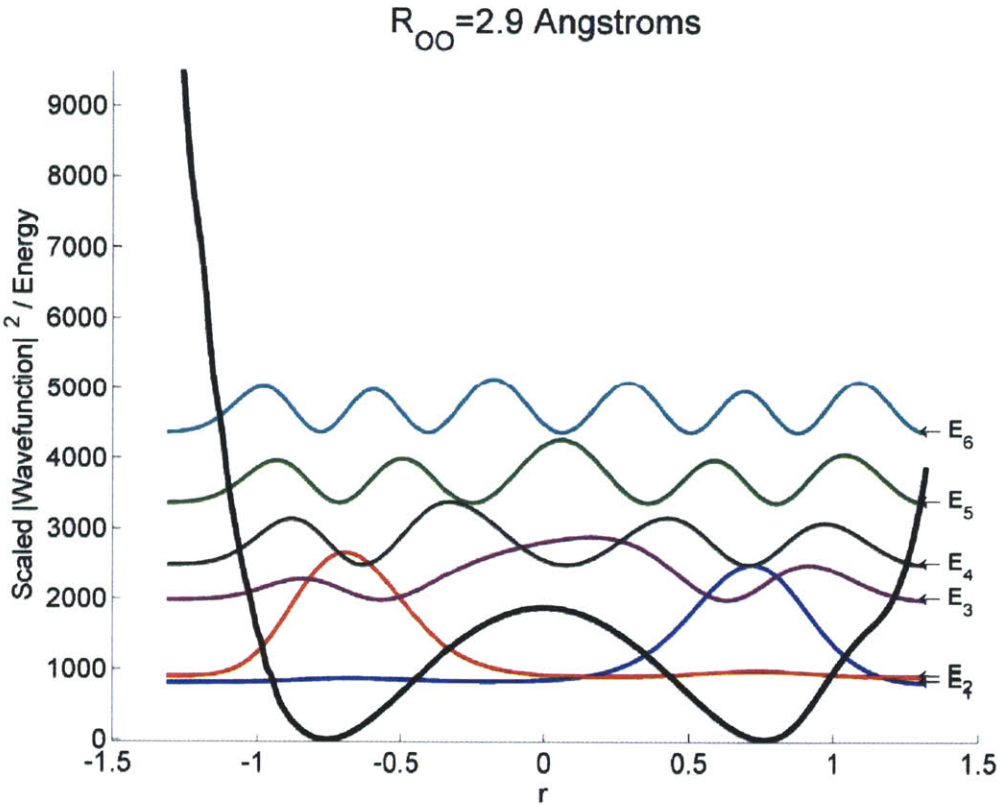

Figure 17: Degeneracy in equally shared proton for $H_3O_2^-$

We then can map as described and plot out transition frequencies as a function of internuclear distance:

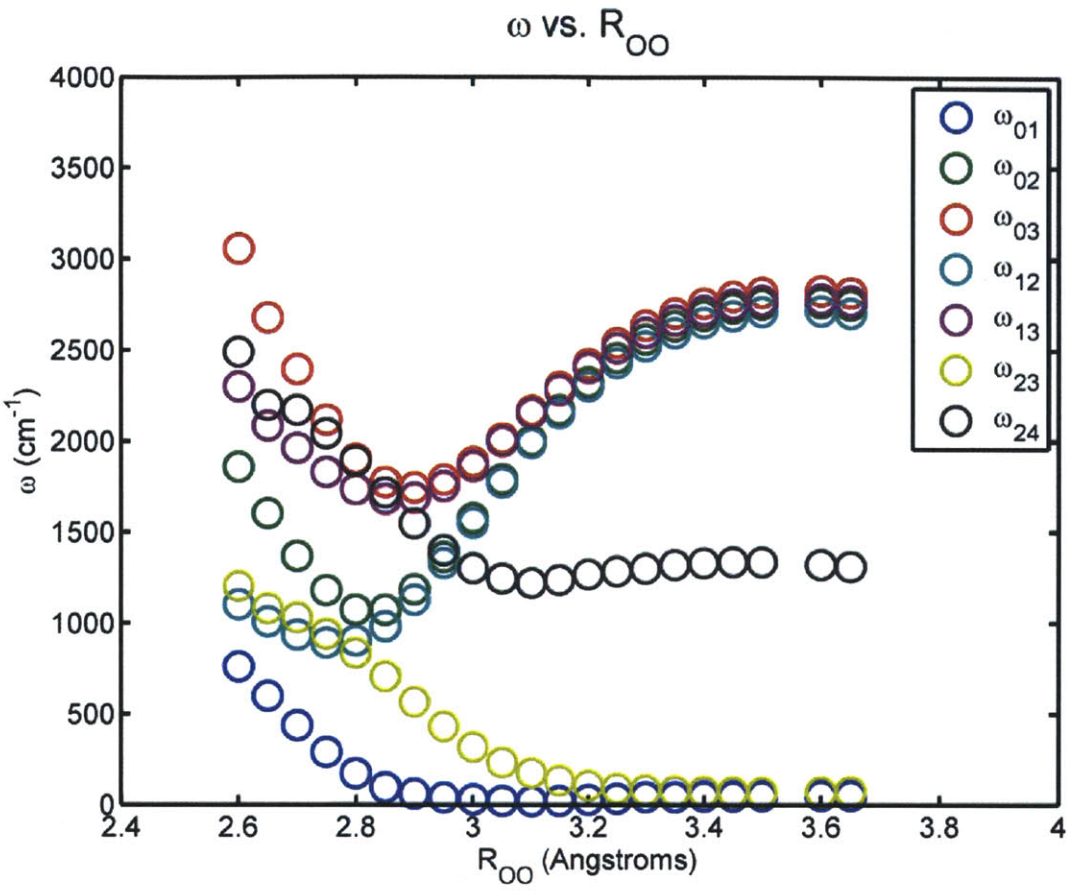

Figure 18: Calculated vibrational stretching frequencies for $H_3O_2^-$ as a function of OO distance

Because of the degeneracies due to the symmetry here, I have chosen to plot a significantly larger number of possible transitions, as the 0→1 transition goes to zero when the proton potential takes the form of two distinct wells.

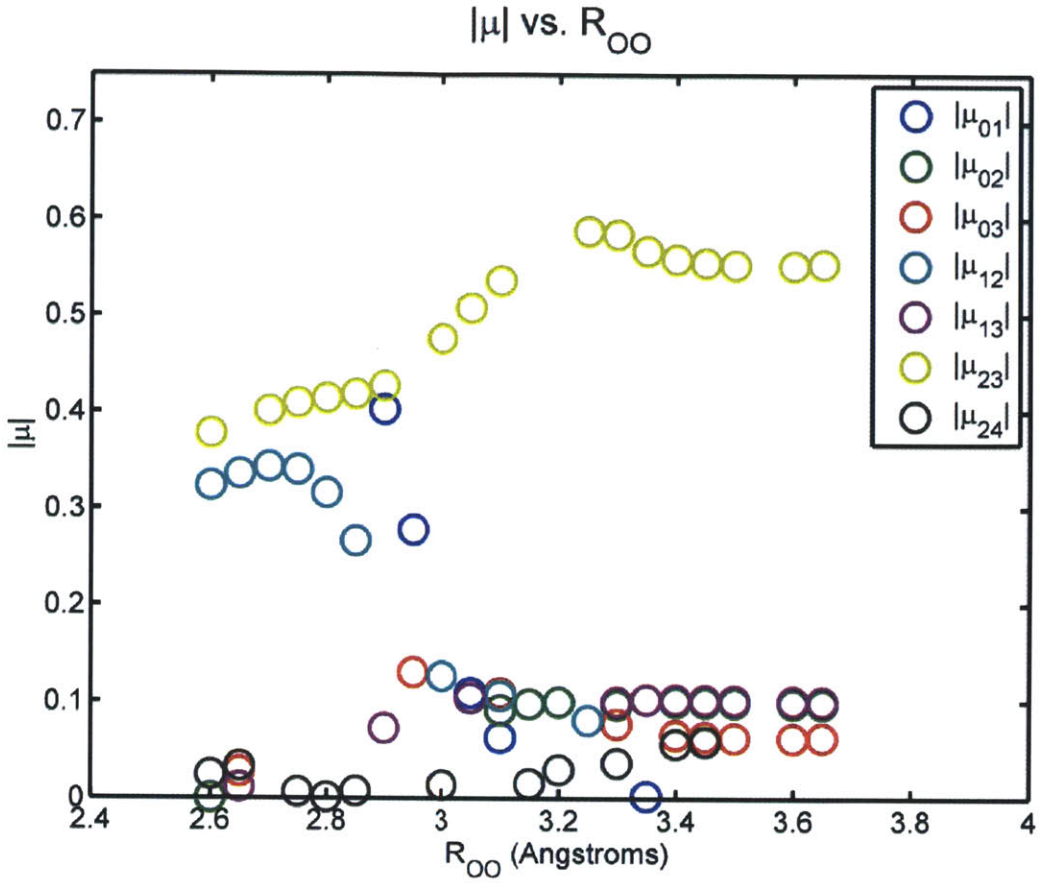

Figure 19: Calculated stretching transition dipoles for $H_3O_2^-$ as a function of OO distance

As we can see here, the dipole strengths of the 0→1 , 1→2, and 2→3 transitions come out as the largest, and thus these transitions may dominate the absorption. All of these stretching frequencies, however, are low in frequency, dipping well below 1500 cm^{-1} for small to mid OO distances. The other transition dipoles remain low, and we begin to see the complexity of the higher vibrational levels, and likely are beginning to enter a regime where more careful, higher level calculations are required, and the neglecting of other solvent molecules likely plays a significant factor here.

After considering the absence of a proton in water, it is also worth considering the effects of an additional proton. The structure of the solvated excess proton defect in the hyperdense hydrogen-bound network of water molecules has been the subject of much controversy, and rightfully so, as this structure is inherently tied to the dynamics of aqueous proton transfer. The current thinking is dominated by two limiting structural motifs: the Eigen cation (H_3O^+ or solvated as $H_9O_4^+$) species, where a proton is largely localized on one water molecule which is triply coordinated, and the Zundel ($H_5O_2^+$) species where it is shared

between a pair of water molecules. As another example, this sort of mapping can also be applied to this Zundel ion, $H_5O_2^+$, as shown in Figure 20and Figure 21 [62-70].

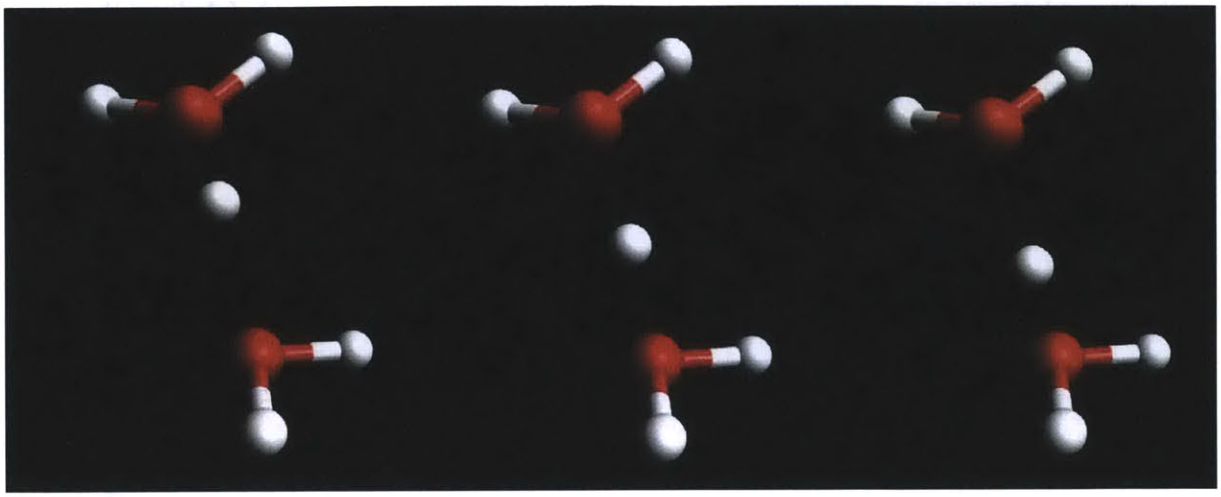

Figure 20: Proton transfer in a Zundel ion

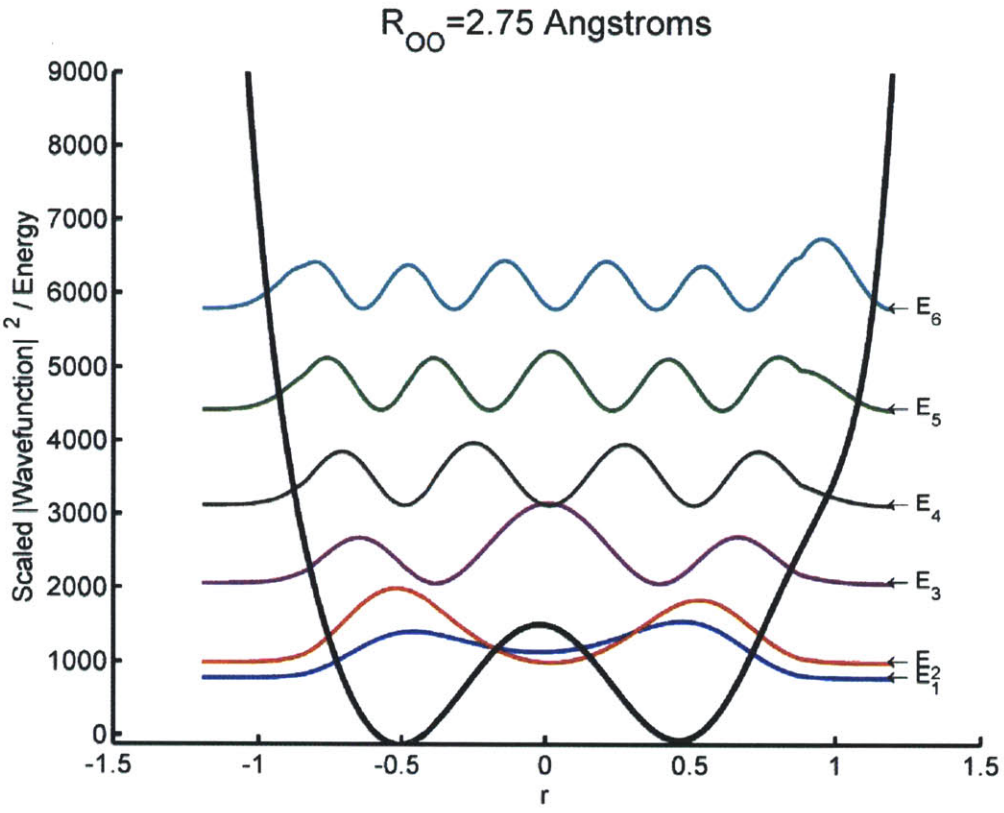

Figure 21: Sample calculated Zundel ion proton potential

For this sample calculated Zundel ion potential, obtained as before with the medium size B3LYP/6-31G(d) functional in the Gaussian 03 software package, the barrier height and well curvature can make it as such that the proton is effectively delocalized even in the ground state. A shared proton like this experiencing various amounts of asymmetry in its potential would appear as a broad IR continuum band spanning many different frequencies, and indeed, the addition of acids to water brings about a few key changes in the IR spectrum, shown in Figure 22 - notably a broad shoulder in the low frequency of the O-H stretch band (normally centered at 3400 cm^{-1}), as well as changes in the stretch and bend regions (1650 cm^{-1} and below), and the development of a broad continuum band between the water OH stretch and the H-O-H bend regions [71, 72]. For the Zundel species, there is evidence of a rather large amount of proton "rattling" between the oxygens (from both computational work and spectroscopy of gas phase clusters), adding IR intensity in the region between the water –OH stretch and bend modes, 1600-3400 cm^{-1}, and it is generally agreed that the intermolecular O---H^+---O Zundel ion stretch and bend peaks lie in the 900-

1200 cm^{-1} regions of the spectrum, respectively, with most results identifying 1200 cm^{-1} as band center for ν(OHO) of $H_5O_2^+$ [68, 69, 73-78].

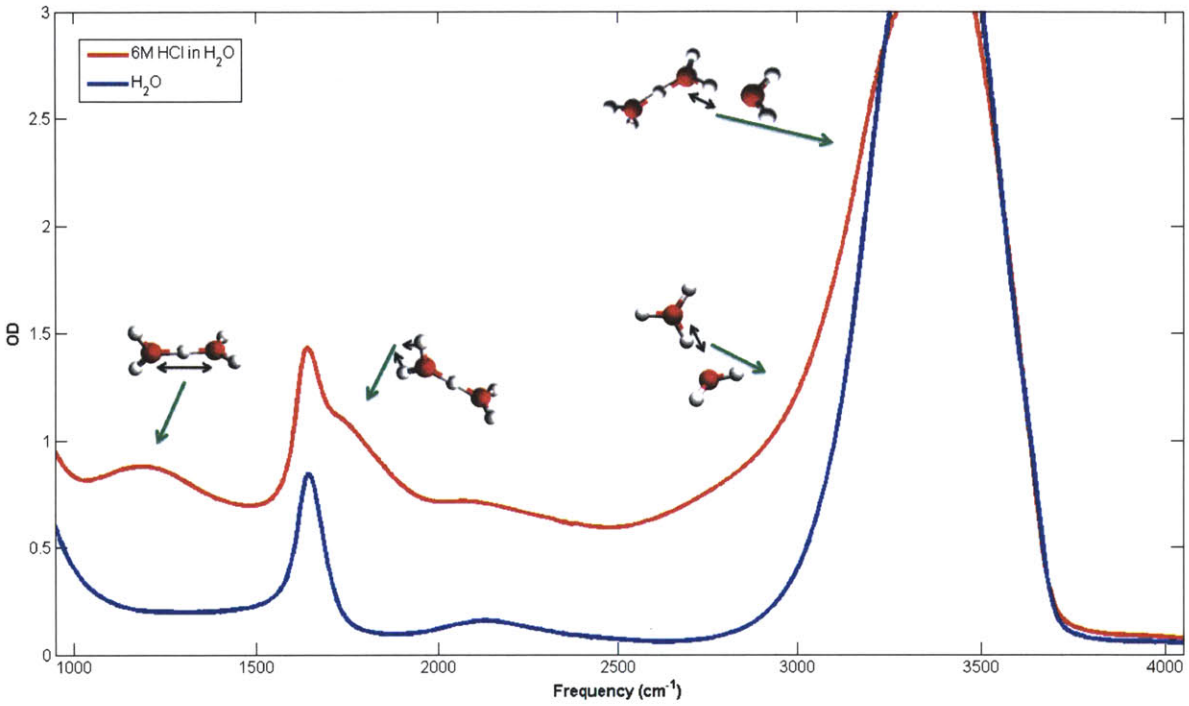

Figure 22: Mid-IR spectrum of HCl in H_2O with proposed Eigen and Zundel vibrational contributions

This sort of broad continuum absorption hints that many different proton potentials may be sampled over a short time span, as a large variety of different vibrational transition frequencies are present, and thus to gain a full understanding of the way these potentials interconvert and change, we need to also consider the dynamics which make this possible. The strong correlation between water's hydrogen bonding network and the motion and stability of the aqueous proton highlights the subtle interplay between structure and dynamics which makes the study of water so complicated, as a complete understanding of one requires a clear picture of the other simultaneously. The next chapter will focus on methods for describing these dynamics, focusing on modeling the bath and its influence on the proton potential itself.

1. Tokmakoff, A., *Time-Dependent Quantum Mechanics and Spectoscopy Notes*. 2003-2011.
2. Nitzan, A., *Chemical dynamics in condensed phases : relaxation, transfer and reactions in condensed molecular systems*. Oxford graduate texts. 2006, Oxford ; New York: Oxford University Press. xxii, 719 p.
3. Berne, B.J. and G.D. Harp, *On the Calculation of Time Correlation Functions*, in *Advances in Chemical Physics*. 2007, John Wiley & Sons, Inc. p. 63-227.
4. Barocchi, F., M. Moraldi, and M. Zoppi, *"Almost classical" many-body systems: The quantum-mechanical corrections to the moments of a general spectrum.* Physical Review A, 1982. **26**(4): p. 2168-2177.
5. Egorov, S.A., K.F. Everitt, and J.L. Skinner, *Quantum Dynamics and Vibrational Relaxation.* The Journal of Physical Chemistry A, 1999. **103**(47): p. 9494-9499.
6. Schatz, G.C. and M.A. Ratner, *Quantum mechanics in chemistry*. 2002, Mineola, N.Y.: Dover Publications. xix, 361 p.
7. Gottfried, K. and T.-m. Yan, *Quantum mechanics : fundamentals*. 2nd ed. Graduate texts in contemporary physics. 2003, New York: Springer. xvii, 620 p.
8. Cohen-Tannoudji, C., B. Diu, and F. Laloë, *Quantum mechanics*. 2005, New York, Paris: Wiley; Hermann. 2 v. (xv, 1524 p.).
9. Jordan, T.F., *Linear operators for quantum mechanics*. 1968, New York,: Wiley. x, 144 p.
10. Stone, M.H., *Linear transformations in Hilbert space and their applications to analysis*. 1932, New York,: The American Mathematical Society. viii, 622 p.
11. Berberian, S.K., *Introduction to Hilbert space*. 1961, New York,: Oxford University Press. 206 p.
12. Young, N., *An introduction to Hilbert space*. 1988, Cambridge [England] ; New York: Cambridge University Press. 239 p.
13. Butcher, P.N. and D. Cotter, *The elements of nonlinear optics*. Cambridge studies in modern optics 9. 1990, Cambridge ; New York: Cambridge University Press. xiv, 344 p.
14. Boyd, R.W., *Nonlinear optics*. 3rd ed. 2008, Amsterdam ; Boston: Academic Press. xix, 613 p.
15. Shen, Y.R., *The Principles of Nonlinear Optics*. Wiley classics library ed. 2003, Hoboken, N.J.: Wiley-Interscience. xii, 563 p.
16. Bloembergen, N., *Nonlinear Optics*. 4th ed. 1996, Singapore ; River Edge, NJ: World Scientific. xiii, 172 p.
17. Mukamel, S., *Principles of nonlinear optical spectroscopy*. 1995, New York: Oxford University Press. xviii, 543 p.
18. Williams, G., *Time-Correlation Functions and Molecular-Motion.* Chemical Society Reviews, 1978. **7**(1): p. 89-131.
19. Jansen, T.l.C., et al., *Stochastic Liouville equations for hydrogen-bonding fluctuations and their signatures in two-dimensional vibrational spectroscopy of water.* The Journal of Chemical Physics, 2005. **123**(11): p. 114504-11.
20. Loparo, J.J., et al., *Variation of the transition dipole moment across the OH stretching band of water.* Chemical Physics, 2007. **341**(1–3): p. 218-229.
21. Knop, S., et al., *On the nature of OH-stretching vibrations in hydrogen-bonded chains: Pump frequency dependent vibrational lifetime.* Physical Chemistry Chemical Physics, 2011. **13**(10).
22. Schmidt, J.R., S.A. Corcelli, and J.L. Skinner, *Pronounced non-Condon effects in the ultrafast infrared spectroscopy of water.* The Journal of Chemical Physics, 2005. **123**(4): p. 044513-13.
23. Nicodemus, R.A., et al., *Hydrogen Bond Rearrangements in Water Probed with Temperature-Dependent 2D IR.* The Journal of Physical Chemistry Letters, 2010. **1**(7): p. 1068-1072.
24. Ramasesha, K., et al., *Ultrafast 2D IR anisotropy of water reveals reorientation during hydrogen-bond switching.* The Journal of Chemical Physics, 2011. **135**(5): p. 054509-11.
25. Roberts, S.T., et al., *Proton Transfer in Concentrated Aqueous Hydroxide Visualized Using Ultrafast Infrared Spectroscopy.* The Journal of Physical Chemistry A, 2011. **115**(16): p. 3957-3972.

26. Piryatinski, A. and J.L. Skinner, *Determining Vibrational Solvation-Correlation Functions from Three-Pulse Infrared Photon Echoes†.* The Journal of Physical Chemistry B, 2002. **106**(33): p. 8055-8063.
27. Schmidt, J.R. and S.A. Corcelli, *Infrared absorption line shapes in the classical limit: A comparison of the classical dipole and fluctuating frequency approximations.* The Journal of Chemical Physics, 2008. **128**(18): p. 184504-7.
28. Roberts, S.T.S.T., *Hydrogen bond rearrangements and the motion of charge defects in water viewed using multidimensional ultrafast infrared spectroscopy*, in *Department of Chemistry.* 2010, Massachusetts Institute of Technology. : Cambridge, MA.
29. Huggins, M.L., *Hydrogen Bridges in Ice and Liquid Water.* The Journal of Physical Chemistry, 1935. **40**(6): p. 723-731.
30. Perrin, C.L., *Are Short, Low-Barrier Hydrogen Bonds Unusually Strong?* Accounts of Chemical Research, 2010. **43**(12): p. 1550-1557.
31. Colbert, D.T. and W.H. Miller, *A novel discrete variable representation for quantum mechanical reactive scattering via the S-matrix Kohn method.* The Journal of Chemical Physics, 1992. **96**(3): p. 1982-1991.
32. Kumar, R., J.R. Schmidt, and J.L. Skinner, *Hydrogen bonding definitions and dynamics in liquid water.* The Journal of Chemical Physics, 2007. **126**(20): p. 204107-12.
33. Steiner, T., *The hydrogen bond in the solid state.* Angewandte Chemie-International Edition, 2002. **41**(1): p. 48-76.
34. Novoa, J.J. and C. Sosa, *Evaluation of the Density Functional Approximation on the Computation of Hydrogen Bond Interactions.* The Journal of Physical Chemistry, 1995. **99**(43): p. 15837-15845.
35. Wendler, K., et al., *Estimating the Hydrogen Bond Energy.* The Journal of Physical Chemistry A, 2010. **114**(35): p. 9529-9536.
36. Ireta, J., J. Neugebauer, and M. Scheffler, *On the Accuracy of DFT for Describing Hydrogen Bonds: Dependence on the Bond Directionality.* The Journal of Physical Chemistry A, 2004. **108**(26): p. 5692-5698.
37. Sholl, D.S. and J.A. Steckel, *Density functional theory : a practical introduction.* 2009, Hoboken, N.J.: Wiley. xii, 238 p.
38. Becke, A.D., *Density-functional thermochemistry. III. The role of exact exchange.* The Journal of Chemical Physics, 1993. **98**(7): p. 5648-5652.
39. Frisch, M.J., et al., *Gaussian 03, Revision C.02.* 2003.
40. Shao, Y., et al., *Advances in methods and algorithms in a modern quantum chemistry program package.* Physical Chemistry Chemical Physics, 2006. **8**(27).
41. Feyereisen, M.W., D. Feller, and D.A. Dixon, *Hydrogen Bond Energy of the Water Dimer.* The Journal of Physical Chemistry, 1996. **100**(8): p. 2993-2997.
42. Xantheas, S.S., *Quantitative Description of Hydrogen Bonding in Chloride − Water Clusters.* The Journal of Physical Chemistry, 1996. **100**(23): p. 9703-9713.
43. Del Bene, J.E., W.B. Person, and K. Szczepaniak, *Properties of Hydrogen-Bonded Complexes Obtained from the B3LYP Functional with 6-31G(d,p) and 6-31+G(d,p) Basis Sets: Comparison with MP2/6-31+G(d,p) Results and Experimental Data.* The Journal of Physical Chemistry, 1995. **99**(27): p. 10705-10707.
44. Lozynski, M., D. Rusinska-Roszak, and H.-G. Mack, *Hydrogen Bonding and Density Functional Calculations: The B3LYP Approach as the Shortest Way to MP2 Results.* The Journal of Physical Chemistry A, 1998. **102**(17): p. 2899-2903.
45. Lee, C., W. Yang, and R.G. Parr, *Development of the Colle-Salvetti correlation-energy formula into a functional of the electron density.* Physical Review B, 1988. **37**(2): p. 785-789.
46. Cramer, C.J., *Essentials of computational chemistry : theories and models.* 2nd ed. 2004, Chichester, West Sussex, England ; Hoboken, NJ: Wiley. xx, 596 p.

47. Peterson, K.A. and J.T.H. Dunning, *Benchmark calculations with correlated molecular wave functions. VII. Binding energy and structure of the HF dimer.* The Journal of Chemical Physics, 1995. **102**(5): p. 2032-2041.
48. Scheiner, S., *AB Initio Studies of Hydrogen Bonds: The Water Dimer Paradigm.* Annual Review of Physical Chemistry, 1994. **45**(1): p. 23-56.
49. Head-Gordon, T. and G. Hura, *Water Structure from Scattering Experiments and Simulation.* Chemical Reviews, 2002. **102**(8): p. 2651-2670.
50. Laasonen, K., et al., *``Ab initio'' liquid water.* The Journal of Chemical Physics, 1993. **99**(11): p. 9080-9089.
51. Sprik, M., J. Hutter, and M. Parrinello, *Ab initio molecular dynamics simulation of liquid water: Comparison of three gradient-corrected density functionals.* The Journal of Chemical Physics, 1996. **105**(3): p. 1142-1152.
52. Paesani, F., S.S. Xantheas, and G.A. Voth, *Infrared Spectroscopy and Hydrogen-Bond Dynamics of Liquid Water from Centroid Molecular Dynamics with an Ab Initio-Based Force Field.* The Journal of Physical Chemistry B, 2009. **113**(39): p. 13118-13130.
53. Park, K., W. Lin, and F. Paesani, *A Refined MS-EVB Model for Proton Transport in Aqueous Environments.* The Journal of Physical Chemistry B, 2011. **116**(1): p. 343-352.
54. VandeVondele, J., et al., *The influence of temperature and density functional models in ab initio molecular dynamics simulation of liquid water.* The Journal of Chemical Physics, 2005. **122**(1): p. 014515-6.
55. Willow, S.Y., N.J. Singh, and K.S. Kim, *NH4+ Resides Inside the Water 20-mer Cage As Opposed to H3O+, Which Resides on the Surface: A First Principles Molecular Dynamics Simulation Study.* Journal of Chemical Theory and Computation, 2011. **7**(11): p. 3461-3465.
56. Cheng, H.-P., *The motion of protons in water--ammonia clusters.* The Journal of Chemical Physics, 1996. **105**(16): p. 6844-6855.
57. Li, Y. and J.M. Farrar, *Proton transfer dynamics of the reaction H[sub 3]O[sup +](NH[sub 3],H[sub 2]O)NH[sub 4][sup +] studied using the crossed molecular beam technique.* The Journal of Chemical Physics, 2004. **120**(1): p. 199-205.
58. Park, S.-C., et al., *Unique Chemistry at Ice Surfaces: Incomplete Proton Transfer in the H3O+–NH3 System.* Angewandte Chemie, 2001. **113**(8): p. 1545-1548.
59. Roberts, S.T., et al., *Observation of a Zundel-like transition state during proton transfer in aqueous hydroxide solutions.* Proceedings of the National Academy of Sciences, 2009. **106**(36): p. 15154-15159.
60. Diken, E.G., et al., *Fundamental Excitations of the Shared Proton in the H3O2- and H5O2+ Complexes.* The Journal of Physical Chemistry A, 2005. **109**(8): p. 1487-1490.
61. Stanton, R.V. and J.K.M. Merz, *Density functional study of symmetric proton transfers.* The Journal of Chemical Physics, 1994. **101**(8): p. 6658-6665.
62. Berkelbach, T.C., H.-S. Lee, and M.E. Tuckerman, *Concerted Hydrogen-Bond Dynamics in the Transport Mechanism of the Hydrated Proton: A First-Principles Molecular Dynamics Study.* Physical Review Letters, 2009. **103**(23): p. 238302.
63. Day, T.J.F., U.W. Schmitt, and G.A. Voth, *The Mechanism of Hydrated Proton Transport in Water.* Journal of the American Chemical Society, 2000. **122**(48): p. 12027-12028.
64. Headrick, J.M., et al., *Spectral Signatures of Hydrated Proton Vibrations in Water Clusters.* Science, 2005. **308**(5729): p. 1765-1769.
65. Kornyshev, A.A., et al., *Kinetics of Proton Transport in Water.* The Journal of Physical Chemistry B, 2003. **107**(15): p. 3351-3366.
66. Marx, D., et al., *The nature of the hydrated excess proton in water.* Nature, 1999. **397**(6720): p. 601-604.
67. Park, M., et al., *Eigen and Zundel Forms of Small Protonated Water Clusters: Structures and Infrared Spectra.* The Journal of Physical Chemistry A, 2007. **111**(42): p. 10692-10702.

68. Vuilleumier, R. and D. Borgis, *Transport and spectroscopy of the hydrated proton: A molecular dynamics study.* The Journal of Chemical Physics, 1999. **111**(9): p. 4251-4266.
69. Borgis, D., G. Tarjus, and H. Azzouz, *An adiabatic dynamical simulation study of the Zundel polarization of strongly H-bonded complexes in solution.* The Journal of Chemical Physics, 1992. **97**(2): p. 1390-1400.
70. Schuster, P., G. Zundel, and C. Sandorfy, *The Hydrogen bond: recent developments in theory and experiments*. 1976, Amsterdam: North-Holland.
71. Zundel, G., *Hydrogen Bonds with Large Proton Polarizability and Proton Transfer Processes in Electrochemistry and Biology*, in *Advances in Chemical Physics*, S.A.R. I. Prigogine, Editor. 2007. p. 1-217.
72. Zundel, G. and M. Eckert, *IR continua of hydrogen bonds and hydrogen-bonded systems, calculated proton polarizabilities and line spectra.* Journal of Molecular Structure: THEOCHEM, 1989. **200**: p. 73-92.
73. Markovitch, O., et al., *Special Pair Dance and Partner Selection: Elementary Steps in Proton Transport in Liquid Water.* The Journal of Physical Chemistry B, 2008. **112**(31): p. 9456-9466.
74. Borgis, D. and J.T. Hynes, *Dynamical theory of proton tunneling transfer rates in solution: general formulation.* Chemical Physics, 1993. **170**(3): p. 315.
75. Wu, Y., et al., *An Improved Multistate Empirical Valence Bond Model for Aqueous Proton Solvation and Transport†.* The Journal of Physical Chemistry B, 2007. **112**(2): p. 467-482.
76. Gardenier, G.H., M.A. Johnson, and A.B. McCoy, *Spectroscopic Study of the Ion−Radical H-Bond in H4O2+†.* The Journal of Physical Chemistry A, 2009. **113**(16): p. 4772-4779.
77. Roscioli, J.R., L.R. McCunn, and M.A. Johnson, *Quantum Structure of the Intermolecular Proton Bond.* Science, 2007. **316**(5822): p. 249-254.
78. Shin, J.-W., et al., *Infrared Signature of Structures Associated with the H+(H2O)n (n = 6 to 27) Clusters.* Science, 2004. **304**(5674): p. 1137-1140.

Chapter 3 : Open Quantum Systems and the Langevin Approach: The Bath

In the previous chapter, methods for evaluating and mapping static spectroscopic variables were discussed – focusing on the vibrational energy gaps and transition dipole moments. These variables were mapped to a variety of model parameters, including double well asymmetry and internuclear distance. The discussion which follows focuses on a dynamical description of the bath which influences the time evolution of these spectroscopic variables. The dominant approach in this chapter is that of Langevin-type equations which treat parts of the bath stochastically, allowing us to write equations of motion for quantum variables in open dissipative systems and calculate the associated correlation functions. We will also examine the useful concept of a bath spectral density and see how this connects to the Langevin approach. This chapter will ultimately bring us to the Brownian oscillator model for the bath and a discussion of its usefulness in modeling strongly hydrogen bonded systems.

Open Quantum Systems

Condensed phase quantum systems, such as a chemical bond surrounded by a collection of solvent molecules, are very often described using a conceptual model consisting of one or a few dynamical variables of interest in contact with a large environment containing many more or infinite degrees of freedom. The choice of "variables of interest" or the "system of interest" is often dictated by what is experimentally accessible (say, for instance, a spectroscopic observable such as the vibrational frequency of a bond), and it is the physical properties of this small system about which we care. To utilize this conceptual partitioning framework, we must treat the quantum system of interest as open, as the interaction between the system and the environment allows for energy and information flow. The system of interest and the external environment (sometimes called the reservoir or the bath) together are part of a larger closed quantum system [1-3].

Langevin Approach

The most common approach to characterize the dynamics of a classical open system is that of the Langevin equation, developed by Paul Langevin as an alternate description of the Brownian motion problem of Einstein and Smoluchowski [4-6]. Langevin managed to establish a stochastic description of Brownian motion by way of careful elimination of bath variables, creating fluctuation terms through which bath variables manifest themselves. In this framework, there is a single degree of freedom q(t) and

an environment which interacts with it via two forces: a frictional force γ (sometimes divided by mass for convenience) which dissipates energy from the system into a bath and a stochastic fluctuating force ξ(t) through which the bath variables interact. In the absence of an external driving force, this interaction with the bath takes the system from an initial state to thermal equilibrium. Note that the presence of a friction term inherently implies that momentum and kinetic energy are transferred to the bath - that is, energy is dissipated out of the system.

Various restrictions can be imposed upon this stochastic force, but to strictly be a "Langevin force" as applied to Brownian motion ξ(t) is generally is considered to be white noise, irregular and unpredictable but with certain properties (namely properties of its moments):

1) It is a stochastic process (that is, for stochastic variable X, $\xi(t) = f(X,t)$ and properties averaged over an ensemble are predictable.

2) $\xi(t)$ acts as an external force with a vanishing average $\langle \xi(t) \rangle = 0$.

3) The autocorrelation function of this force is postulated such that successive collisions are uncorrelated so $\langle \xi(t)\xi(t') \rangle \propto \delta(t-t')$ [4].

This lumping of the bath into a stochastic force is justified when the bath interactions are so fast that they reach equilibrium instantaneously (the so called "repeated randomness assumption"). For such a white noise source with a stochastic force due only to a heat reservoir with no memory (that is, δ-correlated in time) and an optional applied external potential V(q,t) (which in general may be time dependant as well) the differential equation of motion is [4, 7]

$$M\ddot{q}(t) + M\gamma\dot{q}(t') + V'(q,t) = \xi(t) \tag{3.1}$$

Where $V'(q,t) = \frac{\partial}{\partial q} V(q,t)$. If the reservoir is a source of noise which has some finite memory (so-called colored noise), this is generally characterized as a Langevin-like equation and the system dynamics evolve according to the phenomenological stochastic differential equation

$$M\ddot{q}(t) + M\int_{-\infty}^{t} dt'\gamma(t-t')\dot{q}(t') + V'(q,t) = \xi(t) \tag{3.2}$$

which will be more rigorously justified shortly. The difference here lies in the time correlation of the friction term γ, which can also be nonlocal in space. When there is time dependence to this friction, we

often speak of the frequency-dependant dampening which is the Fourier transform of the time dependant friction term above

$$\tilde{\gamma}(\omega) \equiv \tilde{\gamma}'(\omega) + i\tilde{\gamma}''(\omega) = \int_{-\infty}^{\infty} dt\gamma(t)e^{i\omega t} \tag{3.3}$$

The so-called Green-Kubo relations connecting integrals of time correlation functions to transport coefficients allow us to connect this damping coefficient to the time autocorrelation function of the classical stochastic fluctuating force as [8-10]

$$\tilde{\gamma}(\omega) = \frac{1}{Mk_bT}\int_0^{\infty} dt\langle \xi(t)\xi(0)\rangle \cos(\omega t) \tag{3.4}$$

It makes sense that frictional force should be related to the random force, as both come from the same source: the bath. Random collisions with bath molecules when a particle is stationary manifest themselves through $\xi(t)$, and the random collision effects that lead to drag when a particle is moving through the same bath lead to $\gamma(t)$. The relation between the systematic friction and random force interactions of the bath is described by the so-called fluctuation-dissipation theorem, which has been discussed in more detail elsewhere. Briefly, the fluctuation-dissipation theorem ties the dissipative portion of these microscopic forces from the bath, $\gamma(t)$ and $\xi(t)$, which can also be characterized with a correlation function (discussed later with, for example, equations (3.38) and (3.39)) to the response of that system to an external disturbance [11-13].

It is somewhat of a misnomer to refer to the stochastic force term as "random," and a few other properties of this term are worth discussing. First, $\xi(t)$ does not in any way depend on the system coordinate. It is, in a phase space sense, "orthogonal" to the dynamics of the system. It is also somewhat misleading to consider this force as nondeterministic – the force is in fact fully defined by initial positions and momenta, although these initial conditions are oftentimes impossible to know. Instead we commonly describe the statistical distribution of these initial conditions, which still can tell us a great amount about the behavior.

BATH OF HARMONIC OSCILLATORS

It is typical to partition the classical system Hamiltonian into three parts: a system (S) containing the variables of interest, a bath (B) which interacts with this system, and an interaction (I) term describing the coupling between these two. This is written as [14]

$$H = H_S + H_B + H_I \tag{3.5}$$

Where we have the system Hamiltonian with degree of freedom q and conjugate momentum p and mass M

$$H_S = \frac{p^2}{2M} + V(q) \tag{3.6}$$

And the bath, here consisting of N harmonic oscillators each described by oscillator position x_α and momenta p_α with oscillator frequency ω_α and mass m_α

$$H_B = \sum_{\alpha=1}^{N}\left(\frac{1}{2}\frac{p_\alpha^2}{m_\alpha} + \frac{1}{2}m_\alpha\omega_\alpha^2 x_\alpha^2\right) \tag{3.7}$$

Notice that in this notation p refers to the momentum corresponding to the system degree of freedom while p_α refers to the momentum of the α^{th} bath harmonic oscillator. This notation is standard in the literature and is used for this reason and generally does not lead to confusion. Occasionally one sees the system variables as (Q, P, M) with bath variables as (q_α, p_α, m_α) which is clearer. For a single harmonic oscillator as the system degree of freedom, oftentimes $q = x - \bar{x}$. It is worth noting that is approximation – that is, a reservoir of harmonic oscillators, has been shown to be rather general and provide a good description of low temperature environments in a variety of systems [15-18].

We then also introduce an interaction term, in the simplest case linear in bath coordinates

$$H_I = -\sum_{\alpha=1}^{N} F_\alpha(q)x_\alpha + \Delta V(q) \tag{3.8}$$

where the counter term $\Delta V(q)$ is added to renormalize the potential due to the linear coupling term and each $F_\alpha(q)$ describes the coupling of the system degree of freedom to each bath mode. Without this counter term, the minimum of the potential at a given q value is $x_\alpha = \frac{F_\alpha(q)}{m_\alpha\omega_\alpha^2}$. For simple dissipation only without renormalization,

$$\Delta V(q) = \frac{1}{2}\sum_{\alpha=1}^{N}\frac{F_\alpha^2(q)}{m_\alpha\omega_\alpha^2} \tag{3.9}$$

One special case of interaction that is often of interest is that of a separable interaction with the bath, where each bath mode couples in the same way to the system degree of freedom

$$F_\alpha(q) = c_\alpha F(q) \tag{3.10}$$

Which applies in the case of state-independent dissipation (linear dissipation) where F(q)=q and thus

$$F_\alpha(q) = c_\alpha q \tag{3.11}$$

resulting in a coupling of the form $q\sum_{\alpha=1}^{N} c_\alpha x_\alpha$. This sort of coupling is typically referred to as "bilinear" (sometimes it is also called the Caldeira-Leggett model or the Zwanzig-Caldeira-Leggett model). With a separable interaction (but not necessarily bilinear coupling), we obtain the total Hamiltonian of the form

$$H = \underbrace{\frac{p^2}{2M} + V(q,t)}_{System} + \underbrace{\sum_{\alpha=1}^{N}\left(\frac{1}{2}\frac{p_\alpha^2}{m_\alpha} + \frac{1}{2}m_\alpha\omega_\alpha^2 x_\alpha^2\right)}_{Harmonic\ bath} - \underbrace{F(q)\sum_{\alpha=1}^{N} c_\alpha x_\alpha}_{Coupling} + \underbrace{\frac{F(q)^2}{2}\sum_{\alpha=1}^{N}\frac{c_\alpha^2}{m_\alpha\omega_\alpha^2}}_{Counter\ term} \tag{3.12}$$

or

$$H = \underbrace{\frac{p^2}{2M} + V(q,t)}_{System} + \underbrace{\frac{1}{2}\sum_{\alpha=1}^{N}\left[\frac{p_\alpha^2}{m_\alpha} + m_\alpha\omega_\alpha^2\left(x_\alpha - F(q)\frac{c_\alpha^2}{m_\alpha\omega_\alpha^2}\right)^2\right]}_{Bath+couplings} \tag{3.13}$$

In the general case of separable interaction as in (3.10), we can take Hamilton's equations of motion of the form [19]

$$\begin{aligned}
\dot{q} &= \frac{\partial H}{\partial p} = \frac{p}{M} \\
\dot{p} &= -\frac{\partial H}{\partial q} = -\frac{\partial V(q,t)}{\partial q} + \frac{\partial F(q)}{\partial q}\sum_{\alpha=1}^{N} c_\alpha\left(x_\alpha - F(q)\frac{c_\alpha^2}{m_\alpha\omega_\alpha^2}\right) \\
\dot{x}_\alpha &= \frac{\partial H}{\partial p_\alpha} = \frac{p_\alpha}{m_\alpha} \\
\dot{p}_\alpha &= -\frac{\partial H}{\partial x_\alpha} = -m_\alpha\omega_\alpha^2 x_\alpha + c_\alpha F(q)
\end{aligned} \tag{3.14}$$

and rewrite as a second order differential equation, as is standard, to obtain

$$M\ddot{q} + \frac{\partial V(q,t)}{\partial q} + \sum_{\alpha=1}^{N}\frac{c_\alpha^2}{m_\alpha\omega_\alpha^2}F(q)\frac{\partial F(q)}{\partial q} = \frac{\partial F(q)}{\partial q}\sum_{\alpha=1}^{N} c_\alpha x_\alpha \tag{3.15}$$

$$m_\alpha \ddot{x}_\alpha + m_\alpha \omega_\alpha^2 x_\alpha = c_\alpha F(q) \tag{3.16}$$

As shown by Weiss, the use of Green's function techniques (Laplace transforms) for arbitrary initial values $x_\alpha(0)$ and $p_\alpha(0)$ at t=0 results in [7]

$$\begin{aligned} x_\alpha(t) &= x_\alpha(0)\cos(\omega_\alpha t) + \frac{p_\alpha(0)}{m_\alpha \omega_\alpha}\sin(\omega_\alpha t) \\ &+ \frac{c_\alpha}{m_\alpha \omega_\alpha}\int_0^t dt' \sin[\omega_\alpha (t-t')] F[q(t')] \end{aligned} \tag{3.17}$$

and using integration by parts we can get the solution for $x_\alpha(t)$ as a functional of the particle velocity. With this in hand it is then possible to return to the dynamical equation in (3.15) to get

$$\begin{aligned} &M\ddot{q}(t) + \frac{\delta F[q(t)]}{\delta q(t)}\int_0^t dt' \Theta(t-t')\sum_{\alpha=1}^{N}\left[\frac{c_\alpha^2}{m_\alpha \omega_\alpha^2}\cos[\omega_\alpha (t-t')]\right]\frac{\delta F[q(t)]}{\delta q(t)}\dot{q}(t') + \frac{\partial V(q)}{\partial q} \\ &= -M\frac{\delta F[q(t)]}{\delta q(t)}\gamma(t)F[q(0)] + \frac{\delta F[q(t)]}{\delta q(t)}\sum_{\alpha=1}^{N} c_\alpha\left[x_\alpha(0)\cos(\omega_\alpha t) + \frac{p_\alpha(0)}{m_\alpha \omega_\alpha}\sin(\omega_\alpha t)\right] \end{aligned} \tag{3.18}$$

Clearly this equation is hideous looking and one wonders why we would even bother to write it in such a form. But this form of the dynamical equations of motion is more clearly important if we define a memory dependant friction (obeying causality with the Heaviside step function)

$$\gamma(t-t') = \Theta(t-t')\frac{1}{M}\sum_{\alpha=1}^{N}\frac{c_\alpha^2}{m_\alpha \omega_\alpha^2}\cos[\omega_\alpha (t-t')] \tag{3.19}$$

This has the Fourier transform

$$\tilde{\gamma}(\omega) = \lim_{\epsilon \to 0+}\frac{-i\omega}{M}\sum_{\alpha=1}^{N}\frac{c_\alpha^2}{m_\alpha \omega_\alpha^2}\frac{1}{\omega_\alpha^2 - \omega^2 - i\epsilon\,\mathrm{sgn}(\omega)} \tag{3.20}$$

and random force

$$\zeta(t) = \sum_{\alpha=1}^{N} c_\alpha\left[x_\alpha(0)\cos(\omega_\alpha t) + \frac{p_\alpha(0)}{m_\alpha \omega_\alpha}\sin(\omega_\alpha t)\right] \tag{3.21}$$

Substituting these definitions in to (3.18) and shortening the normal and functional derivatives with the notation $V'(q) = \frac{\partial V(q)}{\partial q}$ and $F'[q(t)] = \frac{\delta F[q(t)]}{\delta q(t)}$ we see that we get a Langevin-type equation

$$\begin{aligned} M\ddot{q}(t) + MF'\int_0^t dt'\gamma(t-t')F'[q(t')]\dot{q}(t') + V'(q) \\ = F'[q(t)]\zeta(t) - MF'[q(t)]\gamma(t)F[q(0)] \end{aligned} \tag{3.22}$$

For the case of bilinear coupling, we can reduce this to obtain an ordinary Langevin equation with a friction force containing memory and a transient "slippage term" dependent upon the initial conditions

$$M\ddot{q}(t) + M\int_0^t dt'\gamma(t-t')\dot{q}(t') + V'(q) = \zeta(t) - M\gamma(t)q(0) \tag{3.23}$$

The initial value slip term $M\gamma(t)q(0)$ is often absorbed into a shifted random force

$$\xi(t) = \zeta(t) - M\gamma(t)q(0) \tag{3.24}$$

This gives the standard form of the GLE introduced in equation (3.2).

Environmental Spectral Density

For a particle coupled to a small finite number of oscillators (say, when N is O(10)), the bath reservoir does not truly lead to dissipation. To approximate a real heat bath, we instead introduce the spectral density of the environment which serves as a coupling strength weighted density of bath modes [7, 20]:

$$J(\omega) = \frac{\pi}{2}\sum_{\alpha=1}^{N}\frac{c_\alpha^2}{m_\alpha\omega_\alpha}\delta(\omega-\omega_\alpha) \tag{3.25}$$

If we take this as a smooth function of ω and move to the continuum bath limit, we can replace the sums as integrals, and using the relation [20]

$$\sum_{\alpha=1}^{N}\frac{c_\alpha^2}{m_\alpha\omega_\alpha}f(\omega_\alpha) \to \frac{2}{\pi}\int_0^\infty d\omega J(\omega)f(\omega) \tag{3.26}$$

we obtain a new form of the equation (3.20)

$$\tilde{\gamma}(\omega) = \lim_{\epsilon\to 0+}\frac{-i\omega}{M}\frac{2}{\pi}\int_0^\infty d\omega'\frac{J(\omega')}{\omega'}\frac{1}{\omega'^2-\omega^2-i\epsilon\,\mathrm{sgn}(\omega)} \tag{3.27}$$

or alternatively

$$\gamma(t) = \Theta(t)\frac{1}{M}\frac{2}{\pi}\int_0^\infty d\omega \frac{J(\omega)}{\omega}\cos(\omega t) \tag{3.28}$$

and the inverse of this gives

$$J(\omega) = M\omega\int_0^\infty dt\gamma(t)\cos(\omega t) \tag{3.29}$$

or defining the density of modes for a macroscopic system

$$g(\omega) = \sum_{\alpha=1}^{N}\delta(\omega-\omega_\alpha) \tag{3.30}$$

then defining the coupling density as

$$c^2(\omega)g(\omega) \equiv \sum_{\alpha=1}^{N} c_\alpha^2\delta(\omega-\omega_\alpha) \tag{3.31}$$

we can also write (3.25) as [21, 22]

$$J(\omega) = \frac{\pi}{2}\frac{1}{m}\frac{c^2(\omega)g(\omega)}{\omega} \tag{3.32}$$

Equations (3.28) and (3.29) are important results and we should take some time to consider their consequences. In this case of linear dissipation, that is, where the damping does not depend on the state of the system, the influence of the environment as characterized by the spectral density J(ω) serves to uniquely determine the damping kernel $\tilde{\gamma}(\omega)$ and vice versa. This spectral density can be determined analytically for various model systems, and its behavior can also often be inferred from classical motion. This friction kernel is in principle something that is fully microscopic and well defined, although actually obtaining this is often quite difficult (for the case of harmonic vibrations, projection operator methods have been used formally to derive these, but without a clear microscopic guide to the development). In addition, the sorts of couplings which contribute to a given spectral density can be molecularly motivated – for instance if there is a dominant intermolecular motion in a system, the corresponding vibrational modes can be expected to dominate J(ω).

To explicitly examine the frequency dependence of the frictional damping term, occasionally the Laplace transform $\hat{\gamma}(z)$ is introduced [23, 24]

$$\hat{\gamma}(z) = \mathcal{L}\{\gamma(t)\} = \int_0^\infty ds\gamma(t)e^{-st} \tag{3.33}$$

which, being careful with the domain of the damping functions via analytic continuation

$$\begin{aligned} \hat{\gamma}(z) &= \tilde{\gamma}(\omega = iz) \\ \tilde{\gamma}(\omega) &= \lim_{\epsilon \to 0+} \hat{\gamma}(z = \epsilon - i\omega) \end{aligned} \tag{3.34}$$

gives us

$$\begin{aligned} \hat{\gamma}(z) &= \frac{1}{M}\sum_{\alpha=1}^{N} \frac{c_\alpha^2}{m_\alpha \omega_\alpha^2} \frac{z}{(\omega_\alpha^2 + z^2)} \\ &\Rightarrow \frac{1}{M}\frac{2}{\pi}\int_0^\infty d\omega \frac{J(\omega)}{\omega} \frac{z}{(\omega^2 + z^2)} \end{aligned} \tag{3.35}$$

which can also be used to express the spectral density in term of this transformed damping kernel through inversion of (3.35)

$$J(\omega) = \lim_{\epsilon \to 0+} \frac{1}{2} M\omega\left[\hat{\gamma}(\epsilon + i\omega) + \hat{\gamma}(\epsilon - i\omega)\right] \tag{3.36}$$

These sort of classical damping terms have also been used to model a variety of systems, including for instance some involving explicit quantum mechanical variables such as rates of tunneling though barriers, often describing the dynamics in a manner analogous to what was shown in (3.14) [25, 26].

Connection to Correlation Functions

A particularly important example of the relationship between time correlation functions and stochastic observables is that the spectral density discussed in (3.25) is related to a time correlation function for the bath. For any observable, say bath A represented by a stochastic process x(t) which can be expanded in mass weighted harmonic normal modes with coordinates $\{u_j\}$

$$A(t) = \sum_\alpha c_\alpha^{(A)} u_j(t) \tag{3.37}$$

The correlation function is given by the harmonic oscillator equations of motion resulting in

$$C_{AA}(t) = k_B T \sum_{\alpha} \frac{\left(c_{\alpha}^{(A)}\right)^2}{\omega_{\alpha}^2} \cos(\omega_{\alpha} t)$$
$$\Rightarrow \frac{2k_B T}{\pi} \int_0^{\infty} d\omega \frac{J_A(\omega)}{\omega} \cos(\omega t) \tag{3.38}$$

Where J(ω) is indeed the bath spectral density, which also contains within the dynamics of the variable A [21]. This general connection between the time correlation function and the spectral density is the Wiener-Khinchin (sometimes Wiener-Khintchine or even Khinchin–Kolmogorov) theorem, proven in Nitzan Appendix 7D and van Kampen III.3, which says that the spectral density of a stochastic process is related to the Fourier transform of the corresponding time autocorrelation function [4, 21]

$$I_A(\omega) = \int_{-\infty}^{\infty} dt C_{AA}(t) e^{i\omega t}$$
$$C_{AA}(t) = \frac{1}{2\pi} \int_{-\infty}^{\infty} d\omega I_A(\omega) e^{-i\omega t} \tag{3.39}$$

For consistency with different literature notation styles we have defined

$$I_A(\omega) = \frac{k_B T}{\pi} \frac{J_A(\omega)}{\omega} \tag{3.40}$$

A third notation, with S(ω) as the "power spectrum" is sometimes used. Thus we see that the spectral density can be thought to measure the frequency content of the time variation of a stochastic variable and likewise the autocorrelation of this variable is the Fourier transform of the spectral density.

As an example, for an isotropic system of harmonic modes with N identical atoms, it can be shown that the density of normal modes (see (3.30)) is related to the atomic velocity time correlation function by [21]

$$\frac{g(\omega)}{N} = \frac{3m}{\pi k_B T} \int_{-\infty}^{\infty} dt e^{-i\omega t} \left\langle \dot{x}(0) \dot{x}(t) \right\rangle \tag{3.41}$$

This general connection between correlation functions (which are oftentimes accessible with classical dynamics simulations) and the spectral density has been applied broadly to a number of seemingly disparate systems. For instance, this relationship has been used to calculate the spectral density governing electron transfer in protein environments by calculating the time correlation function for the energy gap between reactant and product states which fluctuates due to thermal motion of the protein, highlighting the relationship between the rate of a chemical process and the motion of the bath environment in which it is embedded [27-29].

Ohmic Friction

We can think of the frequency dependant friction term $\tilde{\gamma}(\omega)$ as describing the timescales of the thermal motion of the bath, and in the case that these motions are all much faster than the oscillator of interest, they become independent of ω. It is common in the case of a harmonic oscillator to impose the condition of Ohmic damping, in which this friction is frequency independent, thus

$$\tilde{\gamma}(\omega) = \gamma \tag{3.42}$$

In this Ohmic regime (so named for similarities to the instance of a series resistor in an electrical circuit which shows a linear I-V curve starting at the origin, thus following Ohm's law) moving to the time domain shows that this corresponds to memory-less friction [14]

$$\gamma(t) = 2\gamma\delta(t) \tag{3.43}$$

For a clearer picture of the "Ohmic" designation, consider the simple example presented by Hanggi and Ingold of the response of the current δI in an electrical circuit when there is a voltage change δV [30]. The basic statement of Ohm's law for electrical circuits is that the current applied I is linearly proportional to the applied voltage V, where the constant of proportionality is the reciprocal of the resistance R. The general current response is determined by Y(ω), the transfer admittance (inverse impedance), which provides a mapping from force to motion such that

$$\delta I(\omega) = Y(\omega)\delta V(\omega) \tag{3.44}$$

In this form it is apparent that the admittance Y(ω) is identical to the susceptibility χ(ω). Here a damping kernel with memory γ(t) corresponds to a frequency dependence in the admittance Y(ω), while in the Ohmic case $Y(\omega) = \frac{1}{R}$ and thus the damping force is proportional only to the velocity, as is immediately evident in (3.1) [7, 12, 31].

If we return to the simple case of Ohmic frequency-independent damping in equation (3.42), where $\tilde{\gamma}(\omega) = \gamma$, this leads to Markovian damping terms in the classical equation of motion, which becomes

$$\ddot{q} + \gamma\dot{q} + \frac{1}{M}\frac{\partial}{\partial q}V = 0 \tag{3.45}$$

Using (3.29) we see that this form of the friction kernel we have a spectral density of the environment which is linear with frequency:

$$J(\omega) = M\gamma\omega \tag{3.46}$$

Clearly this completely memoryless friction is not entirely realistic, as a linearly increasing spectral density diverges instead of vanishes as $\omega \to \infty$ (this also leads to the divergence of certain parameters as which occur in classical Markov processes, for instance, here $\langle p^2 \rangle$ is logarithmically divergent). One reasonable constraint upon this result is to add a cutoff frequency ω_C and impose that the spectral density drop to zero exponentially for $\omega > \omega_C$ [21]

$$J(\omega) = M\gamma\omega e^{\left(-\frac{|\omega|}{\omega_c}\right)} \tag{3.47}$$

This model has been used, for instance, to model the optical Kerr effect in acetonitrile, which based upon Stokes shift data has a cutoff frequency of ~51 cm^{-1} [32].

Oftentimes this problem of divergence at high frequencies is also addressed through what is known as the Drude model (or Lorentz-Drude regularization) by incorporating a microscopic memory time $\tau_D = \frac{1}{\omega_D}$ under which there are effects of inertia in the bath. This serves as a sort of environmental cutoff time longer than which the bath is memoryless but shorter than which there is memory to the friction. With this, the damping kernel can be written as simply

$$\gamma(t) = \gamma\omega_D\Theta(t)e^{-\omega_D t} \tag{3.48}$$

And then in the frequency domain

$$\tilde{\gamma}(\omega) = \frac{\gamma}{\left(1 - \frac{i\omega}{\omega_D}\right)} \tag{3.49}$$

Which corresponds to spectral density of

$$J(\omega) = \frac{M\gamma\omega}{\left(1 + \frac{\omega^2}{\omega_D^2}\right)} \tag{3.50}$$

This Drude model behaves effectively the same as the Ohmic model with $\gamma = \int_0^\infty dt\gamma(t)$ except for times shorter than $\frac{1}{\omega_D}$. We can see the general shape of all three spectral densities, (3.46), (3.47), and (3.50), plotted for the arbitrary values of M=1, γ=550 cm^{-1}, and a cutoff frequency (ω_C or ω_D) of 300 cm^{-1}:

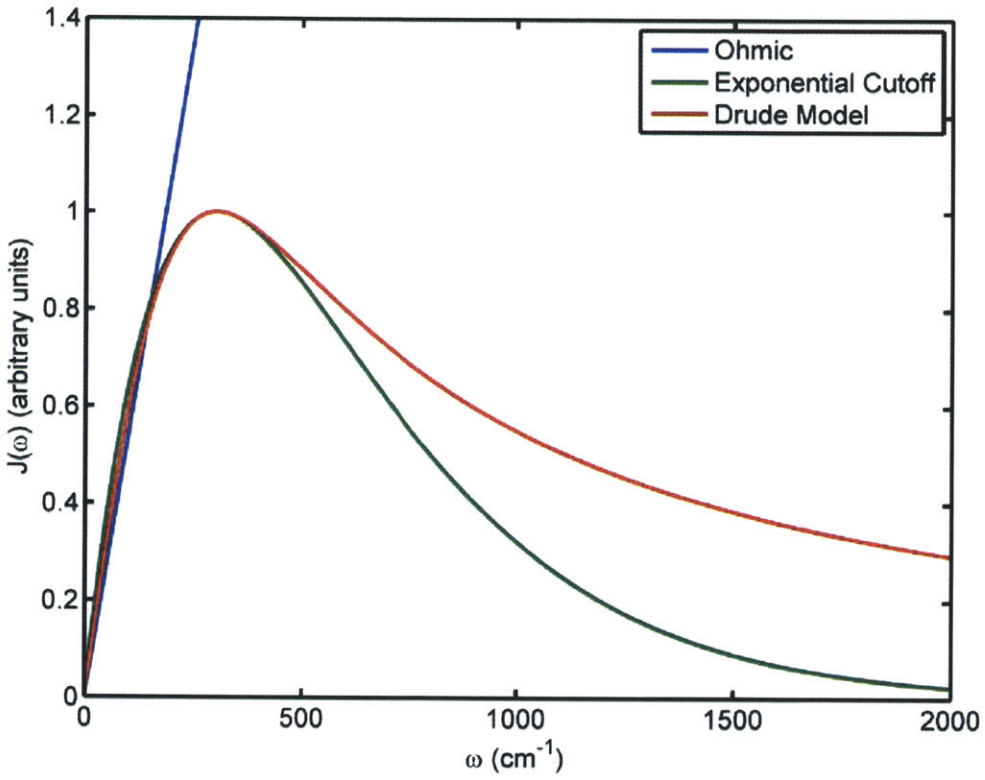

Figure 23: Simple spectral density models

Liquid Friction and Vibrational Relaxation

In moving to a description of liquids on the molecular perspective, this sort of Langevin approach is still broadly applicable, despite the seemingly large number of approximations necessary to describe the bath variables. The harmonic bath model discussed above is useful in that it often provides analytical solutions to the equations and one does not have to think in terms of the timescales of molecular motions. If one uses a simple Onsager model for a liquid, it is actually possible to relate the spectral density to a frequency dependant dielectric function, a measurable quantity [33, 34].

$$J(\omega) = \frac{(\Delta\mu)^2}{2\pi\epsilon_0 a^3} \mathrm{Im}\left[\frac{(\epsilon_s(\omega) - \epsilon_c)}{2\epsilon_s(\omega) + \epsilon_c}\right] \tag{3.51}$$

where $\varepsilon_s(\omega)$ is the complex solvent dielectric function and ε_c is the static dielectric constant of the cavity of radius a in which the solute sits. More complicated Onsager inspired models for chromophores in a variety of solvation scenarios, including more complicated models of chromophores inside a solvated protein cavity can also be solved analytically and related to measurable dielectric responses [33].

For a more general bath, it is possible to consider the density of modes of the condensed phase system, something which can be explicitly computed from the velocity-velocity autocorrelation function from a molecular dynamics trajectory or from the spectrum of eigenvalues for each configuration averaged over a thermal distribution of configurations (the instantaneous normal mode picture) to approximate (3.41). As opposed to the equilibrium normal mode approach where the Hessian is diagonalized at a local potential minimum, the instantaneous normal modes are obtained by diagonalizing the Hessian matrix at each instantaneous configuration, giving a time dependant evolution [35-40]. The frequencies are then the square root of the eigenvalues of this diagonalization, such that negative eigenvalues give imaginary frequencies (often plotted on the negative x axis, as seen in [41]).

This is valid in situations where the solvent motion is rapid and thus successive collisions are largely uncorrelated and where the system is near equilibrium so that imaginary frequencies (which arise because some configurations have negative curvature when they are not local minima) do not contribute [21, 22]. These approximations are relatively good for small solvents such as water, and have been applied to use the velocity-velocity correlation function to calculate the instantaneous normal mode density from classical MD for SPC water at 300K, which has been shown to lead to very good agreement with experimental observables, giving appropriate widths and frequencies for the water bend, stretch, and low frequency intermolecular and librational motions [42].

Independent of the mechanism of friction, the diffusion constant of a Brownian particle is given by the Einstein relation (Einstein–Smoluchowski relation), a consequence of the fluctuation-dissipation theorem [43]

$$D = \frac{k_B T}{\zeta} \tag{3.52}$$

which is a direct consequence of linear response and not debated [44]. The Stokes-Einstein relation can be written from this by assuming friction behavior consistent with classical, non-molecular hydrodynamics for a spherical particle, but this is only appropriate in the large solute (Brownian) limit [45].

The relaxation rate for an oscillator in this picture is often described with a single timescale, $\frac{1}{T_1}$ which has been shown to be well approximated by the Fourier component of the friction at the main oscillator frequency, and it is this friction that leads to population relaxation [46-48]. Actually extracting the friction kernels which govern this relaxation is possible, and is effectively just the correlation function of the force which would be exerted by the solvent upon a rigid vibration [49, 50]. In practice this is often done by freezing the bond of interest then calculating the solvent force autocorrelation function on this frozen rigid bond where $\delta f^{(0)}(t) = f^{(0)}(t) - \overline{f}^{(0)}$

$$C_{\delta f^{(0)}\delta f^{(0)}}(t,t') = \left\langle \delta f^{(0)}(t)\delta f^{(0)}(t') \right\rangle \tag{3.53}$$

As another example, in liquids, Berne et al demonstrate that the dynamic friction can be obtained in a simple case from the velocity autocorrelation function or more completely by taking the fluctuating force δf on a bond a propagating this via the true Liouville propagator $L = -i\{\cdots, H\}$ giving the random force (3.24) as [50, 51]

$$\zeta(t) = M\frac{\left\langle \delta f e^{iQLt}\delta f \right\rangle}{\left\langle p^2 \right\rangle} \tag{3.54}$$

That is, the autocorrelation function of the time-propagated fluctuating force gives us the friction. The static component of this is easy to obtain from MD simulations, as one only needs to calculate how the Hamiltonian evolves:

$$\zeta_0 = \frac{1}{k_B T}\int_0^\infty dt \left\langle \delta f e^{iLt}\delta f \right\rangle \tag{3.55}$$

More recent work has focused on the origin on friction in liquids and what exactly this means molecularly. Effectively the problem is in making a physical assignment of these x_α oscillators and c_α couplings. This can be done by focusing on instantaneous normal modes of the solvent to write the Hamiltonian and obtain the frequencies and coupling coefficients for every mode α for each instantaneous liquid configuration [52, 53]. With this in hand it is possible to calculate from the approach taken in

(3.19) and (3.25) the Hamiltonian-derived friction by averaging over instantaneous liquid configurations to get

$$\gamma(t) = \left\langle \sum_{\alpha=1}^{N} \frac{c_\alpha^2}{\omega_\alpha^2} [\cos \omega_\alpha t - 1] \right\rangle \tag{3.56}$$

which effectively depends only on the spectrum of couplings and a weighted instantaneous normal mode density of states.

QUANTUM DISSIPATION

Coherence in a quantum system can be thought of as an ordering of the relative phases between two states. The major consequence of this is a phase angle between the two states, leading to interference. Using Dirac notation where $|\psi\rangle = \sum_i |i\rangle \psi_i$ and $\psi_i = \langle i | \psi \rangle$, in the case of the traditional probability amplitude, the probability that a system S in the state $|\psi\rangle$ will be found in arbitrary state $|\phi\rangle$ is the number resulting from the square of the modulus of the inner product of the two states [54, 55]

$$\begin{aligned} \text{prob}(\psi \Rightarrow \phi) &= |\langle \phi | \psi \rangle|^2 = |\sum_i \phi_i^* \psi_i|^2 \\ &= \sum_i |\phi_i^* \psi_i|^2 + \sum_{ij;i\neq j} \phi_i^* \phi_j \psi_j^* \psi_i \\ &= \sum_i |\phi_i|^2 |\psi_i|^2 + \sum_{ij;i\neq j} \phi_i^* \phi_j \psi_j^* \psi_i \end{aligned} \tag{3.57}$$

The terms in $\sum_{ij;i\neq j} \phi_i^* \phi_j \psi_j^* \psi_i$ for which i≠j, in explicit Dirac notation written as $\langle \phi | i \rangle \langle j | \phi \rangle \langle \psi | j \rangle \langle i | \psi \rangle$, represent interference between "alternative" intermediate states $|i\rangle$ and $|j\rangle$. These sorts of interference terms vanish in the case that intermediate state $|i\rangle$ is measured or coupled to the environment. This is the effect of the environment – to destroy coherences between quantum states of the system. This loss of phase coherence is not egalitarian, and some subset of states will be more affected by the environment than others. Those that remain (referred to by Zurek as "pointer states") are in a sense selected for by the environmental interaction [54, 56-59]. Zurek refers to this process as einselection (environmentally induced superselection), a selective loss of information due to interactions with the environment which leads to classicality, leaving a collection of those states orthogonal to the environment. These selected for states (pointer states) still stable and the preferred states for observation, as they are persistent and still stable despite the interaction [59-63].

It is worth noting that the term "quantum decoherence" is often used to describe such scenarios, but this is somewhat misleading. This so-called decoherence is not a manifestation of wavefunction collapse, but instead an appearance of a collapse, as the system wavefunction loses its "quantum" nature through thermodynamically irreversible interactions with the environment. An overall global wavefunction still exists and remains coherent, but the individual "system" wavefunction loses coherence due to phases acquired as a result of interactions with the surrounding environment. This is in effect a spreading of correlation from the system to the environment. Caldeira and Leggett wrote in 1981 that what matters here is the "relative importance and nature of the coupling to the environment" and in strongly damped or overdamped systems, "we are often ignorant of the precise details of the coupling and are reduced to describing its effects by phenomenological friction or viscosity coefficients which must be taken from experiment" [14].

In applying the generalized Langevin equation to an actual quantum mechanical system to try and describe this interaction between the system and environment and loss of information, the strategy now commonly taken to obtain formal equations for the quantum Langevin equation (QLE) or quantum master equation (QME) for thermally equilibrated systems is that of the projection operator [15, 20, 30, 64, 65]. The generalized Langevin equation applied to quantum systems first appeared in a paper (without potential renormalization) in a Soviet journal in 1959 taking the form of (3.23) [30, 64, 66, 67]. This quantum Langevin equation is best viewed as an operator equation which is applied over a total Hilbert space of both system (S) and bath (B) which results from the tensor product [30]

$$\mathcal{H} = \mathcal{H}_S \otimes \mathcal{H}_B \tag{3.58}$$

With the total Hamiltonian given by

$$\hat{H} = \hat{H}_S \otimes \hat{I}_B + \hat{I}_S \otimes \hat{H}_B + \hat{H}_I \tag{3.59}$$

With $\hat{I}_B$ and $\hat{I}_S$ being the projection operators of the bath and system, respectively, required for the dimensionality of the addition to be correct. Sometimes this dimensionality issue is ignored or assumed and (3.59) is rewritten as $\hat{H} = \hat{H}_S + \hat{H}_B + \hat{H}_I$. This operator approach applies to the entire space, system and bath, which differs from the classical GLE for which the stochasticity applies only to the system as the random force contains classical noise properties specified in order to account for the bath interactions.

Elimination of the fast bath variables (that is, as in the classical Langevin equation, obtaining a self-contained equation for the system alone such that the stochastic bath dynamics acting solely upon the

system) is difficult if for no other reason than the extra importance of the system-bath interaction in quantum mechanics. This interaction influences the time evolution of both system and bath and thus will be inexorably approximate. In many instances the common approximations fail, for example the use of the rotating-wave approximation has been shown to lead to a violation of the Ehrenfest theorem (which states that mean values obey classical equations of motion – that is, the correspondence between the time evolution of an operator and the commutator of that operator with the Hamiltonian) [68]. Only for very specific situations can an exact QLE be obtained – for instance, when a quantum degree of freedom interacts with the bath in such a way that $[H_I, H_S]=0$ corresponding to pure dephasing, or when the coupling takes the form of a operator-valued function of q or p with linear bath degrees of freedom, but these are generally rare and of limited application [30, 69-71].

BROWNIAN OSCILLATOR

One approach to bridging the gap between the classical Langevin equation and the full quantum counterpart of has been popularized by Mukamel and is known as the Brownian oscillator model [72]. For the Mukamelian multimode Brownian oscillator model, the goal is to provide a detailed picture of the bath influence on a particular quantum mechanical transition. This bath is modeled through a GLE-like equation containing two parts: a few slower primary coordinates which are expected to dominate the interaction with the quantum system and then slow primary nuclear coordinates are then themselves coupled linearly to a bath of harmonic oscillators as is typical for the GLE (the bath is chosen to be harmonic to allow for an arbitrary spectral density and temperature) [72]. This is the case, for instance, in a molecular dimer such as acetic acid, where low frequency dissipative slow nuclear motions couple to one main higher frequency vibrations (say, and –OH stretch) in a larger solvent bath. For primary slow oscillator j the coupling to the bath oscillator α is described in a similar fashion to (3.13) as [15, 20, 73, 74]

$$H' = \frac{1}{2}\sum_{\alpha=1}^{N}\left[\frac{p_\alpha^2}{m_\alpha} + m_\alpha\omega_\alpha^2\left(x_\alpha - q_j\frac{c_\alpha^2}{m_\alpha\omega_\alpha^2}\right)^2\right] \tag{3.60}$$

This allows us to construct a Langevin-like equation for each slow mode, with Brownian force $\xi_j(t)$ on each and an added independent external driving force $F_j(t)$ which couples as $F_j(t)q_j$

$$M_j\ddot{q}_j(t) + m_j\omega_j^2 q_j(t) + M_j\int_{-\infty}^{t} dt'\gamma_j(t-t')\dot{q}_j(t') = \xi_j(t) + F_j(t) \tag{3.61}$$

The solution to (3.61) then provides a description of the coordinates which will influence the primary fast (potentially quantum) degree of freedom – for instance, an electronic transition or a fast vibrational motion such as an –OH stretch.

The problem in application of the classical Langevin equation to quantum systems which becomes immediately apparent is that a quantum correlation function is expected to be complex and satisfy (2.11) while the classical correlation function should be real and obey(2.10). To address this problem in obtaining the quantum correlation function, one calculates the imaginary part of the frequency response spectrum, $\hat{C}''(\omega)$ for each mode based on (3.61). As shown earlier in (2.20), the entire quantum correlation function can be written in terms of just this imaginary part, and so once this is obtained, the entire correlation function $C(t)$ can be obtained in a manner such that it satisfies all the properties of a quantum correlation function (and consequently the fluctuation-dissipation theorem). There are a few approaches to calculating $\hat{C}''(\omega)$ from the GLE. The approach taken by Grabert et al utilizes a Green's function approach and is more mathematically rigorous and general [20]. To provide perhaps somewhat more physical intuition, we can take another approach which leads to the same result. We can use the fact that the linearity of the Langevin equation here allows us to examine the susceptibility $\chi(\omega)$ through ensemble averages and then Fourier transform of both sides of (3.61), giving

$$\begin{aligned} \langle q_j(\omega) \rangle &\equiv \int_{-\infty}^{\infty} dt \langle q_j(t) \rangle e^{i\omega t} \\ &= \chi_j(\omega) \tilde{F}_j(\omega) \end{aligned} \tag{3.62}$$

where

$$\chi_j(\omega) = \frac{1}{m_j} \frac{1}{-\omega^2 + \omega_j^2 - i\omega\gamma_j(\omega)} \tag{3.63}$$

The correlation function of the primary (slow) coordinates we are searching for is

$$C_j(t) \equiv \langle q_j(t) q_j(0) \rho_g \rangle \tag{3.64}$$

Where ρ_g is the ground state density operator of the variable which we wish to interact with the Langevin-like bath system

$$\rho_g \equiv \frac{e^{-\beta H_g}}{Tr\left[e^{-\beta H_g}\right]} \tag{3.65}$$

This gives the response

$$\chi_j(\omega) = \int_0^\infty dt \left\langle -\frac{i}{\hbar}\left[q_j(t), q_j(0)\right]\rho_g \right\rangle e^{i\omega t} \tag{3.66}$$

and then we obtain

$$\tilde{C}_j''(\omega) = \frac{i\hbar}{2}\left[\chi_j(\omega) - \chi_j^*(\omega)\right] \tag{3.67}$$

While results can be obtained from this point on for an arbitrary spectral density / damping, for the case of Ohmic damping for each mode as shown in (3.42), ($\tilde{\gamma}_j(\omega) = \gamma_j$) we can then use (2.20) obtain the imaginary and then real parts of the time correlation function, respectively,

$$C_j''(t) = -\frac{\hbar}{2m_j} \cdot \frac{2}{\sqrt{\omega_j^2 - \gamma_j^2}} \cdot \exp\left(\frac{-\gamma_j t}{2}\right) \sin\left(\sqrt{\omega_j^2 - \gamma_j^2}\, t\right) \tag{3.68}$$

$$\begin{aligned} C_j'(t) = {} & \frac{\hbar}{2m_j} \cdot \frac{2}{\sqrt{\omega_j^2 - \gamma_j^2}} \cdot \left[\coth(i\phi_j \hbar\beta/2) \cdot \exp(-\phi_j t) - \coth(i\phi_j' \hbar\beta/2) \cdot \exp(-\phi_j' t)\right] \\ & - \frac{2\gamma_j}{m_j \beta} \sum_{n=1}^{\infty} \frac{2\pi n}{\hbar\beta} \frac{\exp\left(-\frac{2\pi n}{\hbar\beta} t\right)}{\left(\omega_j^2 + \left(\frac{2\pi n}{\hbar\beta}\right)^2\right) - \gamma_j^2 \left(\frac{2\pi n}{\hbar\beta}\right)^2} \end{aligned} \tag{3.69}$$

where $\phi = \frac{\gamma_j}{2} + \frac{i}{2}\sqrt{\omega_j^2 - \gamma_j^2}$ and $\phi' = \frac{\gamma_j}{2} - \frac{i}{2}\sqrt{\omega_j^2 - \gamma_j^2}$, which are the eigenvalues of a harmonic oscillator with Ohmic damping (although in the case of Mukamel there is an unfortunate albeit not entirely unexpected mixup of φ and φ', here corrected) [20, 72]. This is often slightly simplified by defining another quantity, the frequency of damped oscillations $\zeta_j = \sqrt{\frac{\omega_j^2 - \gamma_j^2}{4}}$ (which becomes imaginary when overdamped, with large γ).

BROWNIAN OSCILLATOR RESULTS

It is useful to examine a few numerical results of this model to get a sense of the types of bath behavior which can be described in this framework. For a single slow bath mode, we can change the damping γ to

range between overdamped ($\gamma_j > \omega_j$, where the system returns to equilibrium without a full oscillation), underdamped ($\gamma_j < \omega_j$. Causing the system to oscillate at a slow frequency down to equilibrium), or critically damped ($\gamma_j = \omega_j$, where the system returns to equilibrium as fast as possible). We can look directly at the components of the time correlation function for these three damping scenarios at a fixed oscillator frequency:

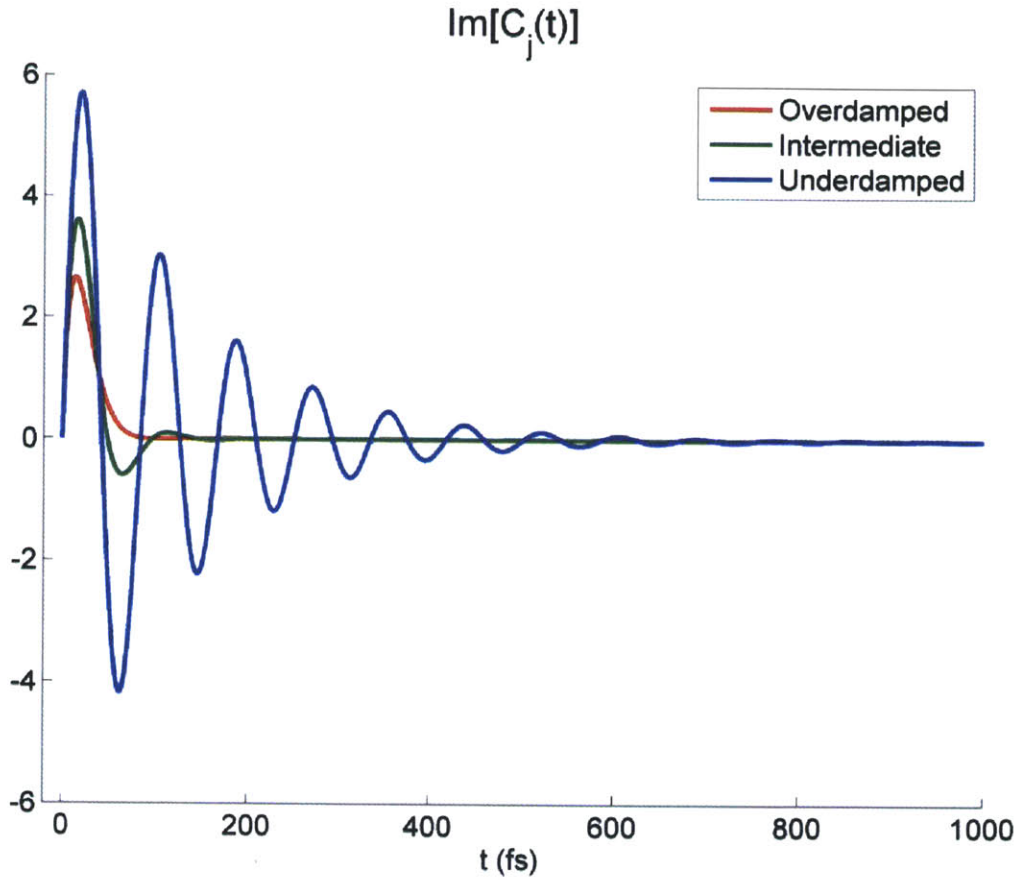

Figure 24: Single Brownian oscillator correlation function for three limiting friction cases

Plotting the frequency domain representation of this result we can see the general shape of the spectral density under various damping regimes:

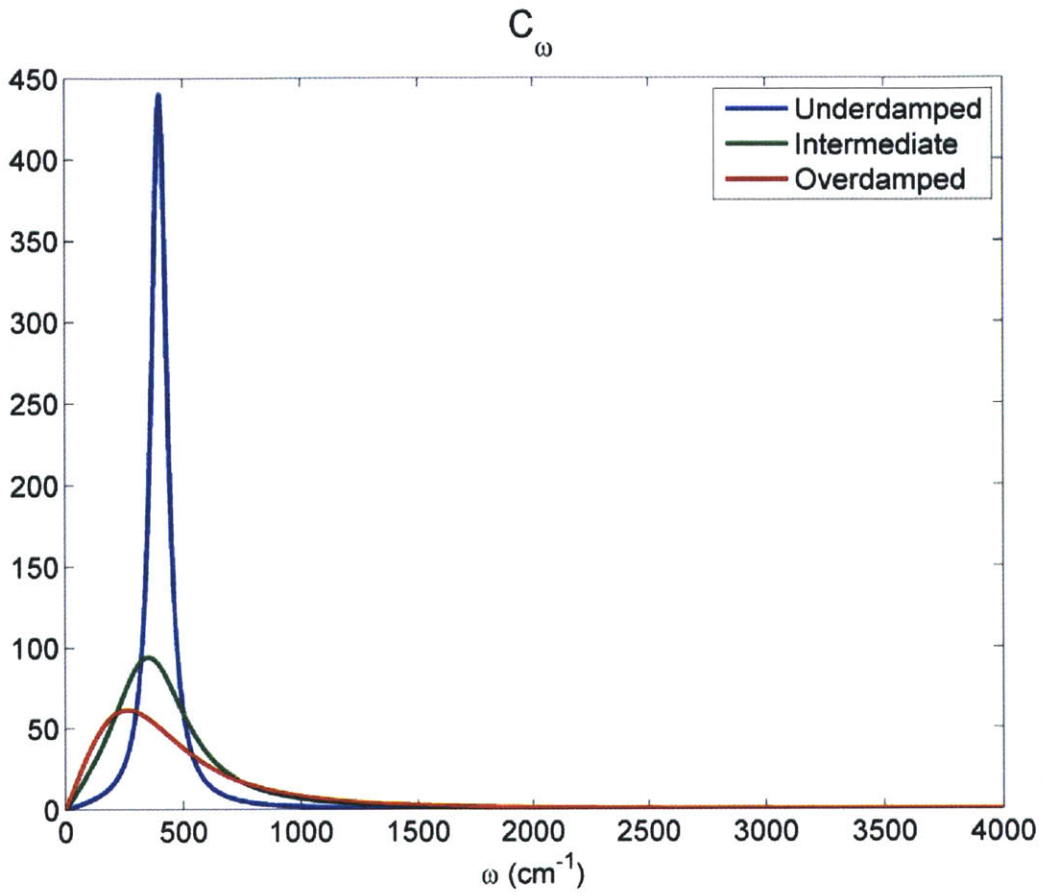

Figure 25: Frequency domain representation of the Brownian oscillator spectral density for three limiting friction cases

These demonstrate the range of damping available in this bath for a single "Brownian oscillator," and additional oscillators add in linearly (see (3.60)), allowing for a bath of arbitrary complexity to be constructed from a series of oscillators at different frequencies and different damping conditions. We will see this bath model applied to spectroscopic systems in the next chapter.

Extracting Time Correlation Information from Molecular Dynamics Simulations

A more computationally expensive but more molecularly motivated approach to quantifying time evolution is to propagate Newton's equations of motion numerically in molecular dynamics to construct classical trajectories. One can then use the results of these dynamics simulations in the construction of frequency and dipole trajectories. These sorts of molecular dynamics simulations (MD) have become a fundamental tool for relating experiments to atomistic and microscopic molecular behavior. As Berkeley's William Miller has been known to say, this is effectively doing 17th century physics on

computers – simply solving the equations of motion in small timesteps based upon an empirical potential energy [75, 76]. It has also insightfully been called "pursuing Laplace's vision on modern computers," as a fully deterministic prediction of all motion, past and present, is given by the forces and positions at a given moment [77].

For two-dimensional infrared spectroscopy this is not a new approach, and many groups now commonly incorporate molecular dynamics in their interpretation of spectra [78-84]. Here it is worth focusing on utilizing MD for time correlation information only and then incorporate mapping results from higher level quantum chemical calculations to construct trajectories. To calculate fluctuating transition frequencies and transition dipoles from molecular dynamics, the most common approach is to extract random small portions of solute and surrounding local solvent environment from a simulation to create a subset of configurations to serve as a sample of the possible solvent environments. For each of these solvent configurations, full electronic structure calculations are performed to calculate points on the potential energy curve for the vibrational motion of interest. Corcelli et al have fit this potential to a Morse oscillator and then with a multiplicative scaling factor to correct for systemic errors in frequency, each local solvent configuration can be assigned a set of transition frequencies [85].

The time trajectory is constructed from the full MD simulation by creating a single mapping coordinate which can be quickly computed for each time point in the molecular configuration and assigning to each time step snapshot (that is, each set of solvent nuclear configurations) a set of transition frequencies and dipoles. For instance, it is common to project the solvent electric field onto the bond of interest, and the transition frequency can be mapped to this projection based upon the *ab initio* calculations of frequencies for the randomly selected solvent cluster configurations [85-89]. It is also possible to compute the classical force exerted on a particular bond over the course and use this to approximate the vibrational frequency by perturbatively calculating the expected frequency shift away from the fundamental frequency if no force is exerted on this oscillator [90].

To demonstrate the extraction of time correlation and force information from a molecular dynamics simulation, we can examine the simple case of pure water. Liquid water is of course known for its complex hydrogen bond dynamics, with rapid bond breaking and forming. Molecular dynamics models for water have been developed for over 40 years, and much insight can be gained from surprisingly simple models [91, 92]. Utilizing the Gromacs 4.5.1 molecular dynamics package, a box of 216 SPC/E water molecules at 300K was equilibrated and allowed to evolve in 2 fs timesteps for a total of 1 ns [93, 94]. The classical SPC/E water model is a simple three-site rigid water molecule, where point charges are located at the nuclear positions of the hydrogen at oxygen atoms with fixed rigid bonds of 1.0 Å, and

HOH angle of 109.47°, and a net dipole of 2.35 D and an average polarization allowed in the potential energy function along with electrostatic interactions and a Lennard-Jones potential for the oxygens [95-97]. For illustrative purposes, a single –OH bond was chosen within the box and the forces projected along this bond were calculated. Force units here are the fundamental units of force in Gromacs, $\frac{kJ}{(mol \cdot nm)}$, approximately 1.66 pN [93, 94].

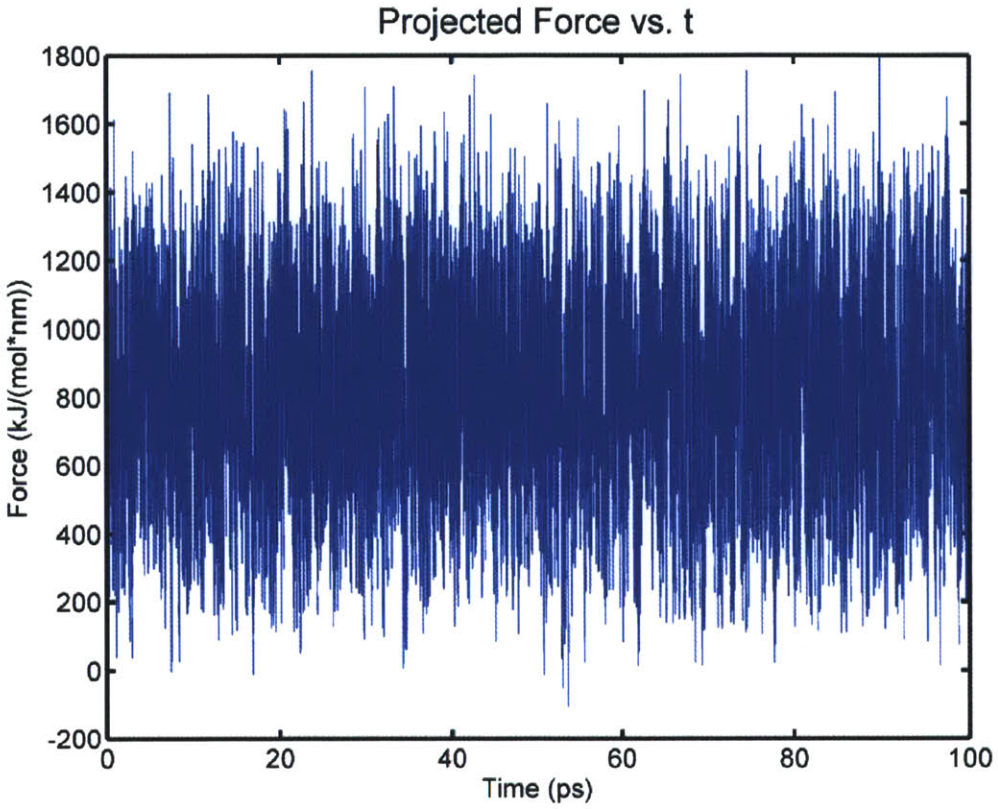

Figure 26: Force projected along the OH bond axis over a portion of an MD trajectory containing SPC/E water

This 100 ps trajectory of projected forces then gives us a histogram of forces along the bond:

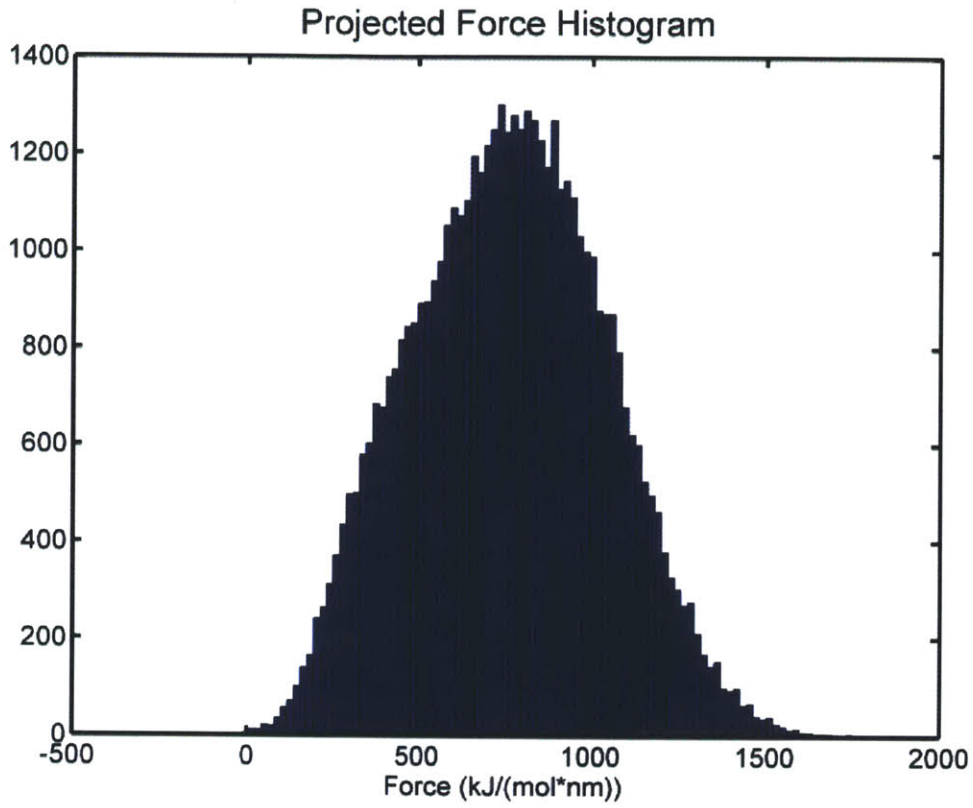

Figure 27: Histogram of projected forces along an SPC/E OH bond over 100ps from a 1ns MD trajectory

And we can calculate the projected force-force correlation function from the trajectory as well:

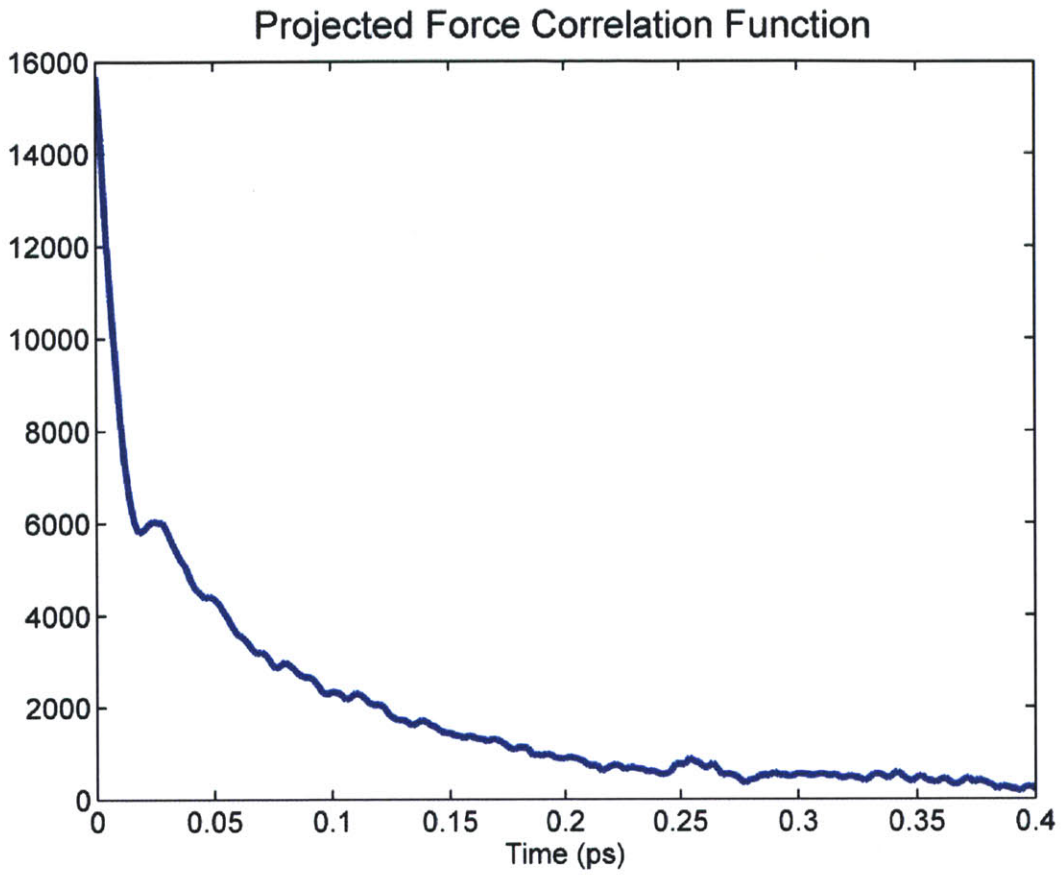

Figure 28: Calculated force-force correlation function for the projection of forces along an OH bond using 100ps of SPC/E water

This classical correlation function then describes the time correlation behavior of the bath, giving us the option of obtaining our dynamics from a simple analytical expression as will be demonstrated shortly, a Langevin-type Brownian oscillator as in (3.68) and (3.69), or from the dynamics of particular variables in molecular dynamics simulations. The molecular dynamics of chemically reactive systems can also be modeled in a similar fashion through a variety of methods – for example, Roberts et al have utilized EVB models to examine the dynamics of proton transfer in aqueous hydroxide, although such techniques oftentimes require significant effort, expertise, and computational resources [98-100].

1. Breuer, H.-P. and F. Petruccione, *The theory of open quantum systems*. 2002, Oxford ; New York: Oxford University Press. xxi, 625 p.
2. Davies, E.B., *Quantum theory of open systems*. 1976, London ; New York: Academic Press. ix, 171 p.
3. Weiss, U., *Quantum dissipative systems*. 3rd ed. 2008, Singapore ; Hackensack, N.J.: World Scientific. xviii, 507 p.
4. Kampen, N.G.v., *Stochastic processes in physics and chemistry*. 3rd ed. 2007, Amsterdam ; Boston ; London: Elsevier. xvi, 463 p.
5. Lemons, D.S. and P. Langevin, *An introduction to stochastic processes in physics : containing "On the theory of Brownian motion" by Paul Langevin, translated by Anthony Gythiel*. 2002, Baltimore: Johns Hopkins University Press. xii, 110 p.
6. Ullersma, P., *An exactly solvable model for Brownian motion: I. Derivation of the Langevin equation*. Physica, 1966. **32**(1): p. 27-55.
7. Weiss, U., *Quantum dissipative systems*. 2nd ed. 1999, Singapore ; River Edge, NJ: World Scientific. xvi, 448 p.
8. Green, M.S., *Markoff Random Processes and the Statistical Mechanics of Time-Dependent Phenomena. II. Irreversible Processes in Fluids*. The Journal of Chemical Physics, 1954. **22**(3): p. 398-413.
9. Green, M.S., *Markoff Random Processes and the Statistical Mechanics of Time-Dependent Phenomena*. The Journal of Chemical Physics, 1952. **20**(8): p. 1281-1295.
10. Kubo, R., *Statistical-Mechanical Theory of Irreversible Processes. I. General Theory and Simple Applications to Magnetic and Conduction Problems*. Journal of the Physical Society of Japan, 1957. **12**(Copyright (C) 1957 The Physical Society of Japan): p. 570.
11. Callen, H.B. and T.A. Welton, *Irreversibility and Generalized Noise*. Physical Review, 1951. **83**(1): p. 34-40.
12. Nyquist, H., *Thermal Agitation of Electric Charge in Conductors*. Physical Review, 1928. **32**(1): p. 110-113.
13. Kubo, R., *The fluctuation-dissipation theorem*. Reports on Progress in Physics, 1966. **29**(1): p. 255.
14. Caldeira, A.O. and A.J. Leggett, *Influence of Dissipation on Quantum Tunneling in Macroscopic Systems*. Physical Review Letters, 1981. **46**(4): p. 211-214.
15. Caldeira, A.O. and A.J. Leggett, *Path integral approach to quantum Brownian motion*. Physica A: Statistical Mechanics and its Applications, 1983. **121**(3): p. 587-616.
16. Caldeira, A.O. and A.J. Leggett, *Quantum tunnelling in a dissipative system*. Annals of Physics, 1983. **149**(2): p. 374-456.
17. Dekker, H., *Classical and quantum mechanics of the damped harmonic oscillator*. Physics Reports, 1981. **80**(1): p. 1-110.
18. Zwanzig, R., *Nonlinear generalized Langevin equations*. Journal of Statistical Physics, 1973. **9**(3): p. 215-220.
19. Goldstein, H., C.P. Poole, and J.L. Safko, *Classical mechanics*. 3rd ed. 2002, San Francisco: Addison Wesley. xviii, 638 p.
20. Grabert, H., P. Schramm, and G.-L. Ingold, *Quantum Brownian motion: The functional integral approach*. Physics Reports, 1988. **168**(3): p. 115-207.
21. Nitzan, A., *Chemical dynamics in condensed phases : relaxation, transfer and reactions in condensed molecular systems*. Oxford graduate texts. 2006, Oxford ; New York: Oxford University Press. xxii, 719 p.
22. Hansen, J.-P. and I.R. McDonald, *Theory of simple liquids*. 3rd ed. 2006, London ; Burlington, MA: Elsevier Academic Press. xi, 416 p.
23. Boas, M.L., *Mathematical methods in the physical sciences*. 3rd ed. 2006, Hoboken, NJ: Wiley. xviii, 839 p.

24. Byron, F.W. and R.W. Fuller, *Mathematics of classical and quantum physics*. 1992, New York: Dover Publications. 2 v. in 1.
25. Grabert, H. and U. Weiss, *Thermal enhancement of the quantum decay rate in a dissipative system.* Zeitschrift für Physik B Condensed Matter, 1984. **56**(2): p. 171-183.
26. Leggett, A.J., *Quantum tunneling in the presence of an arbitrary linear dissipation mechanism.* Physical Review B, 1984. **30**(3): p. 1208-1218.
27. Breton, J., A. Vermeglio, and North Atlantic Treaty Organization. Scientific Affairs Division., *The Photosynthetic bacterial reaction center II : structure, spectroscopy, and dynamics*. 1992, New York: Plenum Press. x, 429 p.
28. Schulten, K. and M. Tesch, *Coupling of protein motion to electron transfer: Molecular dynamics and stochastic quantum mechanics study of photosynthetic reaction centers.* Chemical Physics, 1991. **158**(2–3): p. 421-446.
29. Nonella, M. and K. Schulten, *Molecular dynamics simulation of electron transfer in proteins: theory and application to QA .fwdarw. QB transfer in the photosynthetic reaction center.* The Journal of Physical Chemistry, 1991. **95**(5): p. 2059-2067.
30. Hanggi, P. and G.-L. Ingold, *Fundamental aspects of quantum Brownian motion.* Chaos: An Interdisciplinary Journal of Nonlinear Science, 2005. **15**(2): p. 026105-12.
31. Johnson, J.B., *Thermal Agitation of Electricity in Conductors.* Physical Review, 1928. **32**(1): p. 97-109.
32. Cho, M., et al., *Ultrafast solvent dynamics: Connection between time resolved fluorescence and optical Kerr measurements.* The Journal of Chemical Physics, 1992. **96**(7): p. 5033-5038.
33. Gilmore, J. and R.H. McKenzie, *Quantum Dynamics of Electronic Excitations in Biomolecular Chromophores: Role of the Protein Environment and Solvent.* The Journal of Physical Chemistry A, 2008. **112**(11): p. 2162-2176.
34. Hsu, C.-P., X. Song, and R.A. Marcus, *Time-Dependent Stokes Shift and Its Calculation from Solvent Dielectric Dispersion Data.* The Journal of Physical Chemistry B, 1997. **101**(14): p. 2546-2551.
35. Bastida, A., et al., *Molecular Dynamics Simulations and Instantaneous Normal-Mode Analysis of the Vibrational Relaxation of the C−H Stretching Modes of N-methylacetamide-d in Liquid Deuterated Water.* The Journal of Physical Chemistry A, 2010. **114**(43): p. 11450-11461.
36. Keyes, T., *Instantaneous Normal Mode Approach to Liquid State Dynamics.* The Journal of Physical Chemistry A, 1997. **101**(16): p. 2921-2930.
37. Buchner, M., B.M. Ladanyi, and R.M. Stratt, *The short-time dynamics of molecular liquids. Instantaneous-normal-mode theory.* The Journal of Chemical Physics, 1992. **97**(11): p. 8522-8535.
38. Zwanzig, R., *Elementary Excitations in Classical Liquids.* Physical Review, 1967. **156**(1): p. 190-195.
39. Cho, M., et al., *Instantaneous normal mode analysis of liquid water.* The Journal of Chemical Physics, 1994. **100**(9): p. 6672-6683.
40. Mori, H., *Transport, Collective Motion, and Brownian Motion.* Progress of theoretical physics, 1965. **33**(3): p. 423-455.
41. Gilli, G. and P. Gilli, *The nature of the hydrogen bond: outline of a comprehensive hydrogen bond theory*. 2009, Oxford ; New York: Oxford University Press. xi, 317 p.
42. Yang, C.-Y., et al., *Instantaneous normal mode analysis of hydrated electron solvation dynamics.* The Journal of Chemical Physics, 2001. **114**(8): p. 3598-3611.
43. Einstein, A., *Über die von der molekularkinetischen Theorie der Wärme geforderte Bewegung von in ruhenden Flüssigkeiten suspendierten Teilchen.* Annalen der Physik, 1905. **322**(8): p. 549-560.
44. Zwanzig, R. and A.K. Harrison, *Modifications of the Stokes--Einstein formula.* The Journal of Chemical Physics, 1985. **83**(11): p. 5861-5862.

45. Schmidt, J.R. and J.L. Skinner, *Hydrodynamic boundary conditions, the Stokes--Einstein law, and long-time tails in the Brownian limit.* The Journal of Chemical Physics, 2003. **119**(15): p. 8062-8068.
46. Oxtoby, D.W., *Vibrational Population Relaxation in Liquids*, in *Advances in Chemical Physics.* 2007, John Wiley & Sons, Inc. p. 487-519.
47. Tuckerman, M. and B.J. Berne, *Vibrational relaxation in simple fluids: Comparison of theory and simulation.* The Journal of Chemical Physics, 1993. **98**(9): p. 7301-7318.
48. Stratt, R.M. and M. Maroncelli, *Nonreactive Dynamics in Solution: The Emerging Molecular View of Solvation Dynamics and Vibrational Relaxation.* The Journal of Physical Chemistry, 1996. **100**(31): p. 12981-12996.
49. Shugard, M., J.C. Tully, and A. Nitzan, *Stochastic classical trajectory approach to relaxation phenomena. I. Vibrational relaxation of impurity molecules in solid matrices.* The Journal of Chemical Physics, 1978. **69**(1): p. 336-345.
50. Berne, B.J., et al., *Dynamic friction on rigid and flexible bonds.* The Journal of Chemical Physics, 1990. **93**(7): p. 5084-5095.
51. Straub, J.E., M. Borkovec, and B.J. Berne, *Calculation of dynamic friction on intramolecular degrees of freedom.* The Journal of Physical Chemistry, 1987. **91**(19): p. 4995-4998.
52. Goodyear, G., R.E. Larsen, and R.M. Stratt, *Molecular Origin of Friction in Liquids.* Physical Review Letters, 1996. **76**(2): p. 243-246.
53. Schvaneveldt, S.J. and R.F. Loring, *Vibrational line shapes of solvated molecules with a normal mode approach.* The Journal of Chemical Physics, 1995. **102**(6): p. 2326-2337.
54. Gottfried, K. and T.-m. Yan, *Quantum mechanics : fundamentals.* 2nd ed. Graduate texts in contemporary physics. 2003, New York: Springer. xvii, 620 p.
55. Dirac, P.A.M., *A new notation for quantum mechanics.* Mathematical Proceedings of the Cambridge Philosophical Society, 1939. **35**(03): p. 416-418.
56. Wick, G.C., A.S. Wightman, and E.P. Wigner, *The Intrinsic Parity of Elementary Particles.* Physical Review, 1952. **88**(1): p. 101-105.
57. Wick, G.C., A.S. Wightman, and E.P. Wigner, *Superselection Rule for Charge.* Physical Review D, 1970. **1**(12): p. 3267-3269.
58. Wightman, A., *Superselection rules; old and new.* Il Nuovo Cimento B (1971-1996), 1995. **110**(5): p. 751-769.
59. Zurek, W.H., *Pointer basis of quantum apparatus: Into what mixture does the wave packet collapse?* Physical Review D, 1981. **24**(6): p. 1516-1525.
60. Zurek, W.H., *Decoherence and the Transition from Quantum to Classical.* Physics Today, 1991. **44**(10): p. 36-44.
61. Zurek, W.H., *Decoherence, einselection, and the quantum origins of the classical.* Reviews of Modern Physics, 2003. **75**(3): p. 715-775.
62. Paz, J.P. and W.H. Zurek, *Quantum Limit of Decoherence: Environment Induced Superselection of Energy Eigenstates.* Physical Review Letters, 1999. **82**(26): p. 5181-5185.
63. Zurek, W.H., *Environment-induced superselection rules.* Physical Review D, 1982. **26**(8): p. 1862-1880.
64. Benguria, R. and M. Kac, *Quantum Langevin Equation.* Physical Review Letters, 1981. **46**(1): p. 1-4.
65. Grabert, H., *Projection operator techniques in nonequilibrium statistical mechanics.* 1982, Berlin ; New York: Springer-Verlag. x, 164 p.
66. Magalinskii, V., *Dynamical model in the theory of the Brownian motion.* Sov. Phys. JETP, 1959. **9**: p. 1381-1382.
67. Ford, G.W., J.T. Lewis, and R.F. O'Connell, *Quantum Langevin equation.* Physical Review A, 1988. **37**(11): p. 4419-4428.
68. Ford, G.W. and R.F. O'Connell, *Inconsistency of the rotating wave approximation with the Ehrenfest theorem.* Physics Letters A, 1996. **215**(5–6): p. 245-246.

69. Kampen, N.G.v., *A soluble model for quantum mechanical dissipation.* Journal of Statistical Physics, 1995. **78**(1): p. 299-310.
70. Hänggi, P., *Generalized langevin equations: A useful tool for the perplexed modeller of nonequilibrium fluctuations?*
Stochastic Dynamics, L. Schimansky-Geier and T. Pöschel, Editors. 1997, Springer Berlin / Heidelberg. p. 15-22.
71. Banerjee, D., et al., *Solution of quantum Langevin equation: Approximations, theoretical and numerical aspects.* The Journal of Chemical Physics, 2004. **120**(19): p. 8960-8972.
72. Mukamel, S., *Principles of nonlinear optical spectroscopy.* 1995, New York: Oxford University Press. xviii, 543 p.
73. Tanimura, Y. and S. Mukamel, *Real-time path-integral approach to quantum coherence and dephasing in nonadiabatic transitions and nonlinear optical response.* Physical Review E, 1993. **47**(1): p. 118-136.
74. Mukamel, S., *Femtosecond Optical Spectroscopy: A Direct Look at Elementary Chemical Events.* Annual Review of Physical Chemistry, 1990. **41**(1): p. 647-681.
75. Miller, W.H., *Semiclassical Description of Electronically Non-Adiabatic Processes*, in *Joint Harvard/MIT Physical Chemistry Seminar Series*. 2012: Cambridge, MA.
76. Miller, W.H., *The Semiclassical Initial Value Representation: A Potentially Practical Way for Adding Quantum Effects to Classical Molecular Dynamics Simulations.* The Journal of Physical Chemistry A, 2001. **105**(13): p. 2942-2955.
77. Mesirov, J.P., K. Schulten, and D.W.L. Sumners, *Mathematical approaches to biomolecular structure and dynamics*. 1996, New York: Springer. x, 247 p.
78. Mukamel, S. and D. Abramavicius, *Many-Body Approaches for Simulating Coherent Nonlinear Spectroscopies of Electronic and Vibrational Excitons.* Chemical Reviews, 2004. **104**(4): p. 2073-2098.
79. Cho, M., *Coherent Two-Dimensional Optical Spectroscopy.* Chemical Reviews, 2008. **108**(4): p. 1331-1418.
80. Cho, M. *Two-dimensional optical spectroscopy.* 2009; 1 online resource (378 p.)]. Available from: http://www.crcnetbase.com/isbn/978142008430.
81. Hamm, P. and M.T. Zanni, *Concepts and methods of 2D infrared spectroscopy*. 2011, Cambridge ; New York: Cambridge University Pres. ix, 286 p.
82. Fecko, C.J., et al., *Ultrafast Hydrogen-Bond Dynamics in the Infrared Spectroscopy of Water.* Science, 2003. **301**(5640): p. 1698-1702.
83. Berens, P.H. and K.R. Wilson, *Molecular dynamics and spectra. I. Diatomic rotation and vibration.* The Journal of Chemical Physics, 1981. **74**(9): p. 4872-4882.
84. Gordon, R.G., *Molecular Motion in Infrared and Raman Spectra.* The Journal of Chemical Physics, 1965. **43**(4): p. 1307-1312.
85. Corcelli, S.A., C.P. Lawrence, and J.L. Skinner, *Combined electronic structure/molecular dynamics approach for ultrafast infrared spectroscopy of dilute HOD in liquid H[sub 2]O and D[sub 2]O.* The Journal of Chemical Physics, 2004. **120**(17): p. 8107-8117.
86. Corcelli, S.A. and J.L. Skinner, *Infrared and Raman Line Shapes of Dilute HOD in Liquid H2O and D2O from 10 to 90 °C.* The Journal of Physical Chemistry A, 2005. **109**(28): p. 6154-6165.
87. Schmidt, J.R., S.A. Corcelli, and J.L. Skinner, *Pronounced non-Condon effects in the ultrafast infrared spectroscopy of water.* The Journal of Chemical Physics, 2005. **123**(4): p. 044513-13.
88. Roberts, S.T.S.T., *Hydrogen bond rearrangements and the motion of charge defects in water viewed using multidimensional ultrafast infrared spectroscopy*, in *Department of Chemistry*. 2010, Massachusetts Institute of Technology. : Cambridge, MA.
89. Hudecová, J., K.H. Hopmann, and P. Bouř, *Correction of Vibrational Broadening in Molecular Dynamics Clusters with the Normal Mode Optimization Method.* The Journal of Physical Chemistry B, 2011. **116**(1): p. 336-342.

90. Oxtoby, D.W., D. Levesque, and J.J. Weis, *A molecular dynamics simulation of dephasing in liquid nitrogen.* The Journal of Chemical Physics, 1978. **68**(12): p. 5528-5533.
91. Rahman, A. and F.H. Stillinger, *Molecular Dynamics Study of Liquid Water.* The Journal of Chemical Physics, 1971. **55**(7): p. 3336-3359.
92. Luzar, A. and D. Chandler, *Effect of Environment on Hydrogen Bond Dynamics in Liquid Water.* Physical Review Letters, 1996. **76**(6): p. 928-931.
93. Hess, B., et al., *GROMACS 4: Algorithms for Highly Efficient, Load-Balanced, and Scalable Molecular Simulation.* Journal of Chemical Theory and Computation, 2008. **4**(3): p. 435-447.
94. Lindahl, E., B. Hess, and D. van der Spoel, *GROMACS 3.0: a package for molecular simulation and trajectory analysis.* Journal of Molecular Modeling, 2001. **7**(8): p. 306-317.
95. Berendsen, H.J.C., J.R. Grigera, and T.P. Straatsma, *The missing term in effective pair potentials.* The Journal of Physical Chemistry, 1987. **91**(24): p. 6269-6271.
96. Starr, F.W., J.K. Nielsen, and H.E. Stanley, *Hydrogen-bond dynamics for the extended simple point-charge model of water.* Physical Review E, 2000. **62**(1): p. 579-587.
97. Chatterjee, S., et al., *A computational investigation of thermodynamics, structure, dynamics and solvation behavior in modified water models.* The Journal of Chemical Physics, 2008. **128**(12): p. 124511-9.
98. Roberts, S.T., et al., *Observation of a Zundel-like transition state during proton transfer in aqueous hydroxide solutions.* Proceedings of the National Academy of Sciences, 2009. **106**(36): p. 15154-15159.
99. Car, R. and M. Parrinello, *Unified Approach for Molecular Dynamics and Density-Functional Theory.* Physical Review Letters, 1985. **55**(22): p. 2471-2474.
100. Laasonen, K., et al., *``Ab initio'' liquid water.* The Journal of Chemical Physics, 1993. **99**(11): p. 9080-9089.

Chapter 4 : CALCULATING NONLINEAR SPECTRA

This chapter seeks to unite the static relationships and mappings of Chapter 2 and the tools for describing dynamics introduced in Chapter 3 to calculate nonlinear spectral responses, focusing on the third order response function $\mathbf{R}^{(3)}$ which describes a variety of four wave mixing experiments. A new approach to the construction of time trajectories for transition energy gaps and transition dipole moments is introduced, and these trajectories are used with the semiclassical approximation to calculate spectroscopic observables for a few model systems of chemical interest. This chapter specifically examines the applicability of this approach to the calculation of two dimensional infrared spectra (2D IR) of strongly hydrogen bonded systems and demonstrates a few simple examples of this methodology in practice.

THIRD ORDER RESPONSE

Ultrafast nonlinear spectroscopy has emerged as one of the most information-rich techniques for understanding dynamics of the condensed phase. Linear spectroscopies such as FTIR are sensitive to the distribution of system eigenstates. Nonlinear spectroscopies, however, allow for the possibility of interrogating both the distribution of eigenstates and the dynamics of the molecular environment. The time evolution of spectral variables such as the transition dipole and stretching frequency is by no means simple, and determining the relationship between molecular processes and spectroscopic observables remains a difficult challenge. Comparing experimentally measured spectra to simulated nonlinear spectra allow us to gain insight regarding the molecular microscopic dynamics and can help provide physical intuition with an emphasis on chemically relevant quantities.

The lowest order optical nonlinearity which does not disappear for any point group symmetry is third order (second order signals vanish in isotropic media). Third order nonlinear spectroscopy has proven useful in interrogating chemical processes such as solvation dynamics, vibrational couplings, hydrogen bond dynamics, peptide structure, and proton transfer. Perhaps the most powerful of four-wave mixing third order spectroscopic techniques is that of two dimensional infrared spectroscopy (2D IR) [1-9]. This corresponds to n=3 in (2.60), and can be expressed in the frequency domain using a fourth-rank susceptibility tensor describing the interaction of matter with three separate input electromagnetic fields [10-12]:

$$\mathbf{P}^{(3)}(\omega_1+\omega_2+\omega_3)=\chi\mathbf{E}_1(\mathbf{r},t)\mathbf{E}_2(\mathbf{r},t)\mathbf{E}_3(\mathbf{r},t) \tag{4.1}$$

or utilizing the third-order response function in the time domain

$$\mathbf{P}^{(3)}(t) = \int_0^\infty dt_3 \int_0^\infty dt_2 \int_0^\infty dt_1 \mathbf{R}^{(3)}(t_3,t_2,t_1)\mathbf{E}_1(\mathbf{r},t-\tau_3)\mathbf{E}_2(\mathbf{r},t-\tau_3-\tau_2)\mathbf{E}_3(\mathbf{r},t-\tau_3-\tau_2-\tau_1) \quad (4.2)$$

where the third order response function, per (2.59), is composed of the nested commutators of the transition dipole operator evaluated at the time of interaction with each input field:

$$\begin{aligned}\mathbf{R}^{(3)}(t_3,t_2,t_1) = -\left(\frac{1}{i\hbar}\right)^3 \theta(t_1)\theta(t_2)\theta(t_3) \\ Tr\left(\hat{\mu}(t_3+t_2+t_1)\left[\hat{\mu}(t_2+t_1),\left[\hat{\mu}(t_1),\left[\hat{\mu}(\tau_1=0),\rho(t_0=-\infty)\right]\right]\right]\right)\end{aligned} \quad (4.3)$$

Here in addition to the time intervals introduced in (2.58) we make the choice of time zero as the time of the first interaction with an external field, so τ_1=0, and we also assume that $\rho(t_0)$ does not change when unperturbed (that is, it is at equilibrium under the system Hamiltonian) and thus $\rho(t_0)$ is equivalent to $\rho(-\infty)$.

We can then expand this set of nested commutators, write out each term, and group creatively:

$$\begin{aligned}&\hat{\mu}(t_3+t_2+t_1)\left[\hat{\mu}(t_2+t_1),\left[\hat{\mu}(t_1),\left[\hat{\mu}(0),\rho(-\infty)\right]\right]\right] = \\ &\quad \hat{\mu}(t_3+t_2+t_1)\left[\hat{\mu}(t_2+t_1)\hat{\mu}(t_1)\hat{\mu}(0)\rho(-\infty) - \rho(-\infty)\hat{\mu}(0)\hat{\mu}(t_1)\hat{\mu}(t_2+t_1)\right] + \\ &\quad \hat{\mu}(t_3+t_2+t_1)\left[\hat{\mu}(t_2+t_1)\rho(-\infty)\hat{\mu}(0)\hat{\mu}(t_1) - \hat{\mu}(t_1)\hat{\mu}(0)\rho(-\infty)\hat{\mu}(t_2+t_1)\right] + \\ &\quad \hat{\mu}(t_3+t_2+t_1)\left[\hat{\mu}(t_1)\rho(-\infty)\hat{\mu}(0)\hat{\mu}(t_2+t_1) - \hat{\mu}(t_2+t_1)\hat{\mu}(0)\rho(-\infty)\hat{\mu}(t_1)\right] + \\ &\quad \hat{\mu}(t_3+t_2+t_1)\left[\hat{\mu}(0)\rho(-\infty)\hat{\mu}(t_1)\hat{\mu}(t_2+t_1) - \hat{\mu}(t_2+t_1)\hat{\mu}(t_1)\rho(-\infty)\hat{\mu}(0)\right]\end{aligned} \quad (4.4)$$

Because the dipole operator and the density matrix are Hermitian, we can write each term in brackets in (4.4) as a combination of a term and its associated adjoint ("conjugate"). For example:

$$\hat{\mu}(t_2+t_1)\hat{\mu}(t_1)\hat{\mu}(0)\rho(-\infty) = \left(\rho(-\infty)\hat{\mu}(0)\hat{\mu}(t_1)\hat{\mu}(t_2+t_1)\right)^\dagger \quad (4.5)$$

With this realization we can write the third order response using four components, which we will write as $\mathbf{R}_n$.

$$\mathbf{R}^{(3)}(t_3,t_2,t_1) = -\left(\frac{1}{i\hbar}\right)^3 \sum_{n=1}^{4} \mathbf{R}_n(t_3,t_2,t_1) - \mathbf{R}_n^*(t_3,t_2,t_1) \quad (4.6)$$

For a set of complete system eigenstates and some careful reordering and insertion of the identity, we get:

$$\begin{aligned}
\mathbf{R}_1 &= \sum_{abcd} P_a \left\langle \boldsymbol{\mu}_{ab}(t_3+t_2+t_1)\boldsymbol{\mu}_{bc}(t_2+t_1)\boldsymbol{\mu}_{cd}(t_1)\boldsymbol{\mu}_{da}(0)\right\rangle \\
\mathbf{R}_2 &= \sum_{abcd} P_a \left\langle \boldsymbol{\mu}_{ab}(t_1)\boldsymbol{\mu}_{bc}(t_2+t_1)\boldsymbol{\mu}_{cd}(t_3+t_2+t_1)\boldsymbol{\mu}_{da}(0)\right\rangle \\
\mathbf{R}_3 &= \sum_{abcd} P_a \left\langle \boldsymbol{\mu}_{dc}(t_1)\boldsymbol{\mu}_{cb}(t_3+t_2+t_1)\boldsymbol{\mu}_{ba}(t_2+t_1)\boldsymbol{\mu}_{ad}(0)\right\rangle \\
\mathbf{R}_4 &= \sum_{abcd} P_a \left\langle \boldsymbol{\mu}_{dc}(t_2+t_1)\boldsymbol{\mu}_{cb}(t_3+t_2+t_1)\boldsymbol{\mu}_{ba}(t_1)\boldsymbol{\mu}_{ad}(0)\right\rangle
\end{aligned} \tag{4.7}$$

What has been discussed here so far neglects orientational contributions to the response function. A general treatment of rotational-vibrational coupling has proven exceptionally difficult, and so we typically separate the orientational and vibrational contributions to the response function by adding an additional term Y_{IJKL}^{ijkl} where capital letters refer to the directions in the laboratory frame and lowercase indices are unit vectors in the fixed molecular frame, such that this orientational response tensor projects the laboratory frame onto the molecular frame at each interaction time. Within this term we have all classical rotational and translational motion, and it can be viewed as an inherent property of the medium itself. With this notation we can more carefully note that the vibrational contribution should be expressed in terms of the molecular frame, thus R_{ijkl}. For the isotropic distribution of spherical rotors these orientational response functions can be analytically determined [13-15]. For a full description of the general case of multiple states, see the classic papers of Sung and Silbey [16, 17]. While in general a tensor with 8 indices (i, j, k, l, I, J, K, L) corresponding to spatial dimensions has a total of 3^8 total terms, due to symmetry considerations for isotropic media, only four unique tensor elements remain, and each of these can be independently measured through control of the polarization of the input and detected fields.

In order to obtain an expression for the polarization in (4.2), we must write out an explicit expression for each interaction with the field. We can write each input electric field as a separate pulse E_α, here taken as a simple cosine written in complex form as

$$\mathbf{E}_\alpha(\mathbf{r},t) = \frac{1}{2}\hat{\mathbf{e}}_\alpha^J A_\alpha(t-t_\alpha)\varepsilon_\alpha(\mathbf{r})\exp\left[i\left(\mathbf{k}_\alpha\cdot\mathbf{r}-\omega_\alpha(t-t_\alpha)+\phi_\alpha\right)\right]+c.c. \tag{4.8}$$

Where $\hat{\mathbf{e}}_\alpha^J$ is the vector component of the electric field polarization in the laboratory frame, A_α is the pulse envelope intensity as a function of time, $\mathbf{k}_\alpha$ is the wave vector of the incident field pointing in the propagation direction, ω_α is the pulse frequency, and φ_α is a phase factor. For a third order signal, these electric fields are multiplicative (see (4.1) and (4.2)), giving a sum of complex exponentials. The propagation direction of a third order signal is determined by these different **k** vectors, and utilizing what is referred to as wavevector matching, one can measure different signals independently due to their spatial

separation, according to $\mathbf{k}_{singal} = \mathbf{k}_\alpha \pm \mathbf{k}_\beta \pm \mathbf{k}_\gamma$ for the different possible combinations of signs. For example, the $\mathbf{k}_{singal} = \mathbf{k}_1 - \mathbf{k}_2 + \mathbf{k}_3$ condition gives the "transient grating" or "nonrephasing" signals while spatially separable $\mathbf{k}_{singal} = \mathbf{k}_1 - \mathbf{k}_2 - \mathbf{k}_3$ signal (equivalently, $-\mathbf{k}_1 + \mathbf{k}_2 + \mathbf{k}_3$) is the "photon echo" or "repahsing" contribution. Each of these contributions can be calculated independently utilizing the groupings in (4.7) and made spatially distinct with clever control over the directions of the input fields.

To obtain analytical expressions for these response functions, historically a series of approximations are made, including bilinear coupling between the system and the bath, the second cumulant approximation (the Gaussian approximation), and the Condon approximation for the dipoles. These approximations sacrifice the ability to describe many important kinds of dynamics, including the non-Gaussian sorts of dynamics which dominate hydrogen bonded systems. The approach taken here is mixed quantum-classical model for nonlinear spectra, calculating quantum observables and their static relationships explicitly, creating a mapping of these variables to one another, and then creating time correlated trajectories according to a specific model for the bath. This approach is in many ways analogous to the early Langevin approach, for which details of the bath motions are selectively eliminated and allowed to manifest themselves instead through stochastic forces. Here the details and dynamics of the bath express themselves in the time correlation of the variables of interest, as it is fluctuations in the bulk bath which modulate spectroscopic variables such as the transition dipole moments and the energy gap fluctuations. This approach specifies the dynamical characteristics of the bath and maps this to spectroscopic variables in order to calculate experimental observables.

SEMICLASSICAL APPROXIMATION TO THE THIRD ORDER RESPONSE

Given only a classical trajectory describing the evolution of stochastic variables of a system, we require some simplification of the third order response equations which can be used to calculate spectroscopic observables without the entire full quantum dynamics. With what is known as the "semiclassical approximation," the third order response function (4.3) can be calculated directly from the dynamics of the transition energy gap $\omega_{ab}(t)$ and the transition dipole moments $\mu_{ab}(t)$. Here we consider the weak field limit, where the dipole approximation holds for the interactions between the applied fields and the matter of interest. The semiclassical approximation assumes that we can replace each term in the response function with its classical analogue, which allows us to effectively remove time ordered exponentials in equation (2.72). We can also then replaces the trace over the bath with an equilibrium average over phase space. Without this, we technically require complete knowledge of the quantum dynamics of a system - that is, how the entire quantum system evolves over time, a knowledge which we can never hope to obtain for condensed phase matter, especially interacting molecules in a liquid. With the approximation, we transform quantum time propagator into an ordinary exponential function [18, 19]

$$
\begin{aligned}
\mathbf{R}_1 &= \sum_{abcd} P_a \left\langle \boldsymbol{\mu}_{ab}(t_3+t_2+t_1)\boldsymbol{\mu}_{bc}(t_2+t_1)\boldsymbol{\mu}_{cd}(t_1)\boldsymbol{\mu}_{da}(0)\phi^{(1)}_{abcd} \right\rangle \\
\mathbf{R}_2 &= \sum_{abcd} P_a \left\langle \boldsymbol{\mu}_{ab}(t_1)\boldsymbol{\mu}_{bc}(t_2+t_1)\boldsymbol{\mu}_{cd}(t_3+t_2+t_1)\boldsymbol{\mu}_{da}(0)\phi^{(2)}_{abcd} \right\rangle \\
\mathbf{R}_3 &= \sum_{abcd} P_a \left\langle \boldsymbol{\mu}_{da}(0)\boldsymbol{\mu}_{ab}(t_2+t_1)\boldsymbol{\mu}_{bc}(t_3+t_2+t_1)\boldsymbol{\mu}_{cd}(t_1)\phi^{(3)}_{abcd} \right\rangle \\
\mathbf{R}_4 &= \sum_{abcd} P_a \left\langle \boldsymbol{\mu}_{da}(0)\boldsymbol{\mu}_{ab}(t_1)\boldsymbol{\mu}_{bc}(t_3+t_2+t_1)\boldsymbol{\mu}_{cd}(t_2+t_1)\phi^{(4)}_{abcd} \right\rangle
\end{aligned}
\tag{4.9}
$$

where φ_{abcd} is a set of dephasing functions defined by

$$
\begin{aligned}
\phi^{(1)}_{abcd} &= \exp\left[-i\int_{t_1+t_2}^{t_1+t_2+t_3} \omega_{ba}(\tau)d\tau - i\int_{t_1}^{t_1+t_2} \omega_{ca}(\tau)d\tau - i\int_{0}^{t_1} \omega_{da}(\tau)d\tau \right] \\
\phi^{(2)}_{abcd} &= \exp\left[-i\int_{t_1+t_2}^{t_1+t_2+t_3} \omega_{dc}(\tau)d\tau - i\int_{t_1}^{t_1+t_2} \omega_{db}(\tau)d\tau - i\int_{0}^{t_1} \omega_{da}(\tau)d\tau \right] \\
\phi^{(3)}_{abcd} &= \exp\left[-i\int_{t_1+t_2}^{t_1+t_2+t_3} \omega_{bc}(\tau)d\tau + i\int_{t_1}^{t_1+t_2} \omega_{ca}(\tau)d\tau + i\int_{0}^{t_1} \omega_{da}(\tau)d\tau \right] \\
\phi^{(4)}_{abcd} &= \exp\left[-i\int_{t_1+t_2}^{t_1+t_2+t_3} \omega_{bc}(\tau)d\tau + i\int_{t_1}^{t_1+t_2} \omega_{db}(\tau)d\tau + i\int_{0}^{t_1} \omega_{da}(\tau)d\tau \right]
\end{aligned}
\tag{4.10}
$$

For a third order response, the 2D IR line shape is constructed from the Fourier transform of the sum of the rephasing and non-rephasing signals, where for rephasing (-) signal is emitted in the $\mathbf{k}_R=-\mathbf{k}_1+\mathbf{k}_2+\mathbf{k}_3$ direction and nonrephasing (+) we have $\mathbf{k}_{NR}=\mathbf{k}_1-\mathbf{k}_2-\mathbf{k}_3$ phase matching directions. For a single vibrational resonance ignoring population relaxation and reorientation, can group equation (4.9):

$$
\begin{aligned}
\mathbf{R}^{(3)}_{+} &= \sum_{abcd} \left\langle \boldsymbol{\mu}_{ab}(t_3+t_2+t_1)\boldsymbol{\mu}_{bc}(t_2+t_1)\boldsymbol{\mu}_{cd}(t_1)\boldsymbol{\mu}_{da}(0)f^{(+)}_{abcd} \right\rangle \\
\mathbf{R}^{(3)}_{-} &= \sum_{abcd} \left\langle \boldsymbol{\mu}_{cd}(t_2+t_1)\boldsymbol{\mu}_{bc}(t_3+t_2+t_1)\boldsymbol{\mu}_{ab}(t_1)\boldsymbol{\mu}_{da}(0)f^{(-)}_{abcd} \right\rangle
\end{aligned}
\tag{4.11}
$$

$$
\begin{aligned}
f^{(+)}_{abcd} &= \exp\left[-i\int_{t_2+t_1}^{t_3+t_2+t_1} \omega_{ba}(\tau)d\tau - i\int_{t_1}^{t_2+t_1} \omega_{ca}(\tau)d\tau - i\int_{0}^{t_1} \omega_{da}(\tau)d\tau \right] \\
f^{(-)}_{abcd} &= \exp\left[-i\int_{t_2+t_1}^{t_3+t_2+t_1} \omega_{dc}(\tau)d\tau - i\int_{t_1}^{t_2+t_1} \omega_{db}(\tau)d\tau - i\int_{0}^{t_1} \omega_{da}(\tau)d\tau \right]
\end{aligned}
\tag{4.12}
$$

Where indices *a* through *f* denote vibrational states (v = 1 to 4), including pathways that exclusively involve one- or two-quantum transitions, those that involve mixed one- and two-quantum transitions, and

those pathways that involve coherence during the waiting period t_2. The full response is the sum of these rephrasing and nonrephasing contributions:

$$\mathbf{R}^{(3)}(t_3,t_2,t_1) = \mathbf{R}_{-}^{(3)}(t_3,t_2,t_1) + \mathbf{R}_{+}^{(3)}(t_3,t_2,t_1) \tag{4.13}$$

FLUCTUATIONS

Due to the relatively weak nature of the hydrogen bond, thermal fluctuations alone are enough to cause significant changes in bonding geometry and energy. In liquid water, for instance, fluctuations in the extended hydrogen bonding network are substantial and rapid and thus have significant consequences on chemistry and spectroscopy [4, 6, 20-27]. If the molecular Hamiltonian is fluctuating over time, the time-evolution operator (2.25) must be replaced with the formally integrated solution to the Schrodinger equation (2.23) [28, 29]

$$U(t+\delta t,t) = \exp\left(\frac{1}{i\hbar}\int_0^{\delta t} d\tau H(t+\tau)\right) \tag{4.14}$$

Utilizing the time propagator (4.14) from the formally integrated Schrodinger equation, this equation has also been used to numerically compute the same quantities as our approximation. Regardless, as the system Hamiltonian changes in time, the associated vibrational transition frequency $\omega_{ab}(t)$ of an oscillator inherently changes with time due to the push and pull of solvent molecules. The local electric field change due to differing solvation or bond breaking and forming then technically appears as a time dependant term in the molecular Hamiltonian. For a time dependant transition frequency, we often write two terms – a mean average time-independent frequency and a rapidly fluctuating part $\delta\omega_{01}(t)$ for which $\langle \delta\omega_{01} \rangle = 0$

$$\omega_{01}(t) = \langle \omega_{01} \rangle + \delta\omega_{01}(t) \tag{4.15}$$

The Anderson-Kubo model assumes that the transition frequency fluctuations are due to the time evolution of the environment, and treats this frequency as a classical stochastic variable fluctuating with exponentially correlated Gaussian statistics [30, 31]. In the late 1960's Ryogo Kubo developed a theory to describe the dephasing of NMR transitions which ultimately proved useful for modeling vibrational lineshapes [32]. These fluctuations induced by the solvent can be described with the Langevin approaches mentioned in the previous chapter, and some success has been had in directly propagating the transition frequency as a stochastic variable in a Langevin type-equation [33, 34]. It is also possible to assign these fluctuations to another hidden variable which influences the frequency – for instance, the local electric field along the bond or the number of hydrogen bonds in which the molecule is participating [35].

A Phenomenological Approach

The general approach utilized here for the calculation of spectroscopic observables is illustrated schematically in Figure 29.

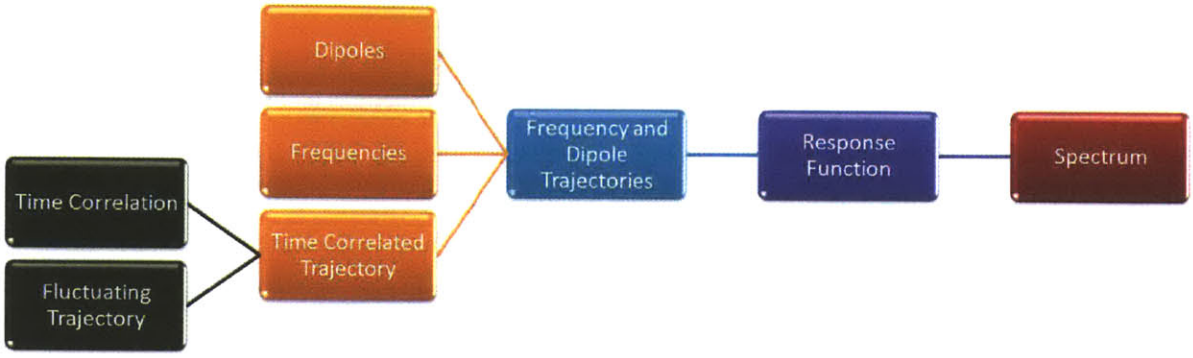

Figure 29: Schematic for spectral calculations

In practice this looks like:

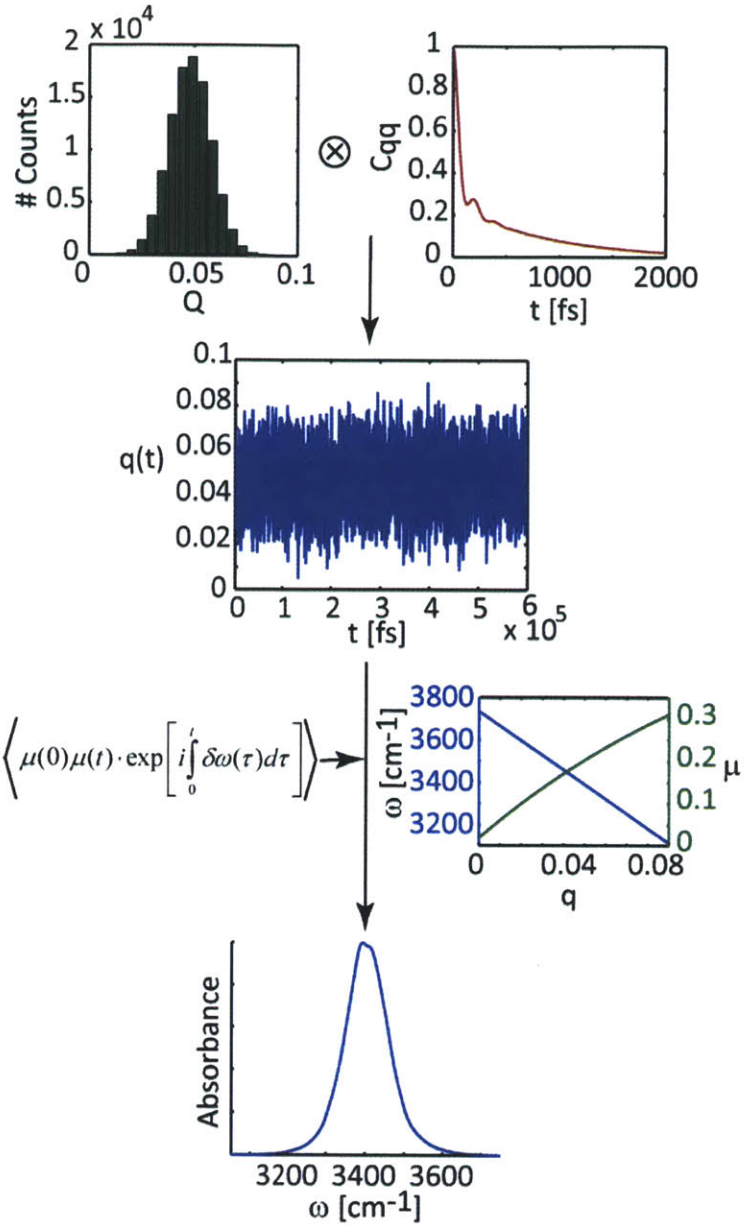

Figure 30: Schematic procedure for calculating a linear spectrum using a time correlated stochastic variable, mapping this to frequencies and dipoles to create trajectories for the semiclassical response function calculation [36]

The main inputs which must be generated to utilize (4.11) are classical frequency and dipole trajectories, which go directly into the calculation of the third order response function using the semiclassical approximation. For the simplest case, one requires the dynamics of the frequencies and transition dipoles of both the 0→1 and 1→2 transitions, $\{\omega_{01}(t), \omega_{12}(t), \mu_{01}(t), \mu_{12}(t)\}$. These in general are obtained by

choosing one dynamic variable of chemical or spectroscopic significance, treating this variable stochastically, constructing a properly time correlated trajectory of this variable, and then mapping the fluctuations in the chosen variable onto variables necessary for the calculation of the response function.

A map relating instantaneous vibrational frequencies and dipoles to the chosen stochastic variable can be generated in a variety of ways. For some variables, these relationships can be determined empirically, such as non-Condon scaling of the transition dipole with frequency or the general trends relating internuclear distance to stretching frequency. These maps can, however, be quite difficult to compute directly. For example one often seeks to create a map which relates microscopic coordinates such as bond distance or proton transfer with transition dipoles and frequencies. The benefit of this approach is that these relationships only need to be determined once, and thus computationally expensive calculations can be utilized at this step to effectively generate a lookup table of relationships.

The choice of this suitable mapping variable upon which is bestowed time correlation is nontrivial and often guided by chemical intuition. We wish for a single valued mapping, linear or nonlinear, with no discontinuities. Clearly one wishes for this variable to be something which can either be treated as a reaction coordinate, has a clear physical motivation, or can be extracted from simulation (say, molecular dynamics) with relative ease. For example, using an EVB simulation of hydroxide in water, it has been shown that the collective electric field projected along the O-H bond is a useful mapping variable essentially directly correlated to the stretching frequency [6, 23, 37]. In some complex systems, there is no clear stochastic variable which contains the majority of the dynamics, in which case this method cannot be easily applied, and the statistical, Langevin approach to dynamics (discussed earlier) becomes the best description of the bath.

The use of a Langevin type equation for IR spectroscopy by calculating the autocorrelation function of the dipole moment operator through the assumption of a randomly modulated oscillator is not new [38, 39]. In fact, for many years it has been possible to take a classical stochastic approach to IR spectroscopy in liquids treating the low frequency modes as randomly modulating, including Fermi resonances [40]. Many others have taken similar stochastic approaches to modeling the anharmonic potential and IR lineshape [41-50]. The extension of this to nonlinear spectroscopies, however, is new and only beginning to be explored [34].

TIME CORRELATION

With a dynamic variable Q chosen, time correlation must be imposed. This is done here by first constructing an uncorrelated trajectory obeying a desired statistical profile. This uncorrelated trajectory is then time-correlated through convolution with a correlation function for this variable,

$C_Q(t) = \langle Q(t)Q(t) \rangle$. The uncorrelated trajectory contains a series of uncorrelated Q values chosen randomly from the desired distribution function P(Q), giving a vector for which the i^{th} entry is Q(i) and $\langle Q(i)Q(j) \rangle = \langle Q^2 \rangle \delta(i-j)$. Given the time correlation function $C_Q(t)$ of equal length with time spacing Δt, the convolution desired that of the uncorrelated trajectory with the time correlation function:

$$\begin{aligned} Q_{correlated}(t) &= C_Q(t) * Q(t) \\ &= \int_0^t d\tau C_Q(t-\tau) Q(\tau) \end{aligned} \tag{4.16}$$

If we realize that for Laplace transforms f(t) = 0 when $t < 0$ and $g(t-\tau) = 0$ for $t > \tau$ we can write this same integral with infinite limits:

$$\int_0^t d\tau C_Q(t-\tau) Q(\tau) = \int_{-\infty}^{\infty} d\tau C_Q(t-\tau) Q(\tau) \tag{4.17}$$

For numerical efficiency this convolution is accomplished through Fourier synthesis utilizing the Cooley-Tukey fast Fourier transform (FFT) algorithm [51, 52]. According to the convolution theorem, for functions f(t) and g(t) and their Fourier transforms $\mathcal{F}\{f(t)\} = F(\omega)$ and $\mathcal{F}\{g(t)\} = G(\omega)$, assuming $\int_{-\infty}^{\infty} dt \, | f(t)g(t) |$ is finite, the product of the two Fourier transforms is the Fourier transform of the convolution. The Wiener-Khinchin theorem mentioned earlier is actually a special case of a related more general cross-correlation theorem. Through the definition of the Fourier transform and a simple variable substitution this can be shown [53]:

$$\begin{aligned} \mathcal{F}\{f(t)\} \cdot \mathcal{F}\{g(t)\} &= F(\omega) \cdot G(\omega) \\ &= \left(\frac{1}{2\pi} \right)^2 \int_{-\infty}^{\infty} \int_{-\infty}^{\infty} dx d\tau e^{-i\omega(x+\tau)} f(x) g(\tau) \\ &= \left(\frac{1}{2\pi} \right)^2 \int_{-\infty}^{\infty} dt e^{-i\omega t} \left[\int_{-\infty}^{\infty} d\tau f(t-\tau) g(\tau) \right] \\ &= \left(\frac{1}{2\pi} \right) \left[\left(\frac{1}{2\pi} \right) \int_{-\infty}^{\infty} dt e^{-i\omega t} f(t) * g(t) \right] \\ &= \left(\frac{1}{2\pi} \right) \mathcal{F}\{ f(t) * g(t) \} \end{aligned} \tag{4.18}$$

And thus we can do the desired convolution through element-by element multiplication in the frequency domain followed by an inverse Fourier transform, noting that care is required in ensuring proper normalization:

$$Q_{correlated}(t) = \mathcal{F}^{-1}\left\{\mathcal{F}\left\{C_Q(t)\right\} \cdot \mathcal{F}\left\{Q(t)\right\}\right\} \tag{4.19}$$

We then take our stochastic variable trajectory with specified dynamics and correlate this to a single valued mapping of the observable variables, here $\left\{\omega_{01}(Q(t)), \omega_{12}(Q(t)),\ \mu_{01}(Q(t)), \mu_{12}(Q(t))\right\}$, that is, we seek to define a set of operations which can map the time trajectory of this single coordinate onto a set of dynamic observable variables, here specifically:

$$Q(t) \rightarrow \left\{\omega_{01}(t), \omega_{12}(t),\ \mu_{01}(t), \mu_{12}(t)\right\} \tag{4.20}$$

VARYING THE FREQUENCY DIRECTLY

Perhaps the easiest and most obvious variable to treat stochastically is the fundamental stretching frequency ω_{01}. As molecules move and rotate in the liquid phase, different electrostatic environments influence each bond and as a result the vibrational energy gap changes dynamically with time. This energy gap has even been examined as a possible reaction coordinate for proton transfer [54]. From a simple linear IR lineshape we can impose a restriction upon the statistical distribution of allowed frequencies, and allow Gaussian frequency fluctuations around this [55]. With the time evolution of the fundamental transition specified, we then map to the rest of the quantities necessary for spectroscopic calculation, $\left\{\omega_{01}(t), \omega_{12}(\omega_{01}(t)),\ \mu_{01}(\omega_{01}(t)), \mu_{12}(\omega_{01}(t))\right\}$.

WATER

The hydrogen bond in water has been modeled as a Brownian oscillator to describe such varied experimental observables as the vibrational Stokes shift and high order Raman spectra [56, 57]. The broad OH stretch absorption is an obvious vibrational target for spectral simulations of hydrogen bonded complexes, and much experimental work has been focused on this transition in the infrared. For the case of an overdamped single OH stretch, the simulated time-time response obtained from (4.11) looks something like:

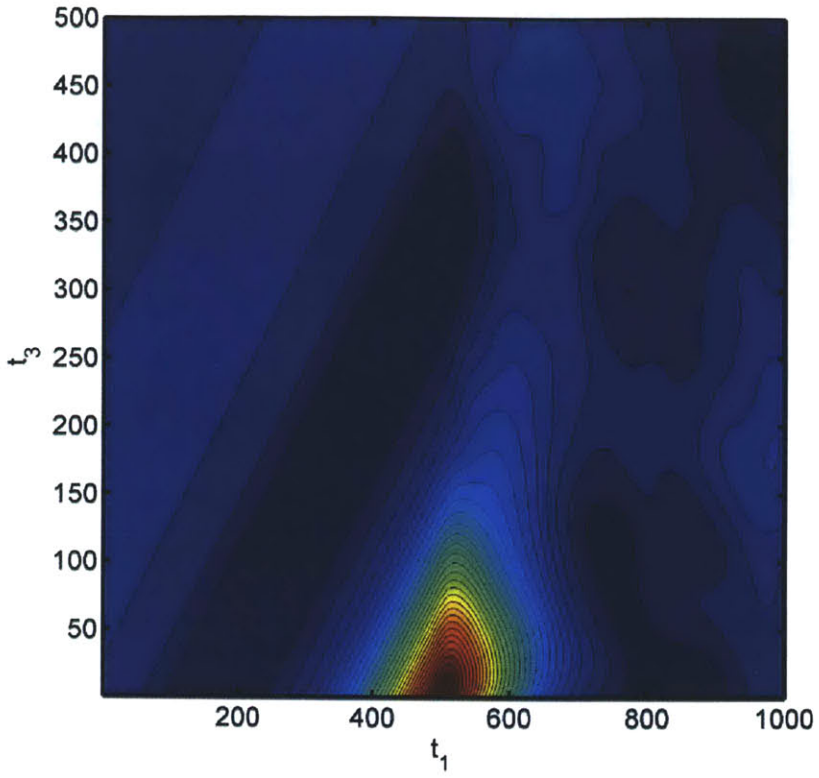

Figure 31: Sample time-time response of overdamped single oscillator at 3400cm^{-1} (timesteps in fs)

As a simple test of the methodology, we can allow ω_{01} to fluctuate according to Gaussian statistics with a full width half max scaled to match the full-width of the linear infrared spectrum of HOD in D_2O.

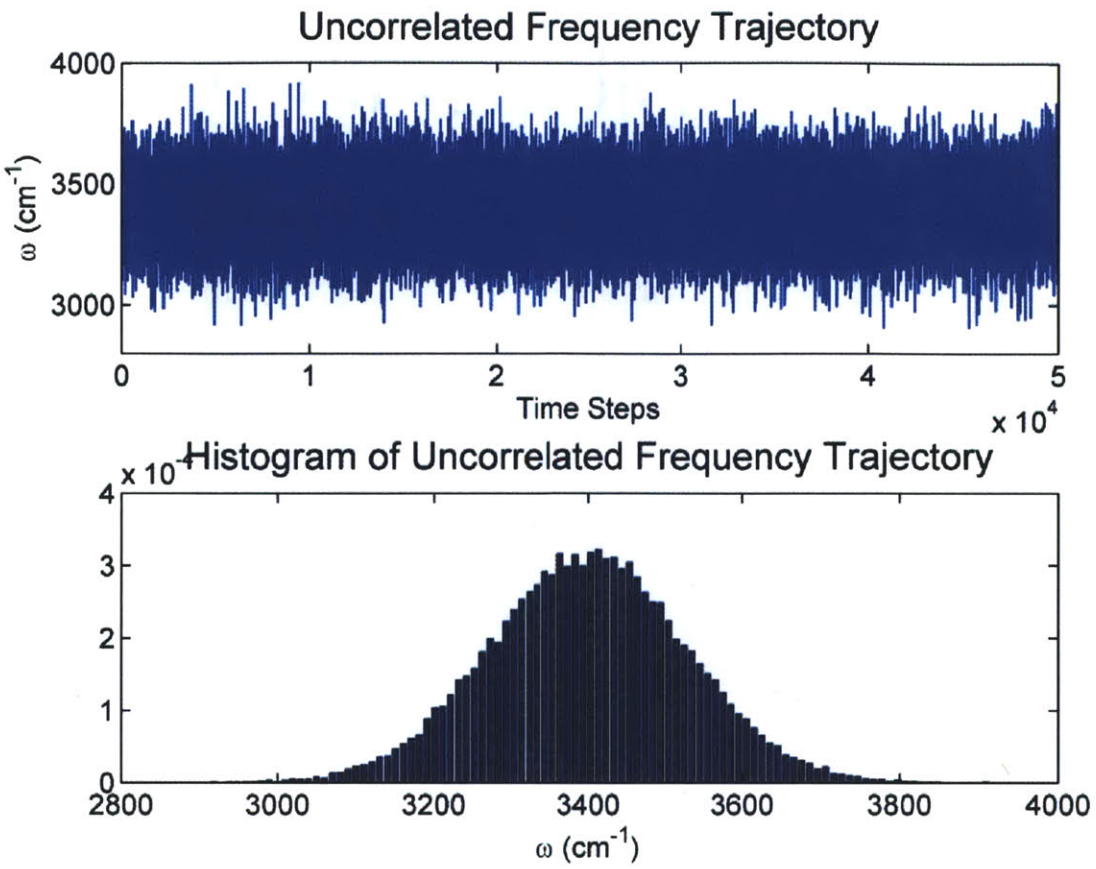

Figure 32: Construction of a sample stochastic trajectory with given statistical distribution

We can then, to continue the example, choose a simple time correlation model to impose upon this trajectory – here a double exponential, a common model for early time water stretching dynamics, with these parameters roughly matching the time correlation function of the OH stretch vibration of HOD solvated in D_2O for the SPC/E water model [37, 58]:

$$C(t) = 0.55 \cdot e^{-\frac{t}{150\,fs}} + 0.45 \cdot e^{-\frac{t}{1000\,fs}} \tag{4.21}$$

Convolution of the uncorrelated stochastic frequency trajectory with this time very simple correlation function as described in (4.19) then produces the desired time correlated frequency trajectory:

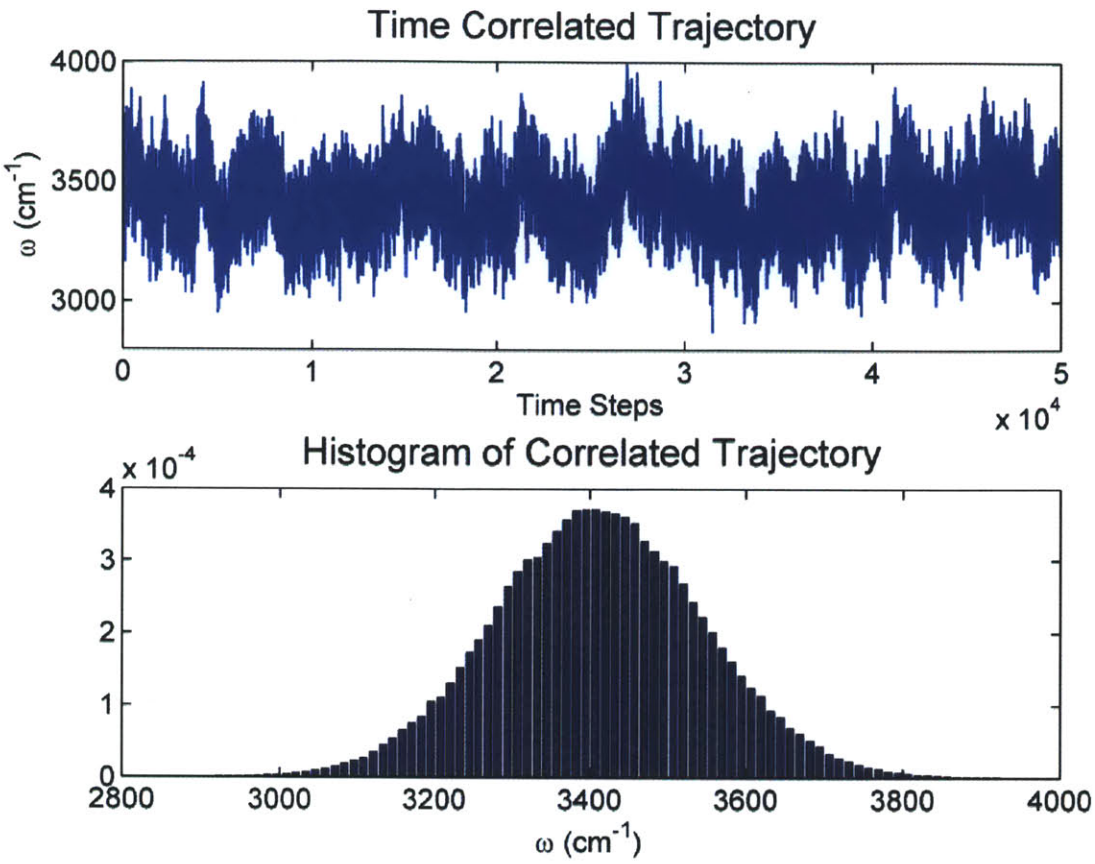

Figure 33: Sample stochastic trajectory after time correlation

To experimentally study the dynamics of OH frequency fluctuations in water, the three-pulse echo peak shift (3PEPS) measurement as been used to extract time correlation information from measurable observables. For instance, Fecko et al. extract the OH frequency correlation function through fitting their experimentally measured three-pulse peak shift decay iteratively utilizing different correlation functions and accounting for long time behavior contributions including real pulse effects, population relaxation, thermally-shifted ground state, and reorientation [2]. In addition, transient hole-burning has been utilized for the same purposes [59, 60].

In the mapping of the stochastic variable to the $\omega_{01}(t) \rightarrow \omega_{12}(t)$ we can choose either a static anhamonicity or a frequency-dependant anharmonicity. For a fixed anharmonicity of $\omega_{12} - \omega_{01} = 200$ cm^{-1} we obtain a spectrum:

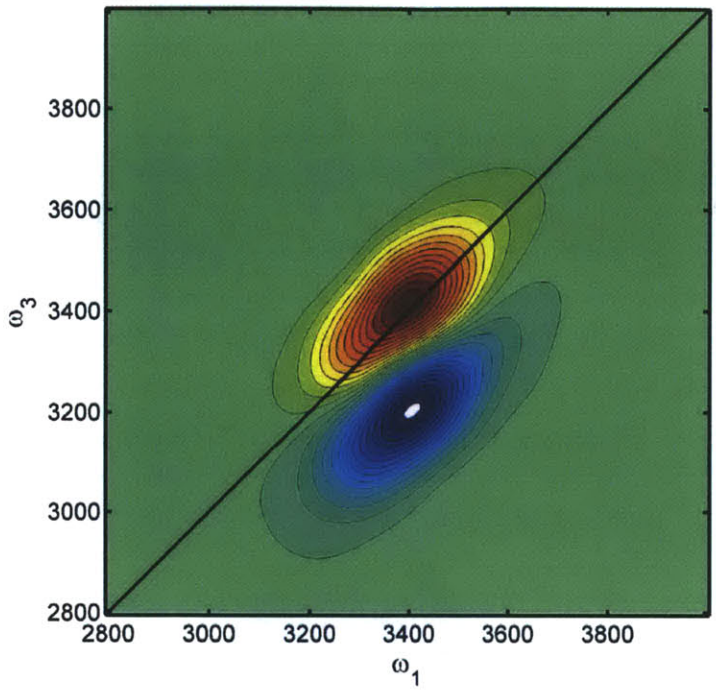

Figure 34: Water OH stretch, Condon approximation, fixed anharmonicity

If there is a frequency dependence to the anharmonicity, we can utilize simple empirical relations for water such as (2.77). With this linear anharmonicity change the spectrum calculated is:

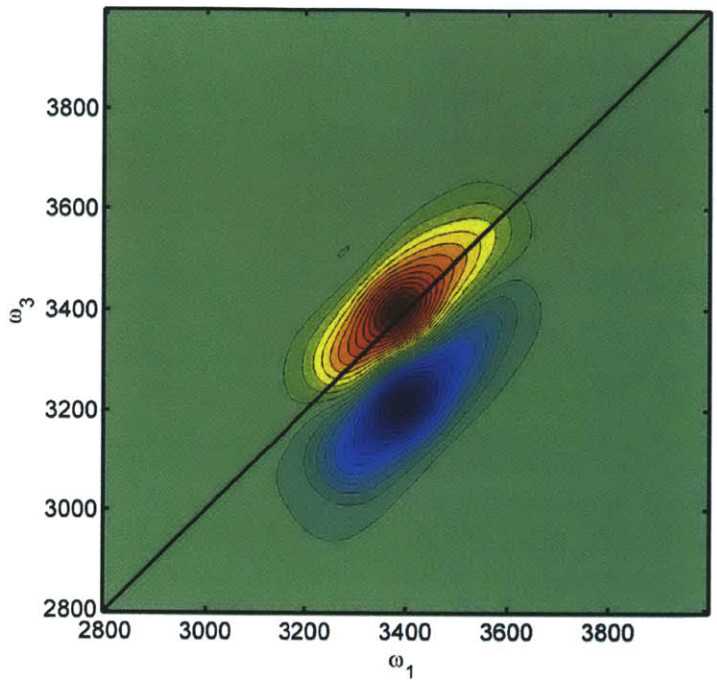

Figure 35: Water OH stretch, Condon approximation, empirical anharmonicity

To map the transition dipoles to the fundamental frequency, $\omega_{01}(t) \rightarrow \mu_{01}(t) \rightarrow \mu_{12}(t)$ we utilize the empirical non-Condon relationship mentioned previously, (2.78). The $1 \rightarrow 2$ transition dipole is assumed to follow harmonic scaling and map directly from the $0 \rightarrow 1$ transition. With this non-Condon effect accounted for, we obtain the following spectrum:

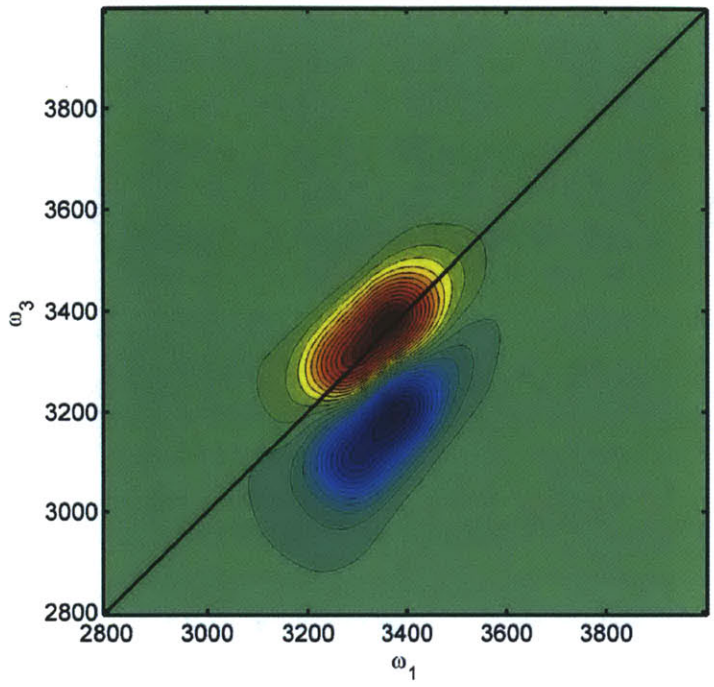

Figure 36: Water OH stretch, non-Condon effects incorporated empirically

These spectral shape changes and subtle but important, and results of this type of model, taking all effects into account, have allowed for the successful calculation of measured 3PEPS data [36].

To demonstrate the effect of the Brownian oscillator model instead of this simple double exponential time correlation, we can time correlate using single mode spectral densities at 200 cm^{-1} in the underdamped and overdamped limits:

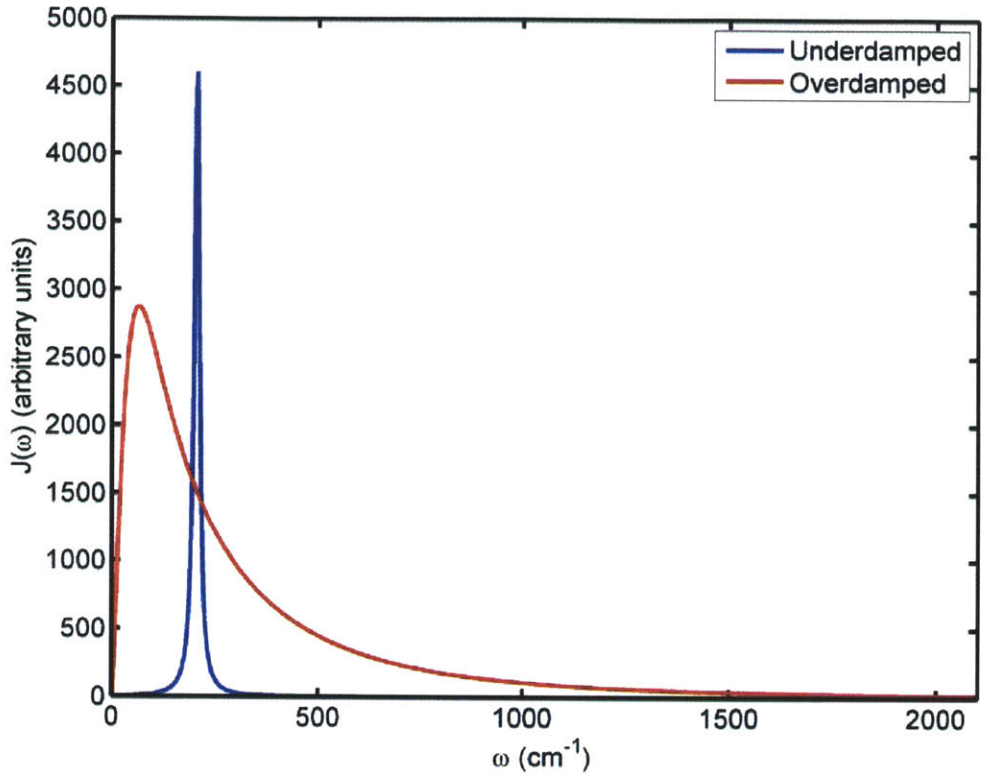

Figure 37: Example spectral densities in the underdamped and overdamped limits used for time correlation

For this illustration we can take the simplest case, fixing the $0 \rightarrow 1$ transition at 3400 cm^{-1} and impose a static anharmonicity of 200 cm^{-1}, treating this fundamental transition stochastically with Gaussian fluctuations with a full width half max of 300 cm^{-1} and using harmonic scaling for the dipole moments. The fluctuating fundamental transition is given time correlation using the underdamped and overdamped time correlation functions. Plotting the lowest 20% contour levels to focus on cross peaks and couplings, we see clear effects of interactions with this 200 cm^{-1} Brownian oscillator mode when underdamped, but a broad single transition with no clear structure for the overdamped limit:

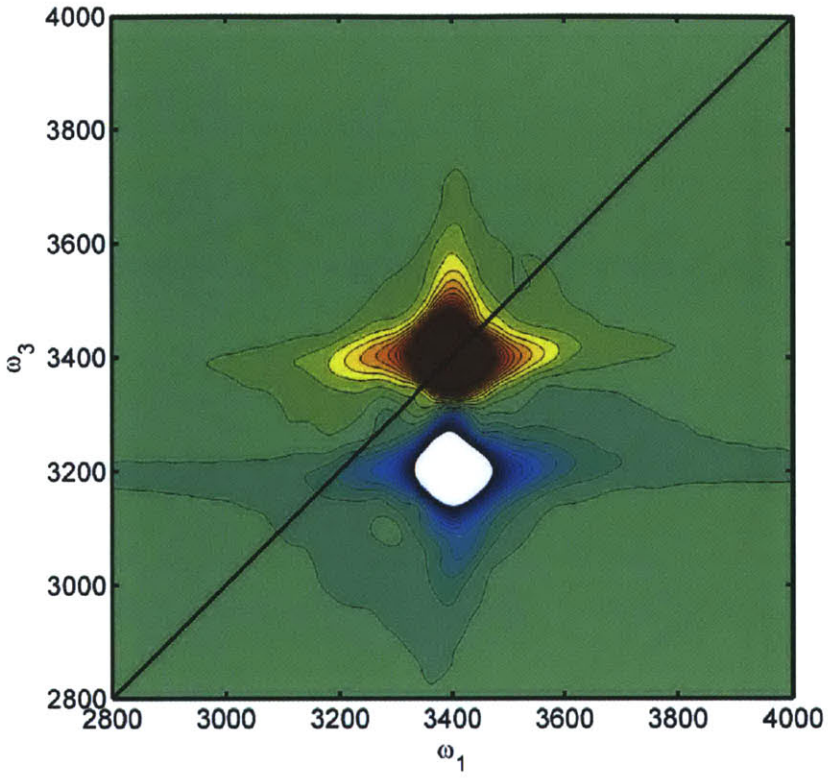

Figure 38: 2D spectrum of a single oscillator with an overdamped spectral density at 200 cm^{-1}

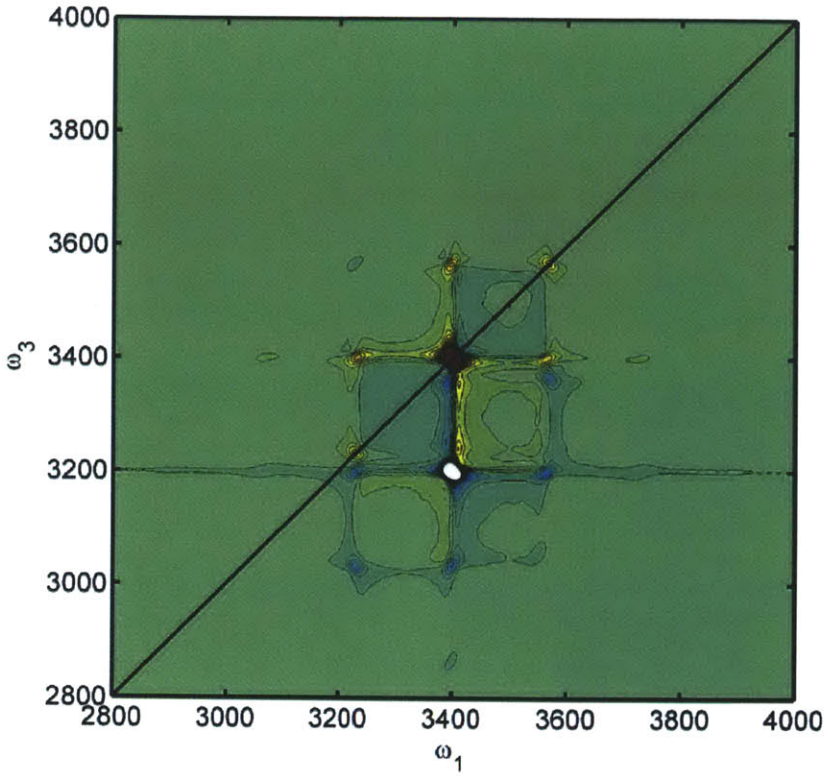

Figure 39: 2D spectrum of a single oscillator with an underdamped spectral density at 200 cm^{-1}

VARYING DOUBLE WELL ASYMMETRY

The next step in complexity in the construction of these classical trajectories is to treat an external variable stochastically and connect this to each of the input trajectories required, as described in (4.20). To model the effect of a direct proton transfer upon the spectrum, we return to the model potential picture presented in Chapter 1. For this model, the fluctuating dynamic variable is not the fundamental frequency but instead the asymmetry of the proton potential, representing the fluctuations in the local electric field experienced by the proton. Chandler et al write that "when such an extreme fluctuation in proton potential occurs, it does not last long, only 0.01 to 0.1 ps. This time interval is nonetheless long enough for the destabilized chemical bond to break" [61]. For the following we will allow for Gaussian fluctuations in the asymmetry parameter, with a full width half max of 2, chosen such that an asymmetry of 3 or -3 gives a fundamental vibrational frequency of 3400 cm^{-1}.

If we use an exaggerated underdamped and an overdamped limit for the Brownian oscillator correlation function, as has been suggested by Ando (who proposed a double well coupled to a dissipative Langevin bath), we can then mapping this fluctuating, time correlated asymmetry to the variables necessary for the

calculation of spectroscopy as in Figure 9 and Figure 10. With these trajectories we can then calculate a spectrum for each average asymmetry value, this time cutting off above 50% to highlight lower intensity features:

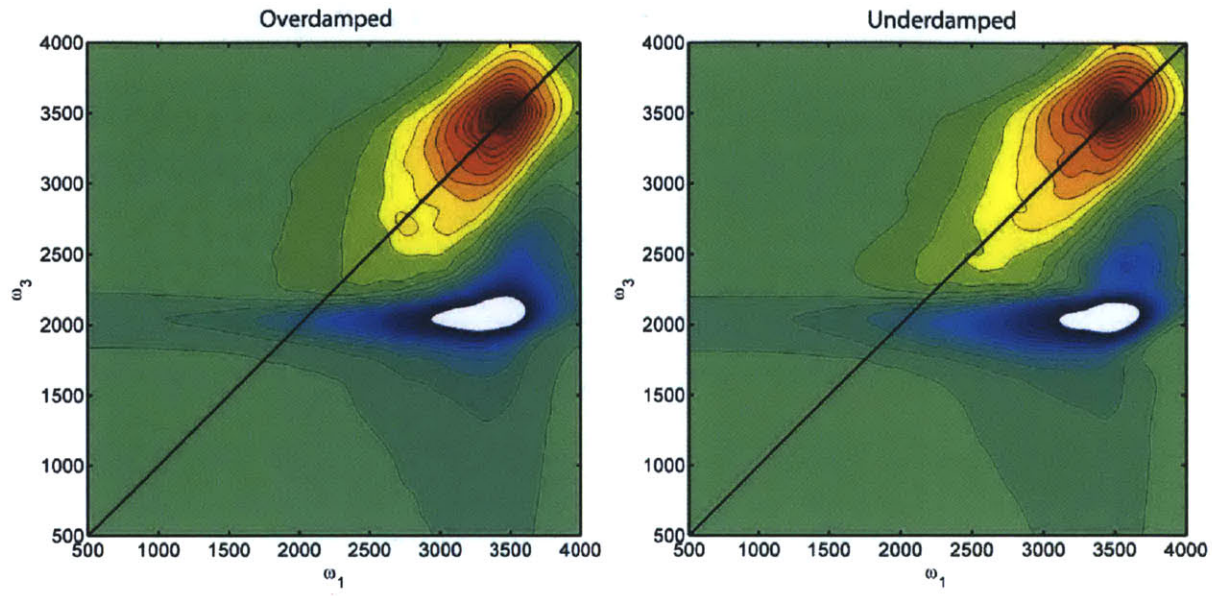

Figure 40: Double well potential with varying asymmetry time correlated using a single mode Brownian oscillator centered at 200 cm^{-1}

With this we obtain subtle but noticeable structure in the measured spectral response of the localized proton species due only to the difference in this single low frequency mode [62].

Imposing time dynamics with the same double exponential correlation function (4.21) instead, we can again map the asymmetry to the transition dipoles and frequencies. We can also allow the asymmetry of the proton potential double well to vary from -3 to zero, with a fixed fluctuation full width half max again of 2:

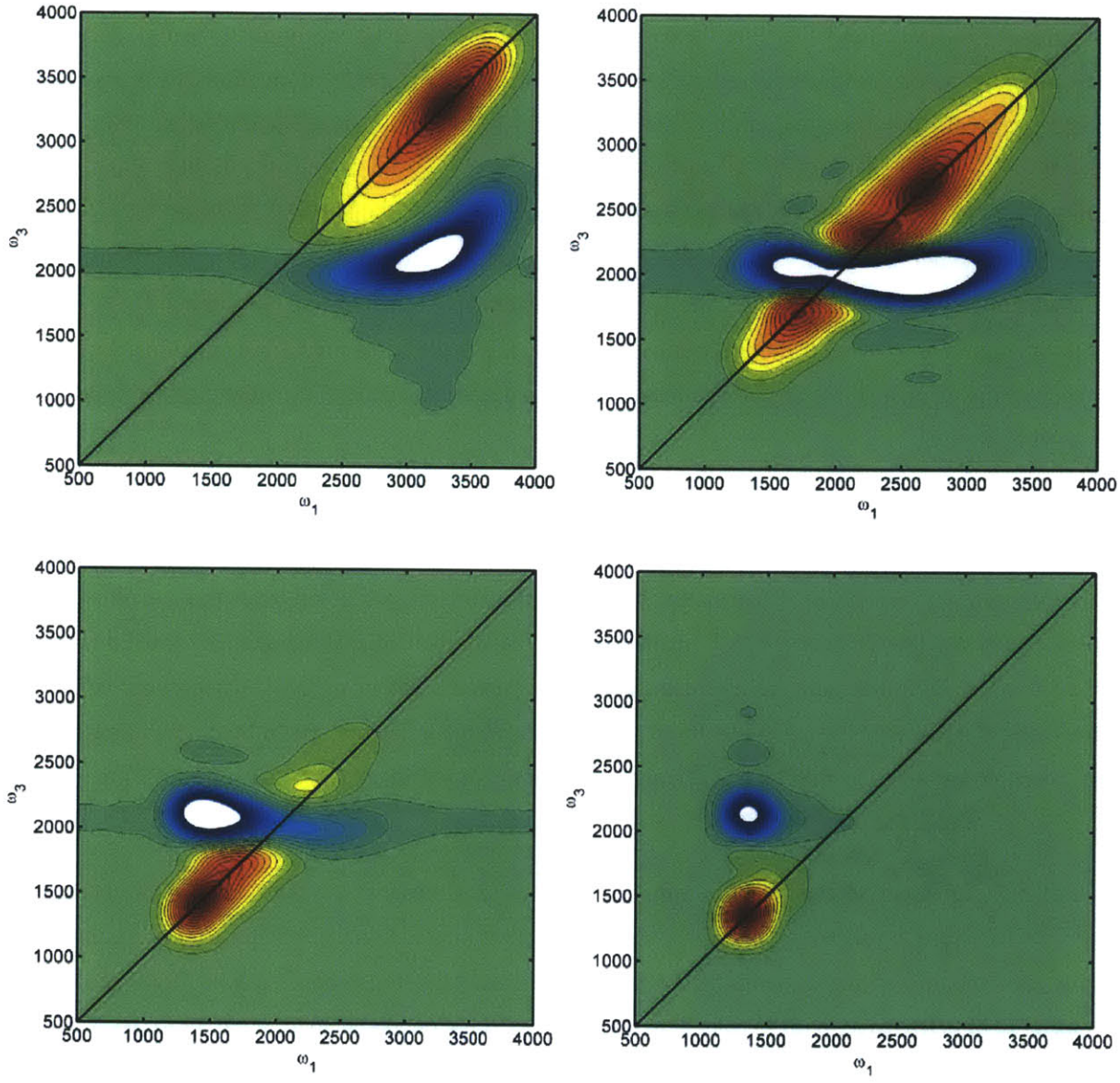

Figure 41: 2D spectra for a model proton transfer: double well asymmetry varying from an asymmetry parameter of -3 (upper left) to 0 (bottom right)

If we were to alter the proton potential smoothly in such a way as to induce a shared proton state – for instance, by creating a stronger and stronger hydrogen bond to an adjacent molecule or by photoinitiation of a proton transfer, altering the environment in such a way that the proton is delocalized over a small barrier, this predicts that we would observe a dramatic shift to lower frequencies as the 1D potential becomes effectively wider, and depending on the potential shape, a negative anharmonicity can be expected for the equally shared state as well.

CONCLUSIONS

Vibrational spectroscopies have, over the past few decades, proven to be exceptionally useful techniques for examining molecules in condensed phases. Common approaches for the calculation of vibrational spectra, especially nonlinear and ultrafast techniques, rely upon a few approximations which limit the sorts of systems to which they can be applied. Popular nonlinear spectroscopic models all rely upon a perturbative approach to describe the dynamics, expanding in terms of the dipole operator, but in order to make this computationally tractable and achieve analytical expressions, other classes of approximations are made, including bilinear coupling, the second cumulant approximation, and the Condon approximation. For systems with highly anharmonic potentials and non-Gaussian fluctuations, such as strong hydrogen bonds, these approximations are not valid and neglect describe much of the important underlying physics.

The trajectory mapping approach discussed here utilizes the semi-classical approximation for calculation of the nonlinear response, but in a manner which is far less restrictive than these other common models. This approach sets a probability distribution for one or more internal variables, treats this variable stochastically and then imposes upon it time correlation based upon either analytical empirical dynamic behavior, a Langevin-like bath model composed of Brownian oscillators, or specific quantities extracted from molecular dynamics simulations. From this time correlated trajectory, the full time evolution of the spectroscopic variables (transition frequencies and transition dipoles) are constructed through mappings in order to evaluate the semiclassical nonlinear response function.

By explicitly constructing classical time trajectories of the spectroscopic variables μ and ω in this manner, a general set of previously intractable dynamics and relationships can now be examined. For example, highly anharmonic potentials governing proton transfer through hydrogen bonds can be postulated or mapped out directly from *ab initio* calculations so that the non-Condon behavior inherent in these systems can be fully incorporated into calculations. In addition, system dynamics which depend on an evolving bath coordinate can be included and modeled, including explicit interdimer modes modulating the stretch in strongly hydrogen bonded dimers. Constructing trajectories utilizing this sort of mapping can be somewhat more computationally intensive, and the numerical integration over these trajectories required for the evaluation of the nonlinear response can be slightly more time consuming, but with this added complexity comes significant added flexibility, allowing for a variety of stochastic variables, experimentally motivated constraints, mapping parameters, and dynamics, with which we can begin to directly correlate infrared spectroscopy and complex chemical dynamics in a multitude of systems.

1. Joo, T., et al., *Third-order nonlinear time domain probes of solvation dynamics.* The Journal of Chemical Physics, 1996. **104**(16): p. 6089-6108.
2. Fecko, C.J., et al., *Local hydrogen bonding dynamics and collective reorganization in water: Ultrafast infrared spectroscopy of HOD/D[sub 2]O.* The Journal of Chemical Physics, 2005. **122**(5): p. 054506-18.
3. Khalil, M. and A. Tokmakoff, *Signatures of vibrational interactions in coherent two-dimensional infrared spectroscopy.* Chemical Physics, 2001. **266**(2-3): p. 213-230.
4. Ramasesha, K., et al., *Ultrafast 2D IR anisotropy of water reveals reorientation during hydrogen-bond switching.* The Journal of Chemical Physics, 2011. **135**(5): p. 054509-11.
5. Roberts, S.T., et al., *Proton Transfer in Concentrated Aqueous Hydroxide Visualized Using Ultrafast Infrared Spectroscopy.* The Journal of Physical Chemistry A, 2011. **115**(16): p. 3957-3972.
6. Roberts, S.T.S.T., *Hydrogen bond rearrangements and the motion of charge defects in water viewed using multidimensional ultrafast infrared spectroscopy*, in *Department of Chemistry.* 2010, Massachusetts Institute of Technology. : Cambridge, MA.
7. Timmer, R.L.A., M.J. Cox, and H.J. Bakker, *Direct Observation of Proton Transfer in Ice Ih Using Femtosecond Spectroscopy.* The Journal of Physical Chemistry A, 2010. **114**(5): p. 2091-2101.
8. Asplund, M.C., M.T. Zanni, and R.M. Hochstrasser, *Two-dimensional infrared spectroscopy of peptides by phase-controlled femtosecond vibrational photon echoes.* Proceedings of the National Academy of Sciences, 2000. **97**(15): p. 8219-8224.
9. Zanni, M.T., et al., *Heterodyned Two-Dimensional Infrared Spectroscopy of Solvent-Dependent Conformations of Acetylproline-NH2†.* The Journal of Physical Chemistry B, 2001. **105**(28): p. 6520-6535.
10. Bloembergen, N., *Nonlinear Optics.* 4th ed. 1996, Singapore ; River Edge, NJ: World Scientific. xiii, 172 p.
11. Shen, Y.R., *The Principles of Nonlinear Optics.* Wiley classics library ed. 2003, Hoboken, N.J.: Wiley-Interscience. xii, 563 p.
12. Butcher, P.N. and D. Cotter, *The elements of nonlinear optics.* Cambridge studies in modern optics 9. 1990, Cambridge ; New York: Cambridge University Press. xiv, 344 p.
13. Tokmakoff, A., *Orientational correlation functions and polarization selectivity for nonlinear spectroscopy of isotropic media. I. Third order.* The Journal of Chemical Physics, 1996. **105**(1): p. 1-12.
14. Tokmakoff, A., *Orientational correlation functions and polarization selectivity for nonlinear spectroscopy of isotropic media. II. Fifth order.* The Journal of Chemical Physics, 1996. **105**(1): p. 13-21.
15. Dick, B., *Response function theory of time-resolved CARS and CSRS of rotating molecules in liquids under general polarization conditions.* Chemical Physics, 1987. **113**(1): p. 131-147.
16. Sung, J. and R.J. Silbey, *Four wave mixing spectroscopy for a multilevel system.* The Journal of Chemical Physics, 2001. **115**(20): p. 9266-9287.
17. Sung, J. and R.J. Silbey, *Optical four wave mixing spectroscopy for multilevel systems coupled to multimode Brownian oscillators.* The Journal of Chemical Physics, 2003. **118**(5): p. 2443-2445.
18. Piryatinski, A. and J.L. Skinner, *Determining Vibrational Solvation-Correlation Functions from Three-Pulse Infrared Photon Echoes†.* The Journal of Physical Chemistry B, 2002. **106**(33): p. 8055-8063.
19. Everitt, K.F., E. Geva, and J.L. Skinner, *Determining the solvation correlation function from three-pulse photon echoes in liquids.* The Journal of Chemical Physics, 2001. **114**(3): p. 1326-1335.
20. Fecko, C.J., et al., *Ultrafast Hydrogen-Bond Dynamics in the Infrared Spectroscopy of Water.* Science, 2003. **301**(5640): p. 1698-1702.

21. Nicodemus, R.A., et al., *Collective Hydrogen Bond Reorganization in Water Studied with Temperature-Dependent Ultrafast Infrared Spectroscopy//.* The Journal of Physical Chemistry B, 2011. **115**(18): p. 5604-5616.
22. Nicodemus, R.A., et al., *Hydrogen Bond Rearrangements in Water Probed with Temperature-Dependent 2D IR.* The Journal of Physical Chemistry Letters, 2010. **1**(7): p. 1068-1072.
23. Roberts, S.T., et al., *Observation of a Zundel-like transition state during proton transfer in aqueous hydroxide solutions.* Proceedings of the National Academy of Sciences, 2009. **106**(36): p. 15154-15159.
24. Roberts, S.T., K. Ramasesha, and A. Tokmakoff, *Structural Rearrangements in Water Viewed Through Two-Dimensional Infrared Spectroscopy.* Accounts of Chemical Research, 2009. **42**(9): p. 1239-1249.
25. Marx, D., *Proton Transfer 200 Years after von Grotthuss: Insights from Ab Initio Simulations.* ChemPhysChem, 2006. **7**(9): p. 1848-1870.
26. Marx, D., et al., *The nature of the hydrated excess proton in water.* Nature, 1999. **397**(6720): p. 601-604.
27. Tuckerman, M.E., et al., *On the Quantum Nature of the Shared Proton in Hydrogen Bonds.* Science, 1997. **275**(5301): p. 817-820.
28. Torii, H., *Time-domain calculations of the polarized Raman and two-dimensional infrared spectra of liquid N,N-dimethylformamide.* Chemical Physics Letters, 2005. **414**(4–6): p. 417-422.
29. Jansen, T.l.C. and J. Knoester, *Nonadiabatic Effects in the Two-Dimensional Infrared Spectra of Peptides: Application to Alanine Dipeptide.* The Journal of Physical Chemistry B, 2006. **110**(45): p. 22910-22916.
30. Kubo, R., *Note on the Stochastic Theory of Resonance Absorption.* Journal of the Physical Society of Japan, 1954 **9**(Copyright (C) 1954 The Physical Society of Japan): p. 935.
31. Anderson, P.W., *A Mathematical Model for the Narrowing of Spectral Lines by Exchange or Motion.* Journal of the Physical Society of Japan, 1954 **9**(Copyright (C) 1954 The Physical Society of Japan): p. 316.
32. Kubo, R., *A Stochastic Theory of Line Shape*, in *Advances in Chemical Physics*, K.E. Shuler, Editor. 2007, John Wiley & Sons, Inc.: Hoboken, NJ, USA. p. 101-127.
33. Jansen, T.l.C., et al., *Stochastic Liouville equations for hydrogen-bonding fluctuations and their signatures in two-dimensional vibrational spectroscopy of water.* The Journal of Chemical Physics, 2005. **123**(11): p. 114504-11.
34. Jansen, T.l.C. and J. Knoester, *Calculation of two-dimensional infrared spectra of ultrafast chemical exchange with numerical Langevin simulations.* The Journal of Chemical Physics, 2007. **127**(23): p. 234502-8.
35. Eaves, J.D., A. Tokmakoff, and P.L. Geissler, *Electric Field Fluctuations Drive Vibrational Dephasing in Water.* The Journal of Physical Chemistry A, 2005. **109**(42): p. 9424-9436.
36. Ramasesha, K., et al., *A phenomenological approach to modeling chemical dynamics in nonlinear and two-dimensional spectroscopy.* The Journal of Chemical Physics, 2012. **136**(13): p. 134507-11.
37. Corcelli, S.A., C.P. Lawrence, and J.L. Skinner, *Combined electronic structure/molecular dynamics approach for ultrafast infrared spectroscopy of dilute HOD in liquid H[sub 2]O and D[sub 2]O.* The Journal of Chemical Physics, 2004. **120**(17): p. 8107-8117.
38. Robertson, G.N. and J. Yarwood, *Vibrational relaxation of hydrogen-bonded species in solution. I. Theory.* Chemical Physics, 1978. **32**(2): p. 267-282.
39. Williams, G., *Time-Correlation Functions and Molecular-Motion.* Chemical Society Reviews, 1978. **7**(1): p. 89-131.
40. Bratos, S., *Profiles of hydrogen stretching ir bands of molecules with hydrogen bonds: A stochastic theory. I. Weak and medium strength hydrogen bonds.* The Journal of Chemical Physics, 1975. **63**(8): p. 3499-3509.

41. Henri-Rousseau, O. and P. Blaise, *The Infrared Spectral Density of Weak Hydrogen Bonds within the Linear Response Theory*, in *Advances in Chemical Physics*. 2007, John Wiley & Sons, Inc. p. 1-186.
42. Hadzi, D., *Theoretical treatments of hydrogen bonding*. 1997, Chichester, England ; New York: John Wiley. xiii, 318 p.
43. Fischer, S.F., G.L. Hofacker, and M.A. Ratner, *Spectral Behavior of Hydrogen-Bonded Systems: Quasiparticle Model.* The Journal of Chemical Physics, 1970. **52**(4): p. 1934-1947.
44. Witkowski, A. and M. Wójcik, *Infrared spectra of hydrogen bond a general theoretical model.* Chemical Physics, 1973. **1**(1): p. 9-16.
45. Witkowski, A., *Separation of electronic and nuclear motions and the dynamical Schrödinger group.* Physical Review A, 1990. **41**(7): p. 3511-3517.
46. Romanowski, H. and L. Sobczyk, *A stochastic approach to their IR spectra of the symmetrical OHO hydrogen bond.* Chemical Physics, 1977. **19**(3): p. 361-370.
47. Guissani, Y. and H. Ratajczak, *Theoritical study on an anomalous isotopic effect on the position and integrated intensity of the ir stretching vibration band for medium-strong and strong hydrogen bonds.* Chemical Physics, 1981. **62**(3): p. 319-331.
48. Witkowski, A., *On quantum molecular dynamics and electrodynamics.* The Journal of Chemical Physics, 1983. **79**(2): p. 852-860.
49. Leviel, J.-L. and Y. Marechal, *Infrared Spectra of H-Bonded Systems : Anharmonicity of the H-Bond Vibrations in Cyclic Dimers.* The Journal of Chemical Physics, 1971. **54**(3): p. 1104-1107.
50. Marechal, Y. and A. Witkowski, *Infrared Spectra of H-Bonded Systems.* The Journal of Chemical Physics, 1968. **48**(8): p. 3697-3705.
51. Cooley, J., P. Lewis, and P. Welch, *Application of the fast Fourier transform to computation of Fourier integrals, Fourier series, and convolution integrals.* Audio and Electroacoustics, IEEE Transactions on, 1967. **15**(2): p. 79-84.
52. Cooley, J. and J. Tukey, *An Algorithm for the Machine Calculation of Complex Fourier Series.* Mathematics of Computation, 1965. **19**(90): p. 297-301.
53. Boas, M.L., *Mathematical methods in the physical sciences*. 3rd ed. 2006, Hoboken, NJ: Wiley. xviii, 839 p.
54. Ka, B.J. and W.H. Thompson, *Sampling the Proton Transfer Reaction Coordinate in Mixed Quantum-Classical Molecular Dynamics Simulations.* The Journal of Physical Chemistry A, 2011. **116**(2): p. 832-838.
55. Lawrence, C.P. and J.L. Skinner, *Vibrational spectroscopy of HOD in liquid D[sub 2]O. II. Infrared line shapes and vibrational Stokes shift.* The Journal of Chemical Physics, 2002. **117**(19): p. 8847-8854.
56. Woutersen, S. and H.J. Bakker, *Hydrogen Bond in Liquid Water as a Brownian Oscillator.* Physical Review Letters, 1999. **83**(10): p. 2077-2080.
57. Palese, S., et al., *Femtosecond Two-Dimensional Raman Spectroscopy of Liquid Water.* The Journal of Physical Chemistry, 1994. **98**(48): p. 12466-12470.
58. Lawrence, C.P. and J.L. Skinner, *Vibrational spectroscopy of HOD in liquid D[sub 2]O. I. Vibrational energy relaxation.* The Journal of Chemical Physics, 2002. **117**(12): p. 5827-5838.
59. Laenen, R., C. Rauscher, and A. Laubereau, *Dynamics of Local Substructures in Water Observed by Ultrafast Infrared Hole Burning.* Physical Review Letters, 1998. **80**(12): p. 2622-2625.
60. Gale, G.M., et al., *Femtosecond Dynamics of Hydrogen Bonds in Liquid Water: A Real Time Study.* Physical Review Letters, 1999. **82**(5): p. 1068-1071.
61. Chandler, D., C. Dellago, and P. Geissler, *Ion dynamics: Wired-up water.* Nat Chem, 2012. **4**(4): p. 245-247.
62. Ando, K., *Semiquantal analysis of a double-well coupled to dissipative bath: effective potential and coupled generalized Langevin equations.* Chemical Physics Letters, 2003. **376**(3-4): p. 532-537.

APPENDIX A: SAMPLE CODE

INTEGRATION OF SEMICLASSICAL APPROXIMATION (MATLAB)

```
function [ xR1 xR2 xNR1 xNR2 R_minus R_plus mean_freq_10] =
wtto2D_parallel_2_water_wt( wt_Trajectory, dt, tau_2, NumberofPoints, delta )
%WTTO2D Construct Response Functions from w01 frequency Trajectory and
Mapping for Water
%    Using R+/-
%    wt_Trajectory = trajectory
%    dt = trajectory timesteps
%    tau2 = waiting time
%    NumberofPoints = duration of t1 and t3
%    delta = anharmonicity, or it can be a mapping


%% Setup
matlabpool open


%% Prep
% Constants
c = 2.99792e-5; %Speed of light [cm fs-1]

% Load
Traj_length = length(wt_Trajectory);
time = linspace(0,Traj_length-1,Traj_length).*dt;
wt_Trajectory_2=wt_Trajectory';
w_10 = wt_Trajectory_2;

%subtract off the mean
mean_freq_10=mean(w_10);
omega_10=(w_10-mean_freq_10)*c*2*pi;

% Create anharmonicity
if delta=='mapping'
    % Empirical linear mapping made up from J.Chem.Phys. 123 114504 (2005)
    omega_21=(((137/126)*w_10-472)-mean_freq_10)*c*2*pi;
else
    omega_21=(w_10-mean_freq_10+delta)*c*2*pi; %static /fixed anharmonicity
end

% Set dipoles
% mu_10=(1.8336 - w_10*1.2973e-3 + (w_10.^2)*4.7136e-7 - (w_10.^3)*6.8016e-
11); %Non-Condon empirical mapping
mu_10=ones(1, Traj_length);  %Condon Approximation
mu_21=sqrt(2)*mu_10; %harmonic scaling

% Integration variables and such
length_t1=NumberofPoints;
length_t3=NumberofPoints;
```

```
tau_1_vector=[1:length_t1];
tau_2=tau_2/dt; %to make it an index not a time

N_averages = Traj_length-2*NumberofPoints-tau_2-1;

% Integral Prep
omega_10_integral = cumtrapz(time, omega_10);
exp_omega_10_integral = exp(1i*omega_10_integral);
omega_21_integral = cumtrapz(time, omega_21);
exp_omega_21_integral = exp(1i*omega_21_integral);

avg_plus_1 = zeros(NumberofPoints);
avg_plus_2 = zeros(NumberofPoints);
avg_minus_1 = zeros(NumberofPoints);
avg_minus_2 = zeros(NumberofPoints);


%% Timing Run
num_cores=4;
parallel_scale_factor=1.3; %Empirical factor to try and guess the timing (not
exactly 4 times faster with 4 cores)

actual_time = clock;
disp(['The time right now is ' sprintf('%02d', actual_time(4)) ':'
sprintf('%02d', actual_time(5)) '.']);
%Note: sprintf('%02d', number) gives 'number' as string, with 2 digits,
including leading zeros

for tau_3=1

    tstart = tic;

    avg_plus_1_temp = zeros(1, NumberofPoints);
    avg_plus_2_temp = zeros(1, NumberofPoints);
    avg_minus_1_temp = zeros(1, NumberofPoints);
    avg_minus_2_temp = zeros(1, NumberofPoints);

    for n_average=1:N_averages
        I1_plus=exp_omega_10_integral(tau_1_vector+n_average-1).*...
            conj(exp_omega_10_integral(n_average));
        I1_minus=conj(I1_plus);
        I2=exp_omega_10_integral((tau_3+tau_2+tau_1_vector+n_average-1)).*...
            conj(exp_omega_10_integral((tau_2+tau_1_vector+n_average-1)));
        I3_plus=I1_plus;
        I3_minus=I1_minus;
        I4=exp_omega_21_integral((tau_3+tau_2+tau_1_vector+n_average-1)).*...
            conj(exp_omega_21_integral((tau_2+tau_1_vector+n_average-1)));

        avg_plus_1_temp = avg_plus_1_temp +...
            mu_10(tau_3+tau_2+tau_1_vector+n_average-1).*...
            mu_10(tau_2+tau_1_vector+n_average-1).*...
            mu_10(tau_1_vector+n_average-1).*...
            mu_10(n_average).*...
            I1_plus.*I2;
        avg_plus_2_temp = avg_plus_2_temp +...
```

```
            mu_21(tau_3+tau_2+tau_1_vector+n_average-1).*...
            mu_21(tau_2+tau_1_vector+n_average-1).*...
            mu_10(tau_1_vector+n_average-1).*...
            mu_10(n_average).*...
            I3_plus.*I4;

        avg_minus_1_temp = avg_minus_1_temp +...
            mu_10(tau_3+tau_2+tau_1_vector+n_average-1).*...
            mu_10(tau_2+tau_1_vector+n_average-1).*...
            mu_10(tau_1_vector+n_average-1).*...
            mu_10(n_average).*...
            I1_minus.*I2;
        avg_minus_2_temp = avg_minus_2_temp +...
            mu_21(tau_3+tau_2+tau_1_vector+n_average-1).*...
            mu_21(tau_2+tau_1_vector+n_average-1).*...
            mu_10(tau_1_vector+n_average-1).*...
            mu_10(n_average).*...
            I3_minus.*I4;
    end

    avg_plus_1(tau_3, :) = avg_plus_1_temp;
    avg_plus_2(tau_3, :) = avg_plus_2_temp;
    avg_minus_1(tau_3, :) = avg_minus_1_temp;
    avg_minus_2(tau_3, :) = avg_minus_2_temp;

    telapsed = toc(tstart);

end

totalt = (length_t3.*telapsed/num_cores)*parallel_scale_factor;
hrs = actual_time(4)+floor(totalt/3600);

mins = actual_time(5)+floor((totalt-3600*floor(totalt/3600))/60);
if mins >= 60
    mins = mins - 60;
    hrs = hrs + 1;
end
if hrs >= 24
    hrs = hrs - 24;
end

disp(['The ' num2str(tau_2*dt) 'fs surface will be done at roughly '...
    sprintf('%02d', hrs) ':' sprintf('%02d', mins) '.']);


%% Response Functions
% Calculate the response function R+-
% R- = rephasing
% R+ = nonrephasing

parfor tau_3=2:length_t3 %picking up where timing run left off

    avg_plus_1_temp = zeros(1, NumberofPoints);
    avg_plus_2_temp = zeros(1, NumberofPoints);
    avg_minus_1_temp = zeros(1, NumberofPoints);
```

```
    avg_minus_2_temp = zeros(1, NumberofPoints);

    for n_average=1:N_averages
        I1_plus=exp_omega_10_integral(tau_1_vector+n_average-1).*...
            conj(exp_omega_10_integral(n_average));
        I1_minus=conj(I1_plus);
        I2=exp_omega_10_integral((tau_3+tau_2+tau_1_vector+n_average-1)).*...
            conj(exp_omega_10_integral((tau_2+tau_1_vector+n_average-1)));
        I3_plus=I1_plus;
        I3_minus=I1_minus;
        I4=exp_omega_21_integral((tau_3+tau_2+tau_1_vector+n_average-1)).*...
            conj(exp_omega_21_integral((tau_2+tau_1_vector+n_average-1)));

        avg_plus_1_temp = avg_plus_1_temp +...
            mu_10(tau_3+tau_2+tau_1_vector+n_average-1).*...
            mu_10(tau_2+tau_1_vector+n_average-1).*...
            mu_10(tau_1_vector+n_average-1).*...
            mu_10(n_average).*...
            I1_plus.*I2;
        avg_plus_2_temp = avg_plus_2_temp +...
            mu_21(tau_3+tau_2+tau_1_vector+n_average-1).*...
            mu_21(tau_2+tau_1_vector+n_average-1).*...
            mu_10(tau_1_vector+n_average-1).*...
            mu_10(n_average).*...
            I3_plus.*I4;

        avg_minus_1_temp = avg_minus_1_temp +...
            mu_10(tau_3+tau_2+tau_1_vector+n_average-1).*...
            mu_10(tau_2+tau_1_vector+n_average-1).*...
            mu_10(tau_1_vector+n_average-1).*...
            mu_10(n_average).*...
            I1_minus.*I2;
        avg_minus_2_temp = avg_minus_2_temp +...
            mu_21(tau_3+tau_2+tau_1_vector+n_average-1).*...
            mu_21(tau_2+tau_1_vector+n_average-1).*...
            mu_10(tau_1_vector+n_average-1).*...
            mu_10(n_average).*...
            I3_minus.*I4;
    end

    avg_plus_1(tau_3, :) = avg_plus_1_temp;
    avg_plus_2(tau_3, :) = avg_plus_2_temp;
    avg_minus_1(tau_3, :) = avg_minus_1_temp;
    avg_minus_2(tau_3, :) = avg_minus_2_temp;

end

avg_plus_1=avg_plus_1./N_averages;
avg_plus_2=avg_plus_2./N_averages;
avg_minus_1=avg_minus_1./N_averages;
avg_minus_2=avg_minus_2./N_averages;

% Put terms together
R_plus=(2*avg_plus_1-avg_plus_2);
R_minus=(2*avg_minus_1-avg_minus_2);
```

```
%%
xR1 = real(R_minus);
xR2 = imag(R_minus);
xNR1 = real(R_plus);
xNR2 = imag(R_plus);


%% Close parallel pool
matlabpool close
end
```

DVR FOR MAPPING TRANSITIONS FROM DOUBLE WELL POTENTIAL (MATLAB)

```
%% Coding Variables
entry_number=1;


% Which Eigenstates to work with
state_i=1;
state_f=6;
n_states=(state_f-state_i)+1;


%% Constants and Variables
hbar=1;
% Mass (reduced mass, in kg/molecule, for water, 1.495_10^-23 g/molecule)
mass=1;

% Variables for the DVR Grid / Matrix
N=600;
xmax=5.5;
xmin=-5.5;
dx=(xmax-xmin)/N;


%% Start varying the potential
for d=-5:0.1:5 %d=linear parameter adding asymmetry to double well

    %% Construct V and T Matricies
    Vm=zeros(N);
    Tm=zeros(N);
    xaxisdata=zeros(N,1);

    %% Fill up matrices
    gp=hbar^2/(2*mass*dx^2); %grid parameter
    for i=1:N
        for j=1:N
            if i==j
                Tm(i,j)=((gp*(-1)^(i-j))*((pi^2)/3));
                ri=xmin+i*dx;
                Vm(i,j)=V(ri, beta, alpha, d);
                %this is where the potential script is called
                %this is where the potential script is called
                xaxisdata(i)=(ri);
            else
                Tm(i,j)=((gp*(-1)^(i-j))*(2/(i-j)^2));
            end
        end
    end


    %% Add to get H
    H=(Tm+Vm);


    %% Compute!
    [Vectors, Values]=eig(H);
```

```
    % Vectors is a matrix with eigenvectors as columns
    % Values is a matrix with eigenvalues along the diagonals
    E=diag(Values);

    for state=state_i:state_f
        % Get Normalization Factor for Wavefunction
        Nstate(state)=(Vectors(:,state)'*Vectors(:,state));
        NormVectors(:,state)=Vectors(:,state)/sqrt(Nstate(state));

        % Frequencies of transitions
        dvalue=d;
        w01=(E(2)-E(1));
        w12=(E(3)-E(2));
        w02=(E(3)-E(1));
        w24=(E(5)-E(3));

    end

    % Vmn = <n|x|m>
    Vmn=zeros(n_states);
    for i=state_i:state_f
        for j=state_i:state_f
            Vmn(i,j)=(NormVectors(:,i)')*(xaxisdata.*NormVectors(:,j));
        end
    end

    % Save data
    mapping(entry_number, :)=[dvalue w01 w12 w02 w24 Vmn(2,1) Vmn(3,2)];
    entry_number=entry_number+1;
end



function [ V_x ] = V( x, beta, alpha, d )
%POTENTIAL The Potential Energy Function in 1D
%   Double Well Potential Here

%% Here's the Potential Function!
% Minima = sqrt(beta/(2*alpha))
% Barrier Height = beta^2/(4alpha)

V_x=alpha*x^4+...
    -beta*x^2+...
    ((beta^2)/(4*alpha))+...
    d*x;
end
```